Loma Linda University

TheScholarsRepository@LLU: Digital Archive of Research, Scholarship & Creative Works

Loma Linda University Electronic Theses, Dissertations & Projects

6-2016

Mechanisms of Post-hemorrhagic Hydrocephalus after Germinal Matrix Hemorrhage

Damon William Klebe

Follow this and additional works at: https://scholarsrepository.llu.edu/etd

Part of the Medical Physiology Commons

Recommended Citation

Klebe, Damon William, "Mechanisms of Post-hemorrhagic Hydrocephalus after Germinal Matrix Hemorrhage" (2016). *Loma Linda University Electronic Theses, Dissertations & Projects*. 385.
https://scholarsrepository.llu.edu/etd/385

This Dissertation is brought to you for free and open access by TheScholarsRepository@LLU: Digital Archive of Research, Scholarship & Creative Works. It has been accepted for inclusion in Loma Linda University Electronic Theses, Dissertations & Projects by an authorized administrator of TheScholarsRepository@LLU: Digital Archive of Research, Scholarship & Creative Works. For more information, please contact scholarsrepository@llu.edu.

LOMA LINDA UNIVERSITY
School of Medicine
in conjunction with the
Faculty of Graduate Studies

Mechanisms of Post-hemorrhagic Hydrocephalus after Germinal Matrix Hemorrhage

by

Damon William Klebe

A Dissertation submitted in partial satisfaction of
the requirements for the degree
Doctor of Philosophy in Physiology

June 2016

© 2016

Damon Klebe
All Rights Reserved

Each person whose signature appears below certifies that this dissertation in his/her opinion is adequate, in scope and quality, as a dissertation for the degree Doctor of Philosophy.

_____, Chairperson

John H. Zhang, Professor of Physiology

_____

Daila S. Gridley, Professor of Microbiology

_____

Richard E. Hartman, Professor of Psychology

_____

Andre Obenaus, Associate Professor of Biochemistry

_____

Jiping Tang, Professor of Physiology

ACKNOWLEDGEMENTS

Thank you Dr. Zhang and Dr. Tang for giving me the opportunity to join your research group during the summer of 2011. You both knew very little of myself and took a huge risk hiring me into your laboratory, a risk I hope paid off well. Thank you for your mentorship and guidance, for challenging me, and for encouraging me on this pursuit. Thank you Dr. Zhang for your constructive criticism, although some was hard to accept at times, all critiques were important for making me into scientist who is well-prepared for a successful career. Thanks to my committee for their guidance and direction. Thanks to past and present members of the Zhang neuroscience laboratory for their contributions and support in my scientific endeavors, in particular Jerry Flores, Devin McBride, Paul Krafft, William Rolland, and Tim Lekic. Thank you to my friends and loved ones for standing by me during both the good and bad times on this journey. Most importantly, thank you to my parents, Dannette Klebe and Douglas Klebe, for your unconditional love and support that made this possible.

CONTENT

Approval Page iii

Acknowledgements iv

List of Figures x

List of Tables xii

List of Abbreviations xiii

Abstract xiv

Chapter

1. Post-hemorrhagic Hydrocephalus Developent after Germinal Matrix Hemorrhage: Established Mechanisms and Proposed Pathways 1

    Abstract 2
    Introduction 3
    Cerebrospinal Fluid Flow Dynamics 6

        Production 6
        Circulation 9
        Reabsorption 10

    Hydrocephalus 15

        Non-communicating Hydrocephalus 16
        Communicating Hydrocephalus 16
        Current Hydrodynamic Theory 17

    Post-hemorrhagic Hydrocephalus Pathophysiology and Potential Mechanisms 24

        Blood Clots, Hemoglobin, and Iron 24
        Inflammation, Fibrosis, and Gliosis 26

    Conclusion 32
    Specific Aims 32

        Aim 1 34
        Aim 2 34

References 37

2. PPARγ-induced Upregulation of CD36 Enhances Hematoma Resolution and Attenuates Long-term Neurological Deficits after Germinal Matrix Hemorrhage in Neonatal Rats 51

Abstract 52
Introduction 53
Materials and Methods 56

Animals and Surgeries 56
Animal Treatments and Experimental Groups 57
Animal Perfusion and Tissue Extraction 58
Hemoglobin Assay 58
Intracranial Pressure Measurements 59
Western blotting 59
Histological Volumetric Analysis 60
Immunohistochemistry 60
Neurobehavioral Analysis 61
Statistical Analysis 62

Results 62

PPARγ Stimulation Ameliorated Long-term Neurological Deficits 62
PPARγ Stimulation Improved Long-term Brain Morphology 64
PPARγ Stimulation Enhanced Hematoma Resolution, Increased Activated Microglia, and Induced M2 Polarization 67
PPARγ Stimulation Increased CD36 and PPARγ Expression at 72 Hours 70
CD36 Knockdown Reversed PPARγ Agonist-enhanced Hematoma Resolution and M2 Expression at 72 Hours 72

Discussion 72
References 79

3. Acute and Delayed Deferoxamine Treatment Attenuates Long-term Sequelae after Germinal Matrix Hemorrhage in Neonatal Rats 85

Abstract 86
Introduction 87
Materials and Methods 88

Animal Surgery and Experimental Groups 88
Behavioral Testing 89
Histopathological Analysis 90
Western blotting 91

Statistical Analysis 91

Results 92

Deferoxamine Improved Brain Morphology after GMH 92
Deferoxamine Reduced Extracellular Matrix Protein Expression after GMH 94
Deferoxamine Improved Long-term Neurofunctional Outcomes after GMH 96

Discussion 98
References 101

4. Protease-activated Receptor 1 and 4 Signal Inhibition Reduces Preterm Neonatal Hemorrhage Brain Injury 103

Abstract 104
Introduction 105
Materials and Methods 105

Animal Surgeries 105
Tissue Processing and Analysis 107
Animal Treatments and Experimental Groups 109
Assessment of Neurological Deficits 109
Statistical Analysis 111

Results 111

GMH Activated Thrombin 111
Molecular Mediators of Post-hemorrhagic Hydrocephalus 111
Western blots 113
Early Signal Inhibition Improved Long-term Outcomes 115

Discussion 117
References 119

5. Dabigatran Ameliorates Post-hemorrhagic Hydrocephalus Development after Germinal Matrix Hemorrhage in Neonatal Rat Pups 121

Abstract 122
Introduction 123
Material and Methods 126

GMH Surgical Procedures 126
Experimental Groups and Treatments 127
Intracranial Pressure Measurement 128

Neurobehavioral Assessments 128
Perfusion and Tissue Extraction 129
Hemoclot Assay 129
Hemoglobin Assay 130
Western blot 130
Histology 131
Statistical Analysis 132

Results 132

Dabigatran Half-life and Hematoma Volume after GMH 132
Thrombin Inhibition Improved Long-term Neurofunctional Recovery, Which Was Not Reversed by PAR-1 Stimulation. PAR-1 Inhibition Alone Was Not Sufficient to Promote Recovery 134
Thrombin Inhibition Improved Long-term Brain Morphological Outcomes, Which Tended to be Reversed by PAR-1 Stimulation. PAR-1 Inhibition Alone Was Not Sufficient to Promote Recovery 136
Short-term p-mTOR and Downstream p-p70s6i Expression Levels are Significantly Increased after GMH 138
Thrombin Inhibition Reduced p-mTOR and p-p70s6k Expression Levels at 3 Days Post-ictus, Which Were Reversed by PAR-1 Stimulation. PAR-1 Inhibition Alone Did Not Significantly Reduced p-mTOR and p-p70s6k Expression 140
Thrombin Inhibition Significantly Reduced Long-term ECM Protein Proliferation after GMH, Which Was Not Reversed by PAR-1 Stimulation. PAR-1 Inhibition Alone Tended to Reduce ECM Protein Proliferation 142

Discussion 144
Conclusion 150
References 151

6. Discussion 155

Summary/Highlights of Findings 155
The State of the Field Prior to this Study 155
How our Findings Advance the Field 156
Summary/Conclusion 158
Prospective 159
References 160

Appendices

A. Modulating the Immune Response towards a Neuroregenerative Peri-injury Milieu after Cerebral Hemorrhage 162

Abstract 163
Cerebral Hemorrhage Pathophysiology 164

Incidence, Outcomes, and Clinical Management 164
Primary Brain Injury 165
Secondary Brain Injury 165
Review Scope 167

Macrophage, Microglia, T-helper Lymphocyte Characterization 168

Macrophage and Microglia Subtypes 168
T-helper Lymphocyte Subtypes 172
Macrophage/Microglia and T-helper Lymphocyte Communication 173

Inflammation after Cerebral Hemorrhage 175

Role of Macrophages and Microglia 175
Role of T-helper Lymphocytes 179

Conclusion 183
References 185

FIGURES

Figures Page

1.1: Overview of the glymphatic system. 14

1.2: Paravascular Virchow-Robin spaces depicted on MRI. 23

1.3: Summary of GMH Pathophysiological Pathways. 31

1.4: Schematic representation of the overall central hypothesis and research aims 36

2.1: Long-term neurocognitive and sensorimotor outcomes after 15d-PGJ_2 treatment and PPARγ inhibition with 15d-PGJ_2 treatment at 3-4 weeks after GMH.....63

2.2: Effects of 15d-PGJ_2 treatment and PPARγ inhibition with 15d-PGJ_2 treatment on brain morphology and intracranial pressure 4 weeks after GMH.....65

2.3: Quantification of brain morphological changes from 15d-PGJ_2 treatment and PPARγ inhibition with 15d-PGJ_2 treatment at 4 weeks post-GMH 66

2.4: Short-term hematoma resolution after GMH from 15d-PGJ_2 treatment, PPARγ inhibition with 15d-PGJ_2 treatment, CD36 knockdown, and CD36 knockdown with 15d-PGJ_2 treatment. 68

2.5: Microglia / Macrophage activation and differentiation into M2 subtypes at 3 days post-GMH following 15d-PGJ_2 treatment, CD36 knockdown, and CD36 knockdown with 15d-PGJ_2 treatment 69

2.6: Short-term time course of CD36 and PPARγ expression after GMH and the effects of 15d-PGJ_2 treatment, PPARγ inhibition with 15d-PGJ_2 treatment, CD36 knockdown, and CD36 knockdown with 15d-PGJ_2 treatment on CD36 and PPARγ expression levels 71

3.1: Long-term brain morphological outcomes after acute and delayed Deferoxamine treatment at 4 weeks post-GMH.....93

3.2: Extracellular matrix protein expression levels after acute and delayed Deferoxamine treatment at 4 weeks post-GMH.....95

3.3: Long-term neurocognitive and sensorimotore recovery after acute and delayed Deferoxamine treatment at 3-4 weeks post-GMH. 97

4.1: Thrombin activity after germinal matrix hemorrhage and association between specific GMH model elements and post-hemorrhagic ventricular dilation development 112

4.2: Dose-response changes of COX-2 and p-mTOR expression after combinatorial PAR-1 and PAR-4 inhibition at 72 hours post-GMH as well as long-term brain morphological outcomes after COX-2 or mTOR inhibition at 4 weeks post-GMH. 114

4.3: Long-term neurocognitive and sensorimotor outcomes after COX-2 or mTOR inhibition at 3-4 weeks post-GMH. 116

5.1: Dabigatran dose response for hematoma volume 24 hours post-GMH and plasma concentration time course. 133

5.2: Long-term neurobehavioral outcomes after thrombin or PAR-1 inhibition at 3-4 weeks post-GMH. 135

5.3: Long-term brain morphological outcomes after thrombin or PAR-1 inhibition at 4 weeks post-GMH 137

5.4: Time course of mTOR/p70s6k activation after GMH 139

5.5: Expression of activated mTOR/p70s6k after thrombin inhibition and PAR-1 stimulation at 72 hours after GMH.....141

5.6: Long-term expression of extracellular matrix proteins after thrombin and PAR-1 inhibition at 4 weeks post-GMH 143

TABLES

Tables Page

A.1: Macrophage/Microglia and T-helper Lymphocyte Subtypes 171

A.2: Current and Past Clinical Trials Evaluating Immunomodulatory Therapies for Cerebral Hemorrhage.....182

ABBREVIATIONS

BID	Twice a Day
CSF	Cerebrospinal Fluid
ECM	Extracellular Matrix
GMH	Germinal Matrix Hemorrhage
ICP	Intracranial Pressure
IL	Interleukin
IVH	Intraventricular Hemorrhage
NIH	National Institute of Health
PHH	Post-hemorrhagic Hydrocephalus
PHVD	Post-hemorrhagic Ventricular Dilation
PPARγ	Peroxisome Proliferator Receptor Gamma
QD	Once a Day
SD	Standard Deviation
SEM	Standard Error of Mean
TGFβ	Tumor Growth Factor Beta
TNFα	Tumor Necrosis Factor Alpha

ABSTRACT OF THE DISSERTATION

Mechanisms of Post-hemorrhagic Hydrocephalus after Germinal Matrix Hemorrhage

by

Damon William Klebe

Doctor of Philosophy, Graduate Program in Physiology
Loma Linda University, June 2016
Dr. John H. Zhang, Chairperson

The inherently fragile vasculature of the germinal matrix is susceptible to rupture, possibly as a result of hemodynamic and cardiorespiratory instability associated with prematurity. Germinal matrix hemorrhage is a leading cause of morbidity and mortality in preterm and/or very low birthweight infants, and post-hemorrhagic hydrocephalus is major consequence of severe grade hemorrhages. Chronic post-hemorrhagic hydrocephalus treatment involves surgical insertion of shunts, which are costly and prone to complications. Thus, a safe non-invasive therapeutic approach towards post-hemorrhagic hydrocephalus clinical management would significantly improve the quality of life for this patient population. Thrombin, cerebroventricular blood clots, and iron have been identified as causative factors of hydrocephalus formation. Thrombin stimulates proteinase-activated receptors, leading to subsequent mTOR activation and extracellular matrix protein proliferation, which possibly obstruct the cerebroventricular system. Blood clots may directly impair cerebrospinal fluid circulation and absorption. PPARγ stimulation enhances micgroglial/macrophage phagocytosis of erythrocytes via CD36 scavenger receptor, augmenting clot resolution and improving outcomes after adult cerebral hemorrhage. Additionally, lysed erythrocytes and metabolized hemoglobin release iron, which is associated with brain injury after adult cerebral hemorrhage and

contribute to post-hemorrhagic hydrocephalus development. The central aim of this proposal is to determine the role of activated thrombin/PAR-1/mTOR pathway as well as the role of hematoma resolution by PPARγ/CD36 and iron chelation by Deferoxamine in hydrocephalus development after germinal matrix hemorrhage. Direct thrombin inhibition reduced short-term mTOR activation and ameliorated long-term post-hemorrhagic hydrocephalus development, neurocogntive deficits, and extracellular matrix protein proliferation, although PAR-1 inhibition alone did not achieve the same therapeutic benefits. PPARγ stimulation improved short-term hematoma resolution, which was reversed by PPARγ antagonism and CD36 knockdown. PPARγ stimulation attenuated long-term neurocognitive deficits and post-hemorrhagic hydrocephalus, which was reversed by PPARγ antagonism. Acute and delayed iron chelation also reduced long-term post-hemorrhagic hydrocephalus development, neurocognitive deficits, and extracellular matrix protein proliferation. Thus, thrombin/PAR/mTOR pathway inhibition, enhanced PPARγ/CD36 mediated hematoma resolution, and iron chelation significantly ameliorated short and long-term brain sequelae after germinal matrix hemorrhage and are clinically viable therapeutic targets warranting further investigation.

CHAPTER ONE

POST-HEMORRHAGIC HYDROCEPHALUS DEVELOPMENT AFTER GERMINAL MATRIX HEMORRHAGE: ESTABLISHED MECHANISMS AND PROPOSED PATHWAYS

Damon Klebe[1], Devin McBride[1], Paul R Krafft[1, 2], Jerry J Flores[1], Jiping Tang[1], John H Zhang[1, 3]

[1]Department of Physiology and Pharmacology, Loma Linda University School of Medicine, Loma Linda, CA 92350

[2]Department of Neurosurgery, Loma Linda University School of Medicine, Loma Linda, CA 92350

[3]Department of Anesthesiology and Neurosurgery, Loma Linda University School of Medicine, Loma Linda, CA 92350

Chapter Content Submitted for Peer-reviewed Publication

Abstract

In addition to being the leading cause of morbidity and mortality in premature infants, germinal matrix hemorrhage (GMH) is also the leading cause of acquired infantile hydrocephalus. The pathophysiology of post-hemorrhagic hydrocephalus development after GMH is complex and vaguely understood, although evidence suggests fibrosis and gliosis in the periventricular and subarachnoid spaces disrupts normal cerebrospinal fluid dynamics. Theories explaining general hydrocephalus etiology have substantially evolved from the original bulk flow theory developed by Dr. Dandy over a century ago. Current clinical and experimental evidence supports a new hydrodynamic theory for hydrocephalus development involving redistribution of vascular pulsations and disruption of starling forces in the brain microcirculation. In this review, we discuss cerebrospinal fluid flow dynamics, history and development of theoretical hydrocephalus pathophysiology, and GMH epidemiology and etiology as it relates to post-hemorrhagic hydrocephalus development. We highlight known mechanisms and propose new avenues that will further elucidate GMH pathophysiology, specifically related to hydrocephalus.

Introduction

Germinal matrix hemorrhage (GMH) occurs in approximately 3 live births per 1,000, has a 20-30% mortality rate, and accounts for 1.7% of all neonatal deaths in the United States (Ballabh 2014; Osterman, Kochanek et al. 2015). Premature infants have a much higher rate of occurrence; for infants born before 32 weeks of gestation up to 20%, (about 12,000 infants) develop GMH each year in the US (Kochanek, Kirmeyer et al. 2012). Fortunately, the premature birthrate and percentage of low birthweight (<2500g) infants have steadily declined between 2006 and 2013, although remaining higher than in the 1980s and 1990s. In 2013, the preterm birthrate was 11.39% and the percentage of low birthweight infants was 8.02%. The percentage of very low birthweight (<1500g) was 1.41% in 2013 (Osterman, Kochanek et al. 2015). A study investigating premature infants dating back to 1914 determined median postnatal survival increased from 2 to 26 days, and median gestational age decreased from 33 to 27 weeks. Interestingly, GMH incidence was 4.7% before 1960, but it increased to 50.0% between 1975 and 1980, and then decreased to 12.5% after 2005 (Hefti, Trachtenberg et al. 2015). The introduction of positive pressure ventilation in preterm clinical management after the 1960s increased survival while simultaneously increasing GMH incidence, which may be attributed to cardiorespiratory and hemodynamic instability associated with mechanical ventilation, and the decline in GMH incidence after the 1980s may be attributed to improvements in mechanical ventilation methodology as well as the use of antenatal steroids and surfactant. Despite improving trends in premature birth incidences and outcomes, GMH remains the leading cause of morbidity and mortality in premature and/or very low birthweight infants, and its incidence has remained steady in the past decade.

Premature and very low birthweight infants are prone to hemodynamic and cardiorespiratory instability, leading to abrupt fluctuations in cerebral blood flow (Ballabh 2014). The fetal brain is hypothesized to lack vascular autoregulatory mechanisms to adequately respond to cerebral blood flow fluctuations, although clinical research involving cerebral blood flow monitoring in preterm infants has produced ambiguous results (Tsuji, Saul et al. 2000; Soul, Hammer et al. 2007; du Plessis 2008; Wong, Leung et al. 2008; Caicedo, De Smet et al. 2011; Alderliesten, Lemmers et al. 2013). The germinal matrix layer, which is present in the fetus and matures by term, contains many neuronal and glial precursor cells and is a site of rapid angiogenesis relative to other parts of the brain (Ballabh, Braun et al. 2004; Ballabh, Xu et al. 2007). The germinal neurovascular unit, consisting of neurons, astrocytes, pericytes, vascular smooth muscle cells, and vascular endothelial cells, is deficient in fibronectin at the endothelial basal lamina, glial fibrillary acidic protein at astrocyte end-feed, and pericyte coverage (Ballabh 2010; Ballabh 2014). Thus, the germinal matrix vasculature is inherently weak and vulnerable to hemorrhage under abnormal conditions, regardless if the premature infant brain has autoregulatory mechanisms to adequately respond to cerebral blood flow fluctuations.

GMH severity is graded on an I-IV scale based on the extent and localization of bleeding. Incidence of higher GMH grades (III-IV) increases as gestational age and/or birthweight decreases (Robinson 2012). Between 50-75% of GMH survivors develop long-term neurocognitive sequelae, including cerebral palsy, learning disabilities, psychiatric disorders, and post-hemorrhagic hydrocephalus (PHH), and higher-grade GMH survivors are most vulnerable to worse long-term outcomes (Ballabh 2010; Ballabh

2014). The mortality rate for severe grade (III-IV) GMH is approximately 44%, with 60% of survivors developing PHH and 25% requiring surgical installation of shunts (Vassilyadi, Tataryn et al. 2009). Another study estimates 10% of GMH patients (any grade) and 20% of severe GMH patients (III-IV) will require surgical insertion of permanent shunts (Robinson 2012). Shunt dependency is not desirable, given the large, costly, detrimental complications that occur due to shunt infection, occlusion, and displacement. Additional approaches to manage or prevent PHH include serial lumbar punctures, ventricular taps, external ventricular drainage, ventricular access device, ventricular-subgaleal shunt, endoscopic third ventriculostomy, and endoscopic coagulation of the choroid plexus (Tully and Dobyns 2014). A non-invasive, therapeutic approach towards ameliorating PHH would significantly improve long-term quality of life for GMH patients.

PHH pathophysiology after GMH remains vague and complex, and minimal advancements have been made in its clinical management. In this review, we discuss CSF flow dynamics, particularly focusing on its importance in GMH. We highlight advancements made in hydrocephalus research after Dr. Dandy first proposed the bulk flow theory over a century ago. We discuss the current hydrodynamic theory for hydrocephalus pathophysiology and how it applies to PHH development after GMH. Special attention is given to the neurovascular unit in both the choroidal and glymphatic microcirculation, where CSF is produced and reabsorbed, respectively. We identify gaps in current research and propose avenues for further exploration.

Cerebrospinal Fluid Flow Dynamics

Cerebrospinal fluid (CSF) is an isotonic solution that primarily acts as a mechanical cushion for the brain, although it serves many other physiologically vital functions as well (Chakravarthi 2012). CSF has a lower specific gravity than brain tissue, creating a buoyant force that reduces the effective mass of the brain. CSF [H^+] concentration is detected by central chemoreceptors located at the ventrolateral medullary surface, which help regulate pulmonary ventilation and cerebral blood flow to ensure the brain receives ample oxygen and nutrients. CSF also maintains a stable external environment for growth and development of neurons and glia (Chakravarthi 2012). Importantly, CSF serves as a cerebral lymphatic conduit utilized for removing metabolic waste and transporting neuropeptides, glucose, and lipids (Iliff, Wang et al. 2012; Xie, Kang et al. 2013).

Production

Between 400-600 mL of CSF is produced per day and the brain renews its CSF between 3-4 times within a 24 hour period (Pierce, Lambertsen et al. 1962; Cutler, Page et al. 1968; Sahar 1972; Sato, Bering et al. 1975). CSF is primarily produced by the ependymal lining of the ventricles, which compose the blood-CSF barrier. Ependymal cells of the blood-CSF barrier are interconnected by tight junctions that are variably distributed and leakier than ependymal cells of the blood-brain barrier. Over two thirds of produced CSF originates from the choroid plexus (Pollay 1975; Segal and Pollay 1977). The choroid plexus lines the lateral ventricles from the inferior horns to the interventricular foramen, where it becomes continuous into the third ventricle and

continues into the fourth ventricle. The choroid epithelium protrudes into the ventricles through invaginations of the pia matter containing choroidal capillaries, called *tela choroidea*, which significantly increase the surface area of the choroidal epithelium (Davson and Segal 1970; Keep and Jones 1990; Speake and Brown 2004; Johanson, Stopa et al. 2011). Non-choroidal ependymal cells, brain interstitial fluid, and capillaries may be other CSF sources as well, which is secreted by transependymal seepage into the brain ventricles or transpinal seepage into the subarachnoid space (Pollay and Curl 1967; Davis and Milhorat 1975; Milhorat, Davis et al. 1975; Saunders, Habgood et al. 1999).

The posterior choroidal, anterior choroidal, inferior cerebellar and superior cerebellar arteries supply the choroid plexus of the lateral ventricles, third ventricle, fourth ventricle, and temporal horns, respectively (Milhorat 1978; Sakka, Coll et al. 2011; Chakravarthi 2012). Blood flow to the choroidal epithelium is estimated at 4 - 6 mL / minute / gram tissue, which is significantly greater than blood flow to other brain tissue estimated at 0.9 - 1.8 mL / minute / gram tissue (Maktabi, Heistad et al. 1991). The choroidal interstitial compartment is the region between choroidal capillaries and choroidal ependymal cells. Choroidal capillaries lack tight junction proteins in their endothelial cells, making them more permeable, and blood plasma filtrate passively crosses into the choroidal interstitial compartment from the choroidal capillaries primarily by Starling forces (Wright 1972; Welch 1975). Thus the main source for produced CSF is technically choroidal capillaries, not the choroid plexus itself (Oreskovic and Klarica 2010; Bulat and Klarica 2011; Oreskovic and Klarica 2011). $[Na^+]$ and $[Cl^-]$ from choroidal interstitium are actively exchanged for $[H^+]$ and $[HCO_3^-]$, generated by cytosolic carbonic anhydrase on choroidal ependymal cells, using carrier

proteins in the choroidal ependymal basolateral membrane. Pumps on the choroidal ependymal apical membrane then expel [Na^+], [Cl^-], [K^+], and [HCO_3^-] into the ventricle lumen, which generates an osmotic pressure (Pollay 1975; Spector and Johanson 1989; Keep and Jones 1990). Water flows down the created osmotic gradient with the help of aquaporin 1 on the choroidal ependymal apical membrane (Reiber 2003). The CSF contains higher concentrations of [Na^+], [Mg^{2+}], and [Cl^-] than blood plasma but less [Ca^{2+}], [K^+], [HCO_3^-], [PO_4^+], protein (contains 0.3% plasma proteins), amino acids, and glucose (Felgenhauer 1974).

The choroidal epithelium can alter CSF secretion in response to multiple factors and mechanisms. Most regulatory mechanisms target membrane transporters, carbonic anhydrase, and aquaporins (Faraci, Mayhan et al. 1990; Sakka, Coll et al. 2011). The NaK2Cl cotransporter, located on the choroidal ependymal apical membrane, helps regulate CSF composition and secretion by its bi-directional transport ability. Arginine vasopressin, atrial natriuretic peptide, serotonin, melatonin, and dopamine receptors are located on choroidal epithelium. Arginine vasopressin and atrial natriuretic peptide decrease CSF secretion. CSF secretion can also be increased by sympathetic innervation and decreased by cholinergic innervation (Chakravarthi 2012). Pharmaceutical drugs that inhibit carbonic anhydrase or sodium transporters, such as diuretics, reduce CSF production, while drugs that augment cerebral blood flow tend to increase CSF production. Increased intracranial pressure also tends to decrease CSF production, although evidence suggests CSF production tends to remain constant despite large increases in hydrostatic pressure (Sakka, Coll et al. 2011).

Circulation

CSF flows from the sites of secretion at the choroidal epithelium to the sites of absorption in the subarachnoid space. The mean CSF volume within the brain is 150 mL, with 25 mL in the ventricles and 125 mL in the subarachnoid space (Sakka, Coll et al. 2011). Generally, CSF flows from the lateral ventricles, passes through the interventricular foramen of Monro into the third ventricle, and finally passes into the cerebral aqueduct of Sylvius into the fourth ventricle. From the fourth ventricle, CSF enters through three openings, the lateral apertures of Lushka and median aperture of Magendie, into the subarachnoid space where it is absorbed. A portion of the CSF exits the cranium through arachnoid villi and cranial nerves while the remainder enters along the spinal cord and exit through spinal nerve roots (Dichiro 1964; Milhorat 1976; Chakravarthi 2012).

CSF circulates through the brain's ventricular system and spinal cord in a pulsatile manner. Cerebral arterial pulse waves are the primary drivers of CSF circulation, although jugular venous pressure, respiratory waves, and even physical activity play minor roles as well (Post, Allen et al. 1974; Williams 1976). CSF flow, however, is very slow and sometimes occurs bi-directionally through ventricle compartments with each cardiac and/or respiratory cycle, but net CSF flow occurs from the lateral ventricles to the subarachnoid space. Additionally, ventricular ependymal cells have cilia that generate current and propel CSF through the brain ventricles. CSF pressure gradients, which are generated by continuous CSF secretion and arterial pulsations, are also important for maintaining CSF flow. This pressure gradient is particularly important in driving CSF flow through the subarachnoid spaces and venous

sinuses. Indeed, CSF flow across the subarachnoid epithelium is driven by a 6 cm H_2O pressure difference between subarachnoid CSF pressure (approximately 15 cm H_2O) and superior sagittal sinus pressure (approximately 9 cm H_2O), and the pressure continues to drop into the jugular vein and systemic venous system (Shulman, Yarnell et al. 1964; Bradley 1970; Sahar, Hochwald et al. 1970; Milhorat 1975).

Reabsorption

Conventionally CSF is reabsorbed in the subarachnoid space and enters through the dural venous sinuses, where it returns to the internal jugular system (Chakravarthi 2012). Subarachnoid villi, called pacchonian bodies, were originally thought to be the main reabsorption sites (Brierley and Field 1948; Welch and Friedman 1960; Welch 1975), but evidence suggests CSF is mainly reabsorbed by capillaries and cerebral lymphatic channels (Bradbury, Cserr et al. 1981; Zakharov, Papaiconomou et al. 2003; Oreskovic and Klarica 2010; Bulat and Klarica 2011; Oreskovic and Klarica 2011). The vast majority of CSF is reabsorbed at the superior sagittal sinus with the remainder reabsorbed at dural sinusoids in dorsal root nerves. Reabsorption is driven by pressure gradients between the subarachnoid space and venous sinuses as well as Starling forces at the capillaries (Cutler, Page et al. 1968; Zlokovic, Segal et al. 1990; Saunders, Habgood et al. 1999; Pollay 2010). Increased intracranial pressure tends to increase CSF reabsorption, but very high intracranial pressure that persists for a long period of time tends to actually decrease CSF reabsorption, mostly because venous pressure tends to increase with intracranial pressure while the overall pressure gradient diminishes. Some evidence suggests CSF flows along cranial nerves and spinal nerve roots and is

reabsorbed in lymphatic channels (Bradbury, Cserr et al. 1981; Zakharov, Papaiconomou et al. 2003). Indeed, CSF reabsorption in the nasal submucosal lymphatic channels through the cribriform plate, which feed into the cervical lymph nodes, is relatively important (Courtice and Simmonds 1951; Erlich, McComb et al. 1986; Cserr, DePasquale et al. 1992; Kida, Pantazis et al. 1993; Silver, Li et al. 1999; Mollanji, Bozanovic-Sosic et al. 2002). Lymphatic vessels have also been recently characterized surrounding the dural sinuses, which are also connected to cervical lymph nodes, further suggesting the lymphatic system plays an important role in CSF reabsorption (Bradbury, Cserr et al. 1981; Zervas, Liszczak et al. 1982; Zakharov, Papaiconomou et al. 2003). Lymphatic-mediated CSF reabsorption is thought to play a greater role in neonates, since subarachnoid granulations are more sparsely distributed.

While the central nervous system lacks a conventional lymphatic system, evidence suggests the presence of a functional waste clearance pathway involving exchange between CSF and interstitial fluid, occurring mostly within perivascular Virchow-Robin spaces in the brain parenchyma (Iliff, Wang et al. 2012; Iliff and Nedergaard 2013; Jessen, Munk et al. 2015). This exchange system is called the glymphatic system for its lymphatic-like function and dependence upon glial cells (Figure 1.1). Cerebral arteries at the cortical surface extend into pial arteries running through the subarachnoid space and subpial space, which turn into arterioles surrounded by astrocyte end-feet as they run deeper into the brain parenchyma. The Virchow-Robin space is the CSF containing perivascular space between the astrocyte end-feet and arteriole, with both walls lined by a leptomeningeal cell layer (Zhang, Inman et al. 1990; Kulik, Kusano et al. 2008; Zlokovic 2011; Prince and Ahn 2013). Virchow-Robin spaces

along veins lack this leptomeningeal cell layer. Arteriole Virchow-Robin spaces become continuous with the basal lamina, which has minimal resistance to CSF flow due to its loosely structured extracellular matrix (ECM). CSF flows along arteriole Virchow-Robin space, through basal lamina surrounding capillaries, and exits through the venous Virchow-Robin space. Arterial pulsation is the main force driving perivascular fluid bulk movement from the subarachnoid space into the Virchow-Robin spaces; although respiration, slow vasomotion, and CSF pressure gradients play minor roles too (Iliff, Wang et al. 2012; Iliff and Nedergaard 2013; Jessen, Munk et al. 2015). Astrocyte end-feet have high expression of aquaporin 4 and are important for CSF exchange with interstitial fluid, since astrocyte end-feet surround perivascular spaces and drive convective interstitial fluid fluxes from periarterial to perivenous spaces. Interstitial fluid then drains into cervical lymph channels from perivenous spaces (Johnston, Zakharov et al. 2004; Murtha, Yang et al. 2014).

The glymphatic system is particularly important for distributing nutrients, such as glucose and lipids, as well as for removing soluble proteins and metabolites from the brain (Rangroo Thrane, Thrane et al. 2013). Glymphatic-mediated exchange is greatest during sleep, which is thought to be important for removing metabolic waste during the resting state (Xie, Kang et al. 2013). In rodent models of Alzheimer's disease, glymphatic-mediated exchange was reduced by 65% in aquaporin 4 knockout mice, resulting in increased accumulation of β-amyloid plaques (Iliff, Wang et al. 2012). In a mouse repeated traumatic brain injury model, glymphatic exchange was reduced at 24 hours after the last injury and persisted for up to 4 weeks, which was attributed to gliosis (Plog, Dashnaw et al. 2015). Furthermore, the glymphatic system was significantly

impaired after subarachnoid hemorrhage, due to blood clots occluding perivascular spaces, and during ischemic stroke, due to reduced arterial pulsations (Gaberel, Gakuba et al. 2014). More research is further elucidating the pathophysiological role the glymphatic system plays in multiple neurodegenerative diseases and injuries, and this system may be particularly important in neonatal GMH and consequent PHH pathophysiology due to the role it plays in CSF dynamics.

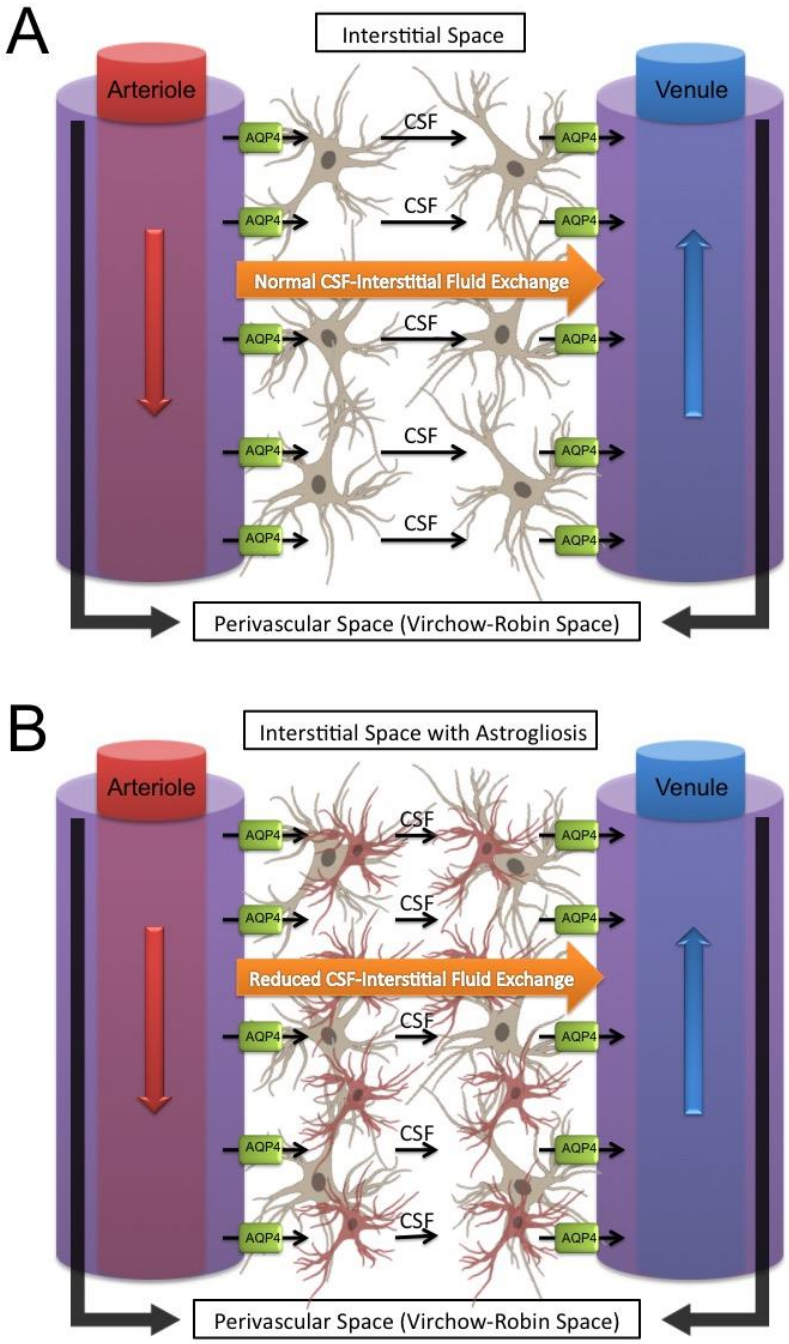

Figure 1.1: Overview of the glymphatic system. Cerebrospinal fluid enters within para-arterial Virchow-Robin spaces in the brain parenchyma and an astroglia-mediated mechanism exchanges cerebrospinal fluid with interstitial fluid and flushes wastes out within para-venous Virchow-Robin spaces (A). Astrogliosis (B) from brain injury possibly disrupts this astroglia-dependent mechanism.

Hydrocephalus

The International Hydrocephalus Imaging Working Group defines hydrocephalus as “an active distension of the ventricular system resulting from inadequate passage of cerebrospinal fluid from its point of production within the cerebral ventricles to its point of absorption into the systemic circulation” (Rekate 2008). Clinical consequences can include increased intracranial pressure, seizures, mental deterioration, and tunnel vision. Most treatments involve surgical implantation of shunts that divert CSF from the brain or surgery, if possible, to repair any malformations that contribute towards hydrocephalus development (Kahle, Kulkarni et al. 2015). Dr. Dandy and Dr. Blackfan classified hydrocephalus into communicating and non-communicating hydrocephalus in 1914 after inducing hydrocephalus in dogs by obstructing the foramen of Monro (Dandy 1914). They proposed the bulk flow theory, which states that CSF flows in bulk from the sites of production in the ventricles to the sites of reabsorption in the subarachnoid space. Hydrocephalus, according to bulk flow theory, had to result from an imbalance in CSF production and absorption. Using the same conceptual framework, Dr. Russell proposed a more specific classification of hydrocephalus in 1949 into non-obstructive and obstructive hydrocephalus, which corresponds to communicating and non-communicating hydrocephalus, respectively (Russell 1949). The original terms proposed by Dr. Dandy, however, remain the most pervasively utilized. Advancements involving CSF tracers and imaging technology, however, has produced evidence challenging the bulk flow theory (Symss and Oi 2013). New hydrocephalus classifications have been proposed based on more recent experimental and clinical evidence, which will be discussed.

Non-communicating Hydrocephalus

Hydrocephalus resulting from an obstruction of CSF flow through ventricular and subarachnoid spaces is called non-communicating hydrocephalus, also known as obstructive hydrocephalus (McAllister 2012; Kahle, Kulkarni et al. 2015). Non-communicating hydrocephalus is typically caused by congenital cerebral malformations. Arnold-Chiari malformation, which is the displacement of the cerebellar tonsils through the foramen magnum, often obstructs the fourth ventricle, leading to dilation of the lateral ventricles and cerebral aqueduct (Gardner 1965). Dandy-Walker malformations, characterized by the absence of the cerebellar vermis, often obstruct the foramina of Luschka and foramen of Magendie, resulting in prominent dilation of the fourth ventricle (Hirsch, Pierre-Kahn et al. 1984). Colloid cysts may obstruct the Foramen of Monro, resulting in lateral ventricular dilation (Camacho, Abernathey et al. 1989). Other lesions may cause abhorrent narrowing of the aqueduct of Sylvius, called aqueductal stenosis, resulting in third and lateral ventricular dilation.

Communicating Hydrocephalus

Communicating hydrocephalus is impaired CSF reabsorption in the absence of any obstruction to CSF flow through the ventricles and subarachnoid spaces (McAllister 2012; Kahle, Kulkarni et al. 2015). Communicating hydrocephalus was believed to primarily result from impaired arachnoid granulations, resulting in reduced reabsorption of CSF. Indeed, cerebral malformations resulting in the absence of arachnoid villi has resulted in hydrocephalus development (Gutierrez, Friede et al. 1975). Subarachnoid hemorrhage and intraventricular hemorrhage, which induce inflammation and glial

scarring in the subarachnoid space, can cause communicating hydrocephalus as well (Korobkin 1975; Vassilouthis and Richardson 1979). Accumulating evidence, however, challenges the presumption that CSF is mostly absorbed by subarachnoid villi (Greitz 2004; Oreskovic and Klarica 2011). Normal pressure hydrocephalus is a form of communicating hydrocephalus that results in ventriculomegaly without increased CSF pressure. CSF pressure readings are within normal range because ventricular dilation compensates for accumulated CSF in the ventricles, thus increased CSF pressure is compensated by increased ventricular volume in this pressure-volume compensatory relationship (Black and Ingraham 2008). In general, the elderly population is most vulnerable to normal pressure hydrocephalus, and causes are either idiopathic or related to other central nervous system diseases and injuries, particularly subarachnoid hemorrhaging. Hydrocephalus ex vacuo is different from normal pressure hydrocephalus because ventricular dilation results from brain tissue atrophy, usually due to a neurodegenerative disorder, and not as a compensatory mechanism for increased CSF pressure (Rekate 2009). Normal pressure hydrocephalus, however, contradicts bulk flow theory, because the ventricles should not dilate without increased mean CSF pressure.

Current Hydrodynamic Theory

Although bulk flow theory is congruent with non-communicating hydrocephalus development, when a ventricular obstruction creates back pressure that dilates the ventricles preceding the obstruction, it is incongruent with communicating hydrocephalus, because the apparent obstruction is within the subarachnoid space, which does not dilate or increase in volume (Greitz 2004; Oreskovic and Klarica 2011). In 1914,

Dr. Weed injected Prussian blue into the ventricles of dog and cat brains and found the dye accumulated near pacchonian bodies (Weed 1914). Prussian blue, however, was also found in other brain parenchymal areas, and further research concluded Prussian blue cannot cross pacchonian bodies under normal conditions (Symss and Oi 2013). Even Dr. Dandy recognized reduced bulk flow across pacchonian bodies should result in subarachnoid CSF pressure being greater than ventricular CSF pressure and the subarachnoid space should expand before the ventricles, neither of which is observed. Dr. Dandy concluded CSF is primarily reabsorbed in the subarachnoid space and quickly enters the circulatory system, based on intrathecal dye injections that rapidly entered the blood and urine (Dandy 1929). The idea that CSF is mostly reabsorbed at pacchonian bodies, however, remained pervasive. In 1960, Dr. Welch reported pacchionian bodies could act as mechanical valves, although future anatomical studies found no mechanical valve presence (Welch and Friedman 1960). Dr. Di Chiro started experimenting with radionuclide cisternography and, in 1966, suggested CSF was reabsorbed at pacchionian bodies because radionuclide accumulated there after 24 hours (Di Chiro 1966). Future studies, however, challenged this conclusion since other radionuclides enter the circulatory system within minutes and most are reabsorbed in the spinal canal (Greitz 1993; Greitz and Hannerz 1996; Greitz, Greitz et al. 1997). Furthermore, sites where radionuclides accumulate after a long period of time may indicate sites where CSF reabsorption is actually very limited. A radionuclide cisternography study in patients with venous vasculitis and high intracranial pressure, performed by Dr. Greitz and Dr. Hannerz in 1996, found no tracer in vessel outlets near capillary beds of pacchonnian bodies, providing evidence for an alternative site of CSF reabsorption (Greitz and

Hannerz 1996). Another major issue is pacchonian bodies are absent in infants and young children, suggesting CSF must be reabsorbed by a different mechanism (Papaiconomou, Bozanovic-Sosic et al. 2002).

Some scientists investigated if abnormal vascular and CSF pulsations may be the root cause for communicating hydrocephalus. In 1943, after observing normal pressure hydrocephalus patients and noting inconsistencies with the bulk flow theory, Dr. O'Connell proposed communicating hydrocephalus may result from increased ventricular pulse pressure (O'Connell 1943). Dr. Bering provided experimental evidence in 1962 that choroid plexus pulsations deliver the means for ventricular enlargement instead of increased mean CSF pressure (Bering 1962). Dr. Bering used a kaolin-induced hydrocephalic dog model and excised the choroid plexus from one lateral ventricle, which resulted in asymmetric ventricular dilation. Increased mean CSF pressure, therefore, could not account for asymmetric ventricular dilation. Dr. Di Rocci provided additional experimental evidence in 1978 in which extreme ventricular pulsation, caused by inflating and deflating a microballon inserted into the lateral ventricles, can produce hydrocephalic ventricular dilation in sheep (Di Rocco, Pettorossi et al. 1978). Concurrently, Dr. Guinane in 1977 produced olfactory ventricular dilation, which lacks a choroid plexus, in rabbits by obstructing surrounding subarachnoid spaces with silicone rubber (Guinane 1977). The silicone rubber obstruction decreased subarachnoid arterial and venous compliance as well as increased capillary pulsations. Increased capillary pulsations, therefore, had to generate the force necessary for the observed ventricular dilation. Using magnetic resonance imaging and radionuclide cisternography, Dr. Greitz reported in the early to mid-1990s arterial pulsation and expansion provides the force

necessary for CSF pulsatile circulation in both the brain and spinal cord, and arterial compliance is important for keeping capillary and venous pulsation low (Greitz 1993; Greitz and Hannerz 1996; Greitz, Greitz et al. 1997; Greitz 2004).

According to bulk flow theory in which CSF malabsorption is a causative factor for communicating hydrocephalus, the subarachnoid CSF-venous pressure gradient would increase, the subarachnoid space would expand, and the ventricles would dilate after subarachnoid space compliance is at maximum. In actuality, the subarachnoid space is smaller, and the subarachnoid CSF-venous pressure gradient is diminished, although both the subarachnoid CSF pressure and venous pressure increase. In 2002, Dr. Egnor developed a mathematical model of communicating hydrocephalus caused by a redistribution of CSF pulsations in the brain (Egnor, Zheng et al. 2002). Decreased intracranial compliance causes abnormal distribution of vascular pulsations, such that arterial pulsations are weaker while capillary and venous pulsations are stronger, and stronger pulsations reach the ventricles while weaker pulsations reach the subarachnoid space. Thus, this vascular pulsation redistribution causes the ventricles to expand at the expense of the subarachnoid space and decreases the subarachnoid CSF-venous pressure gradient. Dr. Edgor's model, based on alternating current electric circuitry, accounted for experimentally and clinically observed CSF malabsorption, increased resistive index, ventricular dilation, intracranial pressure waves, reduced cerebral blood flow, and diminished CSF-venous pressure gradient. Dr. Greitz elaborated on this concept in 2004 in his discussion of hydrodynamic theory of chronic hydrocephalus development. Reduced intracranial compliance causes decreased arterial pulsations and increased compensatory capillary pulsations, generating transmantle pulsatile stress responsible for

hydrocephalus. CSF malabsorption, therefore, is not a causative factor of communicating hydrocephalus but an effect from vascular pulsatile redistribution (Greitz 2004). Dr. Oreskovic further suggests that disruption of Starling forces in the brain parenchymal microvasculature lead to an imbalance in interstitial fluid and CSF exchange, contributing to hydrocephalus development (Oreskovic and Klarica 2011).

In light of our increased understanding of hydrocephalus pathophysiology, Dr. Oi and Dr. Di Rocco proposed a new classification based on the involved pathway: major pathway hydrocephalus and minor pathway hydrocephalus (Oi and Di Rocco 2006). Major pathway hydrocephalus accounts for CSF circulation disruption from the ventricles to the subarachnoid spaces. Major pathway hydrocephalus encompasses most obstructive / non-communicating hydrocephalus cases. Minor pathway hydrocephalus accounts for disruptions in CSF circulation within the subarachnoid space and brain parenchyma. Evidence suggests this pathway is very important for CSF reabsorption in the embryo, fetus, and infants, making it critical for infantile hydrocephalus development (Papaiconomou, Bozanovic-Sosic et al. 2002). Minor pathway hydrocephalus is disruption of CSF flow and reabsorption in newly elucidated channels in the brain parenchyma, which involve deep vascular structures and lymphatic channels (Figure 1.2). Dr. Nedergaard further characterized this pathway in rodents using in vivo two photon imaging and coined the term “glymphatic system”, since this functional waste clearance pathway involves astroglia and lymphatic-like paravascular channels (Iliff, Wang et al. 2012). CSF enters from the subarachnoid space into paravascular artery channels and exchanges with interstitial fluid, which is cleared through paravascular veins. Additional lymphatic channels lining the dural sinuses and meningeal arteries were characterized by

Dr. Louveaue and Dr. Aspelund (Aspelund, Antila et al. 2015; Louveau, Smirnov et al. 2015). These lymphatic vessels connect the meningeal compartment with the glymphatic system. As the cerebral glymphatic / lymphatic systems are further characterized, more research is warranted on their potential pathophysiological roles played in hydrocephalus development.

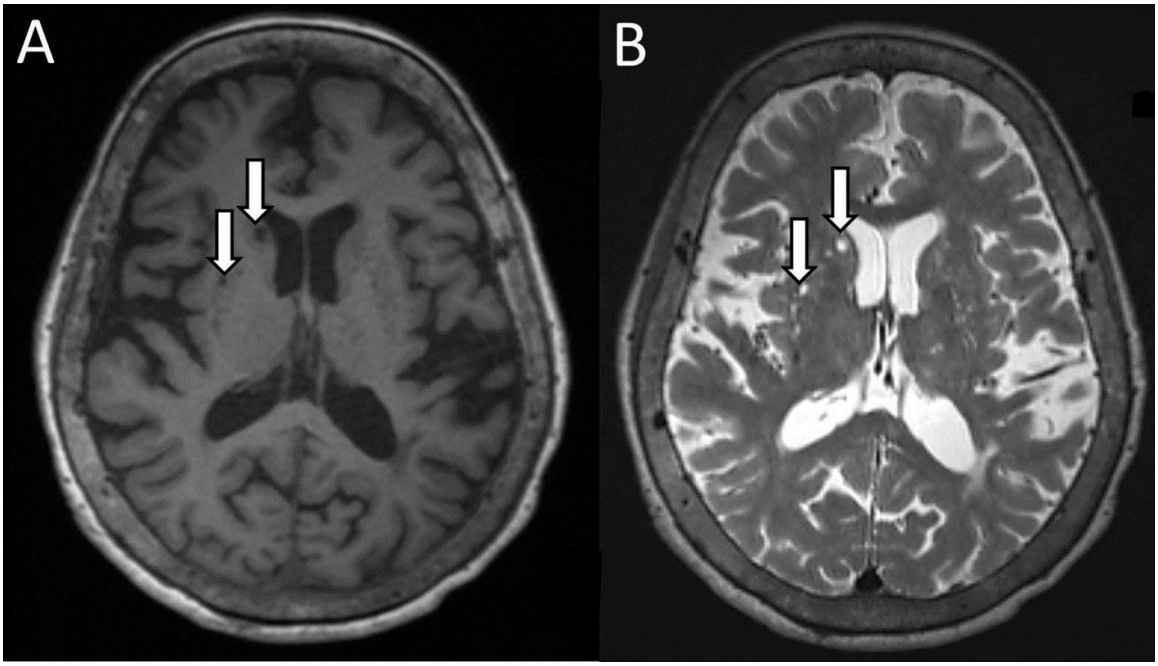

Figure 1.2: Paravascular Virchow-Robin spaces depicted on MRI. Axial non-contrasted brain MRI demonstrating perivascular spaces (arrows) that appear hypointense to brain tissue and isointense to CSF in T1-weighted (A) and T2-weighted (B) sequences.

Post-hemorrhagic Hydrocephalus Pathophysiology and Potential Mechanisms

PHH is a common debilitating consequence of severe grade GMH, and the mechanisms contributing to PHH development remain to be elucidated. Cerebroventricular expansion leads to mechanical compression of surrounding brain tissue, causing injury and consequent neurological deficits in patients surviving the initial bleed (Robinson 2012). PHH was commonly theorized to be caused by blood clots obstructing the cerebral aqueduct or formanina of Luschka and Magendie or by microthrombi obstructing small CSF outflow passages in the subarachnoid space. Much evidence suggests a variety of inter-related pathophysiological mechanisms that potentially alter normal CSF dynamics play significant roles in PHH development as well (Strahle, Garton et al. 2012; Whitelaw and Aquilina 2012; Tang, Tao et al. 2016). Applying concepts in current hydrocephalus theory towards PHH development after GMH may better illuminate potential mechanisms for therapeutic intervention (Figure 1.3).

Blood Clots, Hemoglobin, and Iron

Non-communicating / obstructive PHH may result from cerebroventricular blood clots and microthrombi directly impairing CSF circulation and absorption by obstructing the cerebral aqueduct, formanina of Luschka and Magendia, and subarachnoid CSF outflow passages. Subsequently, it was hypothesized intraventricular fibrinolytic therapy would remove cerebroventricular blood clots and reduce PHH incidence (Whitelaw and Aquilina 2012). In an adult intraventricular hemorrhage dog model, in which intraventricular blood injection resulted in 80% of dogs developing PHH, intraventricular

urokinase injection reduced PHH incidence to 10% (Pang, Sclabassi et al. 1986). Clinical investigations of intraventricular streptokinase, urokinase, or tissue plasminogen activator injections after GMH, however, concluded fibrinolytic therapy did not improve long-term dependence on ventriculo-peritoneal shunts (Whitelaw 1993). Thus, cerebroventricular obstruction from thrombi may play only a minor role in long-term PHH development.

Although intraventricular fibrinolytic therapy failed to improve clinical PHH outcomes, evidence suggests hemoglobin and iron may play an important role in PHH development (Strahle, Garton et al. 2014). Erythrocyte lysis after hemorrhage, typically from complement activation and consequent membrane attack complex formation, releases hemoglobin and iron into surrounding brain tissue. Experimental adult cerebral hemorrhage models conclude hemoglobin metabolites and iron contributes towards brain edema (Chen, Gao et al. 2011). Hemoglobin metabolites were also found in the CSF of rabbit pups with intraventricular hemorrhage, and iron was elevated in the CSF of preterm infants with PHH (Savman, Nilsson et al. 2001; Lee, Keep et al. 2010). Intraventricular injection of hemoglobin or iron into neonatal rat pups also resulted in significant acute ventricular dilation (Strahle, Garton et al. 2014). Additionally, acute and delayed iron chelation by Deferoxamine reduced long-term PHH development in neonatal rats after GMH (Klebe, Krafft et al. 2014). Iron, thus, is a quintessential player in PHH formation, although the exact mechanisms remain unclear.

Gene deletion studies determined iron transport and iron-dependent metabolic proteins are highly expressed in the ependymal lining compared to other brain tissue (Keep and Smith 2011). Thus, the ependymal lining may be adversely affected from iron overload due to GMH. Indeed, ependymal cells are theorized to prevent iron diffusion

into the brain parenchyma by up-taking it from the CSF (Moos 2002). Additionally, iron overload has been associated with increased expression of aquaporin 4 in adult rats with cerebral hemorrhage, and Deferoxamine treatment reduced aquaporin 4 expression (Qing, Dong et al. 2009). Iron, thus, may regulate expression of ependymal ion and water channels, such as aquaporin 4, and contribute towards PHH by altering CSF production dynamics at the ependymal layer. It should be noted, however, that diuretic treatments targeting ependymal channels were evaluated in clinical trials of preterm GMH patients and determined to have no clinical benefit. More research is needed to further elucidate iron's pathophysiological role in development of hydrocephalus.

Inflammation, Fibrosis, and Gliosis

Inflammation has been associated with subependymal gliosis, fibrosing arachnoiditis, and meningeal fibrosis after GMH (Cherian, Whitelaw et al. 2004; Oi and Di Rocco 2006). GMH patients also have increased expression levels of inflammatory markers in their CSF, including TNF-α (Savman, Blennow et al. 2002). Vessel rupture results in blood and serum components entering the brain parenchyma. Resident immune cells, namely microglia, are activated by stimulating toll-like receptors and nod-like receptors with damage-associated molecular patterns, molecules that induce a non-infectious inflammatory response (Klebe, McBride et al. 2015). Activated microglia secrete pro-inflammatory cytokines, extracellular proteases, and oxidative species, which damage surrounding tissue and recruit leukocytes that exacerbate inflammation (Chen, Yang et al. 2015; Yang, Salayandia et al. 2015). In neonatal rat pups with GMH, microglia proliferation was observed in the perihematoma region, microglia activation

was associated with phosphorylated ERK, and modulating microglia activation with minocycline or cannabinoid receptor 2 agonist ameliorate inflammation and improved outcomes (Tang, Chen et al. 2015; Tang, Tao et al. 2015). Interestingly, microglia may play an important role in hematoma resolution, since stimulating PPARγ improved short-term hematoma resolution, which was dependent upon CD36 scavenger receptor and was associated with inducing the alternatively activated M2 microglia/macrophage phenotype (Flores, Klebe et al. 2016).

Fibrosis is the forming of excess connective tissue as a consequence of a reparative process after inflammation (Birbrair, Zhang et al. 2014). Excess fibrous tissue formation may disrupt the normal functioning of surrounding tissue. Multiple factors trigger fibrosis after GMH. Thrombin, which is significantly active up to 10 days after GMH in neonatal rats, cleaves fibrinogen into fibrin to form fibrin clots, activates the complement pathway to augment inflammation, and stimulates protease-activated receptors (PARs), a family of G protein-coupled receptors (Luo, Wang et al. 2007; Babu, Bagley et al. 2012; Lekic, Klebe et al. 2015). PAR stimulation has been associated with fibrosis in several tissues, including liver, renal, pulmonary, and cardiac tissues. PAR stimulation upregulates mammalian target of rapamycin (mTOR), which is associated with ECM protein proliferation. Additionally, PAR stimulation exacerbates inflammation by upregulating cyclo-oxygenase 1 and 2 activity (Kataoka, Hamilton et al. 2003; Steinhoff, Buddenkotte et al. 2005; Luo, Wang et al. 2007). Phosphorylated mTOR and cyclo-oxygenase 2 levels were increased by 72 hours after GMH in rats, which were both reduced by combinatorial PAR-1,4 inhibitor administration (Lekic, Klebe et al. 2015). ECM proteins are theorized to deposit within the cerebroventricular system, similar to

blood clots and microthrombi (Strahle, Garton et al. 2012; Bowen, Jenkins et al. 2013; Tang, Tao et al. 2016). ECM protein overproduction, therefore, may obstruct normal CSF flow pathways. Indeed, fibronectin and vitronectin expression levels are significantly increased in GMH rats with long-term PHH (Klebe, Krafft et al. 2014; Manaenko, Lekic et al. 2014). Inhibiting mTOR with rapamycin and inhibiting cyclo-oxygenase 2 activity ameliorated long-term PHH and neurocognitive deficits in GMH rats, although expression levels of ECM proteins was not determined in this study (Lekic, Klebe et al. 2015).

TGF-β stimulates mesenchymal stem cells and fibroblasts, which produce ECM matrix proteins and deposit connective tissue (Bowen, Jenkins et al. 2013). TGF-β can be secreted from activated microglia, and TGF-β secretion can be induced by thrombin (Schuliga 2015). ECM production induced by TGF-β stimulation may deposit in the cerebroventricular system, disrupting CSF dynamics (Tada, Kanaji et al. 1994). A rabbit pup GMH model indicated TGF-β, fibronectin, and laminin expression levels were significantly increased in the ependymal and subependyma tissue after GMH (Cherian, Thoresen et al. 2004). Mice with transgenic TGF-β overexpression developed hydrocephalus with higher expression of ECM proteins in the brain than wild-types (Wyss-Coray, Feng et al. 1995). In a clinical study, increased TGF-β1 and ECM protein expression in the CSF were associated with PHH development in preterm infants (Aquilina, Chakkarapani et al. 2012; Douglas-Escobar and Weiss 2012). The TGF-β1 isoform is most associated with PHH after IVH in neonates and adults (Gomes, Sousa Vde et al. 2005). Intrathecal TGF-β1 injection in mice resulted in hydrocephalus development, and TGF-β1 expression was significantly increased in brains of neonatal

rats with PHVD after intraventricular blood injection (Tada, Kanaji et al. 1994; Cherian, Thoresen et al. 2004). Indeed, TGF-β1 was elevated in both animal models and premature infants with PHH, although some studies dispute this (Heep, Stoffel-Wagner et al. 2004). In a rat GMH model, TGF-β1 was elevated within hours after GMH, but normalized by 24 hours post-ictus (Tang, Chen et al. 2015). Additionally, inhibiting TGF-β1 ameliorated long-term PHH and neurocognitive deficits as well as reduced vitronectin and GFAP expression in rats (Manaenko, Lekic et al. 2014). Although the mechanism of TGF-β signaling after GMH and its association with PHH development has been established, studies are lacking that discern the changes to CSF dynamics as a consequence of TGF-β signaling and fibrosis.

Gliosis results from damage to the central nervous system and is characterized by the nonspecific reactive proliferation of astrocytes, microglia, and oligodendrocytes (Sofroniew 2009). Hydrocephalus development is also associated with neuroinflammation and reactive gliosis (Del Bigio, Wilson et al. 2003; Deren, Forsyth et al. 2009). Gliosis was observed in cerebral cortical biopsies from hydrocephalic children with shunts (Glees and Hasan 1990). Increased expression of Iba-1 and GFAP, markers for microglia and astrocytes respectively, were also observed in the brains of neonatal rats with hydrocephalus (Deren, Packer et al. 2010). Reactive gliosis in the subarachnoid space was associated with hydrocephalus development after subarachnoid hemorrhage in rats. In an IVH rat model, long-term GFAP expression is markedly increased, and injection of umbilical cord blood-derived mesenchymal stem cells reduced GFAP expression as well as long-term PHH development (Ahn, Chang et al. 2013). Aquaporin 4 knockout mice more rapidly developed hydrocephalus after kaolin injection, although

increased aquaporin 4 expression is observed in hydrocephalus too (Bloch, Auguste et al. 2006; Mao, Enno et al. 2006). Aquaporin 1 is expressed on the choroid plexus apical membrane and aquaporin 1 knockout mice had decreased CSF production (Oshio, Watanabe et al. 2005). Given the important role astrocytes play in the blood-brain and blood-CSF barrier functions as well as in glymphatic mediated CSF-interstitial fluid exchange, gliosis may have a profound effect on CSF dynamics and PHH development, which warrants further investigation.

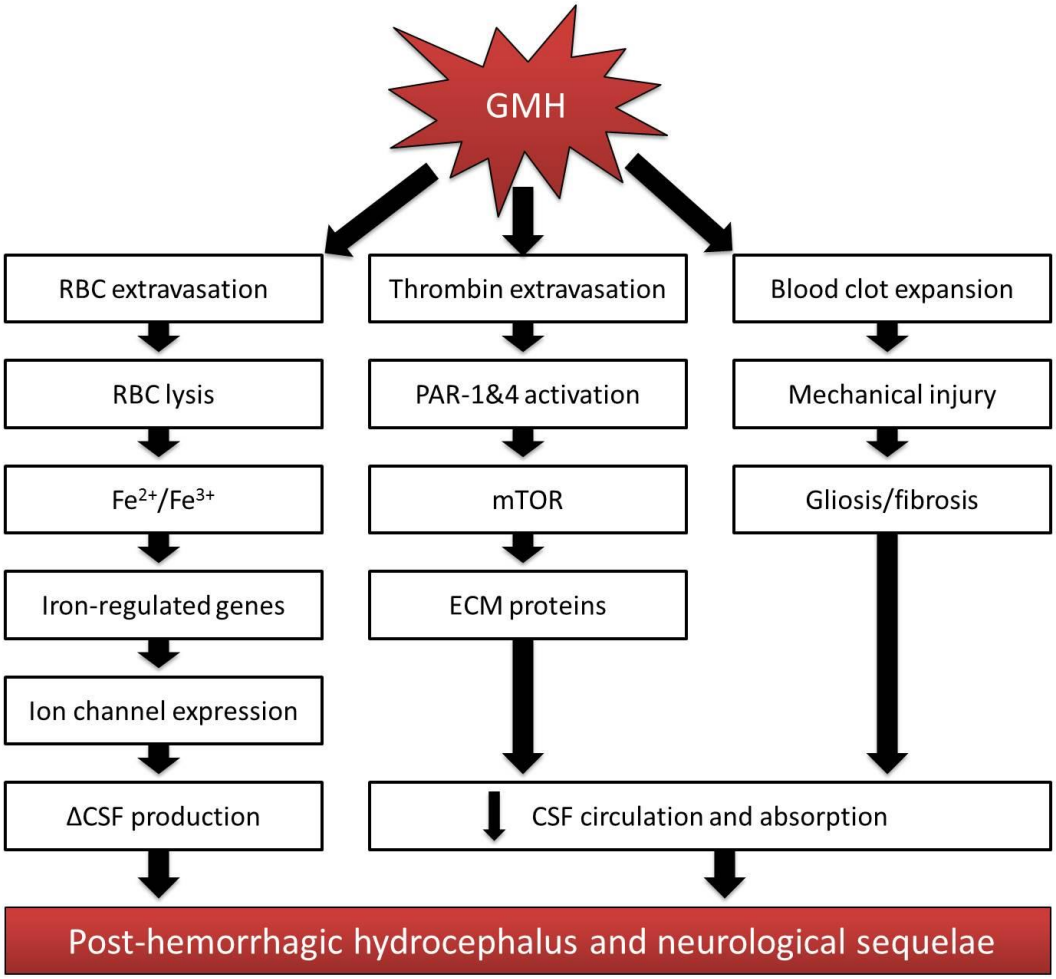

Figure 1.3: Summary of GMH Pathophysiological Pathways. Know pathways and potential mechanisms disrupting cerebrospinal fluid dynamics and contributing to post-hemorrhagic hydrocephalus development after germinal matrix hemorrhage**.**

Conclusions

Our understanding of hydrocephalus has changed significantly since Dr. Dandy's first experiments in the early 20th century and the bulk flow theory was proposal. The source for CSF production is choroidal and ependymal capillaries, and the source for CSF reabsorption are subarachnoid and parenchymal capillaries as well as perivascular channels following glymphatic mediated CSF-interstitial fluid exchange. The current hydrodynamic theory suggests hydrocephalus develops from disruptions in hydrostatic and osmotic pressures in the brain microvasculature as well as disruptions in vascular pulsatile distribution due to alterations in overall brain compliance. Our purpose is to reconcile our knowledge of GMH and PHH development with the current hydrodynamic theory of hydrocephalus. Indeed, many GMH/IVH studies suggest PHH is a consequence of obstructions within the cerebroventricular system and subarachnoid drainage pathways due to thrombi, gliosis, and fibrosis. In line with current hydrocephalus school of thought, we suggest thrombi, gliosis, and fibrosis after GMH are not merely obstructing CSF passages but are altering barrier dynamics in the microvasculature and ependymal lining, altering CSF dynamics and CSF-interstitial fluid exchange to cause PHH development. Future research should elucidate these potential mechanisms.

Specific Aims

Post-hemorrhagic hydrocephalus is a debilitating consequence of germinal matrix hemorrhage (Ballabh 2010; Heron, Sutton et al. 2010). Thrombin as well as intracerebroventricular blood clots have been identified as causative factors of hydrocephalus formation. Thrombin initiates inflammatory responses, gliosis, and

overproduction of ECM proteins that may permanently obstruct the cerebroventricular system (Xue, Balasubramaniam et al. 2003; Cherian, Whitelaw et al. 2004; Volpe 2009). Thrombin mediates brain injury by activating PARs (Kataoka, Hamilton et al. 2003; Steinhoff, Buddenkotte et al. 2005). PAR stimulation leads to phosphorylation and subsequent activation of mTOR, which is linked to overproduction of ECM proteins that cause impaired CSF circulation and absorption (Paul, Leef et al. 2000; Crews, Wyss-Coray et al. 2004; Del Bigio 2004; Xue and Del Bigio 2005; Ballabh, Xu et al. 2007; Dummula, Vinukonda et al. 2010). Blood clots directly impair CSF circulation and absorption. Previous studies of adult hemorrhagic stroke suggest activation of PPARγ enhances microglial phagocytosis of red blood cells via CD36 scavenger receptor, which results in enhanced clot resolution and improved neurobehavioral outcomes (Zhao, Zhang et al. 2006; Zhao, Sun et al. 2007). Additionally, lysed red blood cells and metabolized hemoglobin releases non-protein bound iron, which mediates brain injury and is associated with PHH development. The objective of this proposal is to characterize the extent of GMH-induced brain injury and evaluate the implications of thrombin, PARs, PPARγ, CD36, and iron in GMH pathophysiology. The long-term goals are to provide non-invasive, therapeutic approaches for GMH patients. The central hypothesis is the inhibition of thrombin or thrombin's downstream effectors PAR-1 and mTOR as well as enhancement of clot and iron clearance via PPARγ and iron chelation respectively reduces GMH-induced hydrocephalus and improves long-term neurological function in rats. The hypothesis will be tested in two specific aims.

Aim 1

Determine the role of PPARγ in clot clearance as well as iron chelation by Deferoxamine after GMH. PPARγ activation will enhance CD36-mediated microglial phagocytosis of red blood cells and, thus, reduce blood clots and subsequent hydrocephalus after GMH. Iron chelation will also improve long-term neurological and brain morphological outcomes after GMH. Aim 1A will investigate the time-course of PPARγ and CD36 expression as well as the time course of hematoma resolution after PPARγ stimulation or inhibition after GMH. Long-term brain morphological and neurological outcomes following PPARγ stimulation or inhibition will also be evaluated. Short-term hematoma resolution from PPARγ stimulation will be reversed by CD36 knockdown. Aim 1B will investigate if acute or delayed iron chelation treatment will improve long-term neurological and brain morphological outcomes as well as reduce ECM protein proliferation after GMH.

Aim 2

Determine the role of activated thrombin/PAR-1/mTOR pathway in GMH induced hydrocephalus. Thrombin activation and stimulation of its downstream receptor, PAR-1, will lead to mTOR activation and consequent ECM overproduction after GMH, resulting in long-term post-hemorrhagic hydrocephalus development and neurological deficits. Aim 2A will investigate the time course of thrombin activation and if combinatorial PAR-1 and PAR-4 inhibition will reduce short-term COX-2 and mTOR activation as well as if COX-2 and mTOR inhibition will improve long-term neurobehavioral and brain morphological outcomes. Aim 2B will investigate if direct

thrombin or PAR-1 inhibition will reduce short-term mTOR activation, improve neurobehavioral and brain morphological outcomes, and reduce long-term ECM protein proliferation. PAR-1 stimulation will attempt to reverse effects from PAR-1 inhibition.

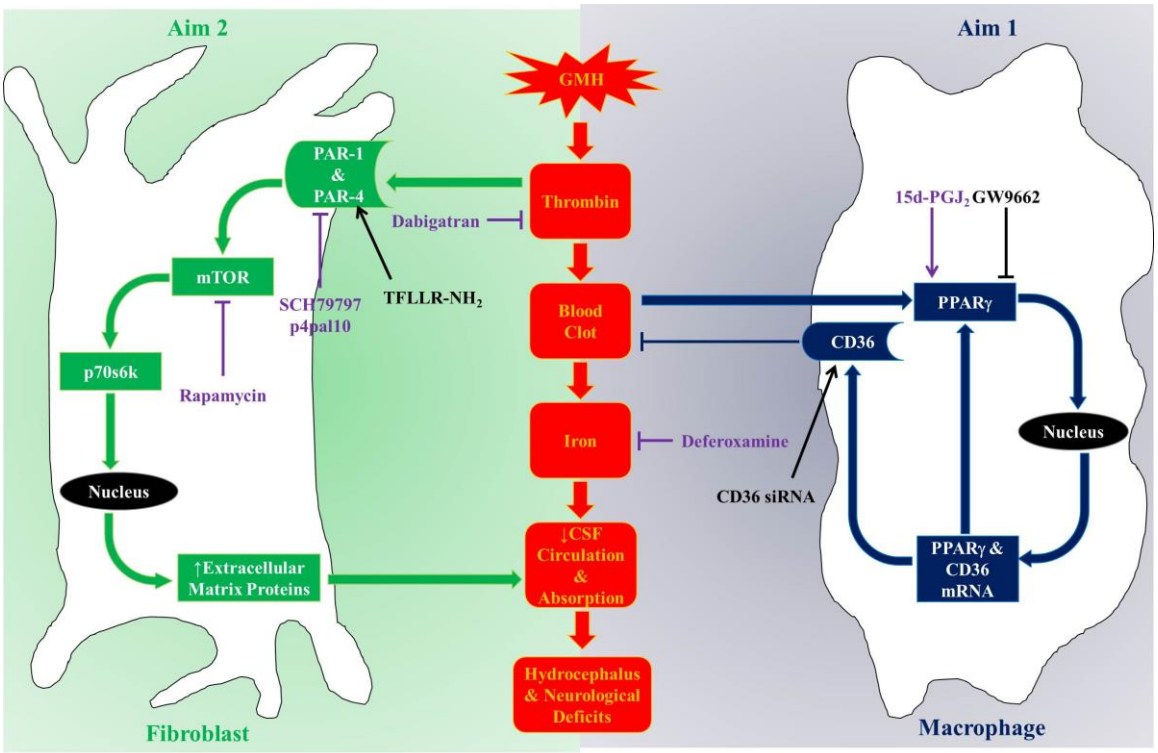

Figure 1.4: Schematic representation of the overall central hypothesis and research aims. Our central hypothesis is thrombin/PAR-1/mTOR pathway inhibition, enhanced PPARγ/CD36 mediated phagocytosis of blood clots, and iron chelation after germinal matrix hemorrhage will ameliorate long-term post-hemorrhagic hydrocephalus and consequent neurofunctional deficits. Aim 1 will investigate PPARγ/CD36 mediated hematoma resolution by microglia/macrophage phagocytosis as well as iron chelation by Deferoxamine. Aim 2 will investigate the thrombin/PAR-1/mTOR pathway and extracellular matrix protein proliferation.

References

Ahn SY, Chang YS, Sung DK, Sung SI, Yoo HS, Lee JH, Oh WI, and Park WS (2013). "Mesenchymal Stem Cells Prevent Hydrocephalus after Severe Intraventricular Hemorrhage." Stroke **44**(2): 497-504.

Alderliesten T, Lemmers PM, Smarius JJ, van de Vosse RE, Baerts W, and van Bel F (2013). "Cerebral Oxygenation, Extraction, and Autoregulation in Very Preterm Infants Who Develop Peri-Intraventricular Hemorrhage." J Pediatr **162**(4): 698-704 e692.

Aquilina K, Chakkarapani E, and Thoresen M (2012). "Early Deterioration of Cerebrospinal Fluid Dynamics in a Neonatal Piglet Model of Intraventricular Hemorrhage and Posthemorrhagic Ventricular Dilation." J Neurosurg Pediatr **10**(6): 529-537.

Aspelund A, Antila S, Proulx ST, Karlsen TV, Karaman S, Detmar M, Wiig H, and Alitalo K (2015). "A Dural Lymphatic Vascular System That Drains Brain Interstitial Fluid and Macromolecules." J Exp Med **212**(7): 991-999.

Babu R, Bagley JH, Di C, Friedman AH, and Adamson C (2012). "Thrombin and Hemin as Central Factors in the Mechanisms of Intracerebral Hemorrhage-Induced Secondary Brain Injury and as Potential Targets for Intervention." Neurosurg Focus **32**(4): E8.

Ballabh P (2010). "Intraventricular Hemorrhage in Premature Infants: Mechanism of Disease." Pediatr Res **67**(1): 1-8.

Ballabh P (2014). "Pathogenesis and Prevention of Intraventricular Hemorrhage." Clin Perinatol **41**(1): 47-67.

Ballabh P, Braun A, and Nedergaard M (2004). "Anatomic Analysis of Blood Vessels in Germinal Matrix, Cerebral Cortex, and White Matter in Developing Infants." Pediatr Res **56**(1): 117-124.

Ballabh P, Xu H, Hu F, Braun A, Smith K, Rivera A, Lou N, Ungvari Z, Goldman SA, Csiszar A, and Nedergaard M (2007). "Angiogenic Inhibition Reduces Germinal Matrix Hemorrhage." Nat Med **13**(4): 477-485.

Bering EA, Jr. (1962). "Circulation of the Cerebrospinal Fluid. Demonstration of the Choroid Plexuses as the Generator of the Force for Flow of Fluid and Ventricular Enlargement." J Neurosurg **19**: 405-413.

Birbrair A, Zhang T, Files DC, Mannava S, Smith T, Wang ZM, Messi ML, Mintz A, and Delbono O (2014). "Type-1 Pericytes Accumulate after Tissue Injury and Produce Collagen in an Organ-Dependent Manner." Stem Cell Res Ther **5**(6): 122.

Black P, and Ingraham FD (2008). "Normal Pressure Hydrocephalus." Progress in Clinical Neurosciences **22**: 289.

Bloch O, Auguste KI, Manley GT, and Verkman AS (2006). "Accelerated Progression of Kaolin-Induced Hydrocephalus in Aquaporin-4-Deficient Mice." J Cereb Blood Flow Metab **26**(12): 1527-1537.

Bowen T, Jenkins RH, and Fraser DJ (2013). "Micrornas, Transforming Growth Factor Beta-1, and Tissue Fibrosis." J Pathol **229**(2): 274-285.

Bradbury MW, Cserr HF, and Westrop RJ (1981). "Drainage of Cerebral Interstitial Fluid into Deep Cervical Lymph of the Rabbit." Am J Physiol **240**(4): F329-336.

Bradley KC (1970). "Cerebrospinal Fluid Pressure." J Neurol Neurosurg Psychiatry **33**(3): 387-397.

Brierley JB, and Field EJ (1948). "The Connexions of the Spinal Sub-Arachnoid Space with the Lymphatic System." J Anat **82**(3): 153-166.

Bulat M, and Klarica M (2011). "Recent Insights into a New Hydrodynamics of the Cerebrospinal Fluid." Brain Res Rev **65**(2): 99-112.

Caicedo A, De Smet D, Naulaers G, Ameye L, Vanderhaegen J, Lemmers P, Van Bel F, and Van Huffel S (2011). "Cerebral Tissue Oxygenation and Regional Oxygen Saturation Can Be Used to Study Cerebral Autoregulation in Prematurely Born Infants." Pediatr Res **69**(6): 548-553.

Camacho A, Abernathey CD, Kelly PJ, and Laws Jr ER (1989). "Colloid Cysts: Experience with the Management of 84 Cases since the Introduction of Computed Tomography." Neurosurgery **24**(5): 693-700.

Chakravarthi A (2012). "Cerebrospinal Fluid Dynamics." Textbook of Contemporary Neurosurgery (Volumes 1 & 2).

Chen S, Yang Q, Chen G, and Zhang JH (2015). "An Update on Inflammation in the Acute Phase of Intracerebral Hemorrhage." Transl Stroke Res **6**(1): 4-8.

Chen Z, Gao C, Hua Y, Keep RF, Muraszko K, and Xi G (2011). "Role of Iron in Brain Injury after Intraventricular Hemorrhage." Stroke **42**(2): 465-470.

Cherian S, Thoresen M, Silver IA, Whitelaw A, and Love S (2004). "Transforming Growth Factor-Betas in a Rat Model of Neonatal Posthaemorrhagic Hydrocephalus." Neuropathol Appl Neurobiol **30**(6): 585-600.

Cherian S, Whitelaw A, Thoresen M, and Love S (2004). "The Pathogenesis of Neonatal Post-Hemorrhagic Hydrocephalus." Brain Pathol **14**(3): 305-311.

Courtice FC, and Simmonds WJ (1951). "The Removal of Protein from the Subarachnoid Space." Aust J Exp Biol Med Sci **29**(4): 255-263.

Crews L, Wyss-Coray T, and Masliah E (2004). "Insights into the Pathogenesis of Hydrocephalus from Transgenic and Experimental Animal Models." Brain Pathol **14**(3): 312-316.

Cserr HF, DePasquale M, Harling-Berg CJ, Park JT, and Knopf PM (1992). "Afferent and Efferent Arms of the Humoral Immune Response to Csf-Administered Albumins in a Rat Model with Normal Blood-Brain Barrier Permeability." J Neuroimmunol **41**(2): 195-202.

Cutler RW, Page L, Galicich J, and Watters GV (1968). "Formation and Absorption of Cerebrospinal Fluid in Man." Brain **91**(4): 707-720.

Dandy WE (1914). "Internal Hydrocephalus. An Experimental, Clinical and Pathological Study." Am J Dis Child **8**: 406-482.

Dandy WE (1929). "Where Is Cerebrospinal Fluid Absorbed?" Journal of the American Medical Association **92**(24): 2012-2014.

Davis DA, and Milhorat TH (1975). "The Blood-Brain Barrier of the Rat Choroid Plexus." Anat Rec **181**(4): 779-789.

Davson H, and Segal MB (1970). "The Effects of Some Inhibitors and Accelerators of Sodium Transport on the Turnover of 22na in the Cerebrospinal Fluid and the Brain." J Physiol **209**(1): 131-153.

Del Bigio MR (2004). "Cellular Damage and Prevention in Childhood Hydrocephalus." Brain Pathol **14**(3): 317-324.

Del Bigio MR, Wilson MJ, and Enno T (2003). "Chronic Hydrocephalus in Rats and Humans: White Matter Loss and Behavior Changes." Ann Neurol **53**(3): 337-346.

Deren KE, Forsyth J, Abdullah O, Hsu EW, Klinge PM, Silverberg GD, Johanson CE, and McAllister JP, 2nd (2009). "Low Levels of Amyloid-Beta and Its Transporters in Neonatal Rats with and without Hydrocephalus." Cerebrospinal Fluid Res **6**: 4.

Deren KE, Packer M, Forsyth J, Milash B, Abdullah OM, Hsu EW, and McAllister JP, 2nd (2010). "Reactive Astrocytosis, Microgliosis and Inflammation in Rats with Neonatal Hydrocephalus." Exp Neurol **226**(1): 110-119.

Di Chiro G (1966). "Observations on the Circulation of the Cerebrospinal Fluid." Acta Radiol Diagn (Stockh) **5**: 988-1002.

Di Rocco C, Pettorossi VE, Caldarelli M, Mancinelli R, and Velardi F (1978). "Communicating Hydrocephalus Induced by Mechanically Increased Amplitude of the Intraventricular Cerebrospinal Fluid Pressure: Experimental Studies." Exp Neurol **59**(1): 40-52.

Dichiro G (1964). "Movement of the Cerebrospinal Fluid in Human Beings." Nature **204**: 290-291.

Douglas-Escobar M, and Weiss MD (2012). "Biomarkers of Brain Injury in the Premature Infant." Front Neurol **3**: 185.

du Plessis AJ (2008). "Cerebrovascular Injury in Premature Infants: Current Understanding and Challenges for Future Prevention." Clin Perinatol **35**(4): 609-641, v.

Dummula K, Vinukonda G, Xu H, Hu F, Zia MT, Braun A, Shi Q, Wolk J, and Ballabh P (2010). "Development of Integrins in the Vasculature of Germinal Matrix, Cerebral Cortex, and White Matter of Fetuses and Premature Infants." J Neurosci Res **88**(6): 1193-1204.

Egnor M, Zheng L, Rosiello A, Gutman F, and Davis R (2002). "A Model of Pulsations in Communicating Hydrocephalus." Pediatr Neurosurg **36**(6): 281-303.

Erlich SS, McComb JG, Hyman S, and Weiss MH (1986). "Ultrastructural Morphology of the Olfactory Pathway for Cerebrospinal Fluid Drainage in the Rabbit." J Neurosurg **64**(3): 466-473.

Faraci FM, Mayhan WG, and Heistad DD (1990). "Effect of Vasopressin on Production of Cerebrospinal Fluid: Possible Role of Vasopressin (V1)-Receptors." Am J Physiol **258**(1 Pt 2): R94-98.

Felgenhauer K (1974). "Protein Size and Cerebrospinal Fluid Composition." Klin Wochenschr **52**(24): 1158-1164.

Flores JJ, Klebe D, Rolland WB, Lekic T, Krafft PR, and Zhang JH (2016). "Ppargamma-Induced Upregulation of Cd36 Enhances Hematoma Resolution and Attenuates Long-Term Neurological Deficits after Germinal Matrix Hemorrhage in Neonatal Rats." Neurobiol Dis **87**: 124-133.

Gaberel T, Gakuba C, Goulay R, Martinez De Lizarrondo S, Hanouz JL, Emery E, Touze E, Vivien D, and Gauberti M (2014). "Impaired Glymphatic Perfusion after Strokes Revealed by Contrast-Enhanced Mri: A New Target for Fibrinolysis?" Stroke **45**(10): 3092-3096.

Gardner W (1965). "Arnold-Chiari Malformation and Hydrocephalus." J. of Neurology, Neurosurgery and Psychiatry **28**: 247.

Glees P, and Hasan M (1990). "Ultrastructure of Human Cerebral Macroglia and Microglia: Maturing and Hydrocephalic Frontal Cortex." Neurosurg Rev **13**(3): 231-242.

Gomes FC, Sousa Vde O, and Romao L (2005). "Emerging Roles for Tgf-Beta1 in Nervous System Development." Int J Dev Neurosci **23**(5): 413-424.

Greitz D (1993). "Cerebrospinal Fluid Circulation and Associated Intracranial Dynamics. A Radiologic Investigation Using Mr Imaging and Radionuclide Cisternography." Acta Radiol Suppl **386**: 1-23.

Greitz D (2004). "Radiological Assessment of Hydrocephalus: New Theories and Implications for Therapy." Neurosurg Rev **27**(3): 145-165; discussion 166-147.

Greitz D, Greitz T, and Hindmarsh T (1997). "A New View on the Csf-Circulation with the Potential for Pharmacological Treatment of Childhood Hydrocephalus." Acta Paediatr **86**(2): 125-132.

Greitz D, and Hannerz J (1996). "A Proposed Model of Cerebrospinal Fluid Circulation: Observations with Radionuclide Cisternography." AJNR Am J Neuroradiol **17**(3): 431-438.

Guinane JE (1977). "Why Does Hydrocephalus Progress?" J Neurol Sci **32**(1): 1-8.

Gutierrez Y, Friede RL, and Kaliney WJ (1975). "Agenesis of Arachnoid Granulations and Its Relationship to Communicating Hydrocephalus." J Neurosurg **43**(5): 553-558.

Heep A, Stoffel-Wagner B, Bartmann P, Benseler S, Schaller C, Groneck P, Obladen M, and Felderhoff-Mueser U (2004). "Vascular Endothelial Growth Factor and Transforming Growth Factor-Beta1 Are Highly Expressed in the Cerebrospinal Fluid of Premature Infants with Posthemorrhagic Hydrocephalus." Pediatr Res **56**(5): 768-774.

Hefti MM, Trachtenberg FL, Haynes RL, Hassett C, Volpe JJ, and Kinney HC (2015). "A Century of Germinal Matrix Intraventricular Hemorrhage in Autopsied Premature Infants: A Historical Account." Pediatr Dev Pathol.

Heron M, Sutton PD, Xu J, Ventura SJ, Strobino DM, and Guyer B (2010). "Annual Summary of Vital Statistics: 2007." Pediatrics **125**(1): 4-15.

Hirsch J-F, Pierre-Kahn A, Renier D, Sainte-Rose C, and Hoppe-Hirsch E (1984). "The Dandy-Walker Malformation: A Review of 40 Cases." J Neurosurg **61**(3): 515-522.

Iliff JJ, and Nedergaard M (2013). "Is There a Cerebral Lymphatic System?" Stroke **44**(6 Suppl 1): S93-95.

Iliff JJ, Wang M, Liao Y, Plogg BA, Peng W, Gundersen GA, Benveniste H, Vates GE, Deane R, Goldman SA, Nagelhus EA, and Nedergaard M (2012). "A Paravascular Pathway Facilitates Csf Flow through the Brain Parenchyma and the Clearance of Interstitial Solutes, Including Amyloid Beta." Sci Transl Med **4**(147): 147ra111.

Jessen NA, Munk AS, Lundgaard I, and Nedergaard M (2015). "The Glymphatic System: A Beginner's Guide." Neurochem Res **40**(12): 2583-2599.

Johanson CE, Stopa EG, and McMillan PN (2011). "The Blood-Cerebrospinal Fluid Barrier: Structure and Functional Significance." Methods Mol Biol **686**: 101-131.

Johnston M, Zakharov A, Papaiconomou C, Salmasi G, and Armstrong D (2004). "Evidence of Connections between Cerebrospinal Fluid and Nasal Lymphatic Vessels in Humans, Non-Human Primates and Other Mammalian Species." Cerebrospinal Fluid Res **1**(1): 2.

Kahle KT, Kulkarni AV, Limbrick DD, Jr., and Warf BC (2015). "Hydrocephalus in Children." Lancet.

Kataoka H, Hamilton JR, McKemy DD, Camerer E, Zheng YW, Cheng A, Griffin C, and Coughlin SR (2003). "Protease-Activated Receptors 1 and 4 Mediate Thrombin Signaling in Endothelial Cells." Blood **102**(9): 3224-3231.

Keep RF, and Jones HC (1990). "A Morphometric Study on the Development of the Lateral Ventricle Choroid Plexus, Choroid Plexus Capillaries and Ventricular Ependyma in the Rat." Brain Res Dev Brain Res **56**(1): 47-53.

Keep RF, and Smith DE (2011). "Choroid Plexus Transport: Gene Deletion Studies." Fluids Barriers CNS **8**(1): 26.

Kida S, Pantazis A, and Weller RO (1993). "Csf Drains Directly from the Subarachnoid Space into Nasal Lymphatics in the Rat. Anatomy, Histology and Immunological Significance." Neuropathol Appl Neurobiol **19**(6): 480-488.

Klebe D, Krafft PR, Hoffmann C, Lekic T, Flores JJ, Rolland W, and Zhang JH (2014). "Acute and Delayed Deferoxamine Treatment Attenuates Long-Term Sequelae after Germinal Matrix Hemorrhage in Neonatal Rats." Stroke **45**(8): 2475-2479.

Klebe D, McBride D, Flores JJ, Zhang JH, and Tang J (2015). "Modulating the Immune Response Towards a Neuroregenerative Peri-Injury Milieu after Cerebral Hemorrhage." J Neuroimmune Pharmacol **10**(4): 576-586.

Kochanek KD, Kirmeyer SE, Martin JA, Strobino DM, and Guyer B (2012). "Annual Summary of Vital Statistics: 2009." Pediatrics **129**(2): 338-348.

Korobkin R (1975). "The Relationship between Head Circumference and the Development of Communicating Hydrocephalus in Infants Following Intraventricular Hemorrhage." Pediatrics **56**(1): 74-77.

Kulik T, Kusano Y, Aronhime S, Sandler AL, and Winn HR (2008). "Regulation of Cerebral Vasculature in Normal and Ischemic Brain." Neuropharmacology **55**(3): 281-288.

Lee JY, Keep RF, He Y, Sagher O, Hua Y, and Xi G (2010). "Hemoglobin and Iron Handling in Brain after Subarachnoid Hemorrhage and the Effect of Deferoxamine on Early Brain Injury." J Cereb Blood Flow Metab **30**(11): 1793-1803.

Lekic T, Klebe D, McBride DW, Manaenko A, Rolland WB, Flores JJ, Altay O, Tang J, and Zhang JH (2015). "Protease-Activated Receptor 1 and 4 Signal Inhibition Reduces Preterm Neonatal Hemorrhagic Brain Injury." Stroke **46**(6): 1710-1713.

Louveau A, Smirnov I, Keyes TJ, Eccles JD, Rouhani SJ, Peske JD, Derecki NC, Castle D, Mandell JW, Lee KS, Harris TH, and Kipnis J (2015). "Structural and Functional Features of Central Nervous System Lymphatic Vessels." Nature **523**(7560): 337-341.

Luo W, Wang Y, and Reiser G (2007). "Protease-Activated Receptors in the Brain: Receptor Expression, Activation, and Functions in Neurodegeneration and Neuroprotection." Brain Res Rev **56**(2): 331-345.

Maktabi MA, Heistad DD, and Faraci FM (1991). "Effects of Central and Intravascular Angiotensin I and Ii on the Choroid Plexus." Am J Physiol **261**(5 Pt 2): R1126-1132.

Manaenko A, Lekic T, Barnhart M, Hartman R, and Zhang JH (2014). "Inhibition of Transforming Growth Factor-Beta Attenuates Brain Injury and Neurological Deficits in a Rat Model of Germinal Matrix Hemorrhage." Stroke **45**(3): 828-834.

Mao X, Enno TL, and Del Bigio MR (2006). "Aquaporin 4 Changes in Rat Brain with Severe Hydrocephalus." Eur J Neurosci **23**(11): 2929-2936.

McAllister JP, 2nd (2012). "Pathophysiology of Congenital and Neonatal Hydrocephalus." Semin Fetal Neonatal Med **17**(5): 285-294.

Milhorat TH (1975). "The Third Circulation Revisited." J Neurosurg **42**(6): 628-645.

Milhorat TH (1976). "Structure and Function of the Choroid Plexus and Other Sites of Cerebrospinal Fluid Formation." Int Rev Cytol **47**: 225-288.

Milhorat TH (1978). "Pediatric Neurosurgery." Contemp Neurol Ser **16**: 1-389.

Milhorat TH, Davis DA, and Hammock MK (1975). "Localization of Ouabain-Sensitive Na-K-Atpase in Frog, Rabbit and Rat Choroid Plexus." Brain Res **99**(1): 170-174.

Mollanji R, Bozanovic-Sosic R, Zakharov A, Makarian L, and Johnston MG (2002). "Blocking Cerebrospinal Fluid Absorption through the Cribriform Plate Increases Resting Intracranial Pressure." Am J Physiol Regul Integr Comp Physiol **282**(6): R1593-1599.

Moos T (2002). "Brain Iron Homeostasis." Dan Med Bull **49**(4): 279-301.

Murtha LA, Yang Q, Parsons MW, Levi CR, Beard DJ, Spratt NJ, and McLeod DD (2014). "Cerebrospinal Fluid Is Drained Primarily Via the Spinal Canal and Olfactory Route in Young and Aged Spontaneously Hypertensive Rats." Fluids Barriers CNS **11**: 12.

O'Connell JE (1943). "The Vascular Factor in Intracranial Pressure and the Maintenance of the Cerebrospinal Fluid Circulation." Brain **66**(3): 204-228.

Oi S, and Di Rocco C (2006). "Proposal of "Evolution Theory in Cerebrospinal Fluid Dynamics" and Minor Pathway Hydrocephalus in Developing Immature Brain." Childs Nerv Syst **22**(7): 662-669.

Oreskovic D, and Klarica M (2010). "The Formation of Cerebrospinal Fluid: Nearly a Hundred Years of Interpretations and Misinterpretations." Brain Res Rev **64**(2): 241-262.

Oreskovic D, and Klarica M (2011). "Development of Hydrocephalus and Classical Hypothesis of Cerebrospinal Fluid Hydrodynamics: Facts and Illusions." Prog Neurobiol **94**(3): 238-258.

Oshio K, Watanabe H, Song Y, Verkman AS, and Manley GT (2005). "Reduced Cerebrospinal Fluid Production and Intracranial Pressure in Mice Lacking Choroid Plexus Water Channel Aquaporin-1." FASEB J **19**(1): 76-78.

Osterman MJ, Kochanek KD, MacDorman MF, Strobino DM, and Guyer B (2015). "Annual Summary of Vital Statistics: 2012-2013." Pediatrics **135**(6): 1115-1125.

Pang D, Sclabassi RJ, and Horton JA (1986). "Lysis of Intraventricular Blood Clot with Urokinase in a Canine Model: Part 3. Effects of Intraventricular Urokinase on Clot Lysis and Posthemorrhagic Hydrocephalus." Neurosurgery **19**(4): 553-572.

Papaiconomou C, Bozanovic-Sosic R, Zakharov A, and Johnston M (2002). "Does Neonatal Cerebrospinal Fluid Absorption Occur Via Arachnoid Projections or Extracranial Lymphatics?" American Journal of Physiology-Regulatory, Integrative and Comparative Physiology **283**(4): R869-R876.

Paul DA, Leef KH, and Stefano JL (2000). "Increased Leukocytes in Infants with Intraventricular Hemorrhage." Pediatr Neurol **22**(3): 194-199.

Pierce EC, Jr., Lambertsen CJ, Deutsch S, Chase PE, Linde HW, Dripps RD, and Price HL (1962). "Cerebral Circulation and Metabolism During Thiopental Anesthesia and Hyper-Ventilation in Man." J Clin Invest **41**: 1664-1671.

Plog BA, Dashnaw ML, Hitomi E, Peng W, Liao Y, Lou N, Deane R, and Nedergaard M (2015). "Biomarkers of Traumatic Injury Are Transported from Brain to Blood Via the Glymphatic System." J Neurosci **35**(2): 518-526.

Pollay M (1975). "Formation of Cerebrospinal Fluid. Relation of Studies of Isolated Choroid Plexus to the Standing Gradient Hypothesis." J Neurosurg **42**(6): 665-673.

Pollay M (2010). "The Function and Structure of the Cerebrospinal Fluid Outflow System." Cerebrospinal Fluid Res **7**: 9.

Pollay M, and Curl F (1967). "Secretion of Cerebrospinal Fluid by the Ventricular Ependyma of the Rabbit." Am J Physiol **213**(4): 1031-1038.

Post RM, Allen FH, and Ommaya AK (1974). "Cerebrospinal Fluid Flow and Iodide 131 Transport in the Spinal Subarachnoid Space." Life Sci **14**(10): 1885-1894.

Prince EA, and Ahn SH (2013). "Basic Vascular Neuroanatomy of the Brain and Spine: What the General Interventional Radiologist Needs to Know." Semin Intervent Radiol **30**(3): 234-239.

Qing WG, Dong YQ, Ping TQ, Lai LG, Fang LD, Min HW, Xia L, and Heng PY (2009). "Brain Edema after Intracerebral Hemorrhage in Rats: The Role of Iron Overload and Aquaporin 4." J Neurosurg **110**(3): 462-468.

Rangroo Thrane V, Thrane AS, Plog BA, Thiyagarajan M, Iliff JJ, Deane R, Nagelhus EA, and Nedergaard M (2013). "Paravascular Microcirculation Facilitates Rapid Lipid Transport and Astrocyte Signaling in the Brain." Sci Rep **3**: 2582.

Reiber H (2003). "Proteins in Cerebrospinal Fluid and Blood: Barriers, Csf Flow Rate and Source-Related Dynamics." Restor Neurol Neurosci **21**(3-4): 79-96.

Rekate HL (2008). "The Definition and Classification of Hydrocephalus: A Personal Recommendation to Stimulate Debate." Cerebrospinal Fluid Res **5**: 2.

Rekate HL (2009). A Contemporary Definition and Classification of Hydrocephalus. Seminars in pediatric neurology, Elsevier.

Robinson S (2012). "Neonatal Posthemorrhagic Hydrocephalus from Prematurity: Pathophysiology and Current Treatment Concepts." J Neurosurg Pediatr **9**(3): 242-258.

Russell DS (1949). Observations on the Pathology of Hydrocephalus, HM Stationery Office.

Sahar A (1972). "Choroidal Origin of Cerebrospinal Fluid." Isr J Med Sci **81**(5): 594-596.

Sahar A, Hochwald GM, and Ransohoff J (1970). "Cerebrospinal Fluid and Cranial Sinus Pressures. Relationship in Normal and Hydrocephalic Cats." Arch Neurol **23**(5): 413-418.

Sakka L, Coll G, and Chazal J (2011). "Anatomy and Physiology of Cerebrospinal Fluid." Eur Ann Otorhinolaryngol Head Neck Dis **128**(6): 309-316.

Sato O, Bering EA, Jr., Yagi M, Tsugane R, Hara M, Amano Y, and Asai T (1975). "Bulk Flow in the Cerebrospinal Fluid System of the Dog." Acta Neurol Scand **51**(1): 1-11.

Saunders NR, Habgood MD, and Dziegielewska KM (1999). "Barrier Mechanisms in the Brain, I. Adult Brain." Clin Exp Pharmacol Physiol **26**(1): 11-19.

Savman K, Blennow M, Hagberg H, Tarkowski E, Thoresen M, and Whitelaw A (2002). "Cytokine Response in Cerebrospinal Fluid from Preterm Infants with Posthaemorrhagic Ventricular Dilatation." Acta Paediatr **91**(12): 1357-1363.

Savman K, Nilsson UA, Blennow M, Kjellmer I, and Whitelaw A (2001). "Non-Protein-Bound Iron Is Elevated in Cerebrospinal Fluid from Preterm Infants with Posthemorrhagic Ventricular Dilatation." Pediatr Res **49**(2): 208-212.

Schuliga M (2015). "The Inflammatory Actions of Coagulant and Fibrinolytic Proteases in Disease." Mediators Inflamm **2015**: 437695.

Segal MB, and Pollay M (1977). "The Secretion of Cerebrospinal Fluid." Exp Eye Res **25 Suppl**: 127-148.

Shulman K, Yarnell P, and Ransohoff J (1964). "Dural Sinus Pressure. In Normal and Hydrocephalic Dogs." Arch Neurol **10**: 575-580.

Silver I, Li B, Szalai J, and Johnston M (1999). "Relationship between Intracranial Pressure and Cervical Lymphatic Pressure and Flow Rates in Sheep." Am J Physiol **277**(6 Pt 2): R1712-1717.

Sofroniew MV (2009). "Molecular Dissection of Reactive Astrogliosis and Glial Scar Formation." Trends Neurosci **32**(12): 638-647.

Soul JS, Hammer PE, Tsuji M, Saul JP, Bassan H, Limperopoulos C, Disalvo DN, Moore M, Akins P, Ringer S, Volpe JJ, Trachtenberg F, and du Plessis AJ (2007). "Fluctuating Pressure-Passivity Is Common in the Cerebral Circulation of Sick Premature Infants." Pediatr Res **61**(4): 467-473.

Speake T, and Brown PD (2004). "Ion Channels in Epithelial Cells of the Choroid Plexus Isolated from the Lateral Ventricle of Rat Brain." Brain Res **1005**(1-2): 60-66.

Spector R, and Johanson CE (1989). "The Mammalian Choroid Plexus." Sci Am **261**(5): 68-74.

Steinhoff M, Buddenkotte J, Shpacovitch V, Rattenholl A, Moormann C, Vergnolle N, Luger TA, and Hollenberg MD (2005). "Proteinase-Activated Receptors: Transducers of Proteinase-Mediated Signaling in Inflammation and Immune Response." Endocr Rev **26**(1): 1-43.

Strahle J, Garton HJ, Maher CO, Muraszko KM, Keep RF, and Xi G (2012). "Mechanisms of Hydrocephalus after Neonatal and Adult Intraventricular Hemorrhage." Transl Stroke Res **3**(Suppl 1): 25-38.

Strahle JM, Garton T, Bazzi AA, Kilaru H, Garton HJ, Maher CO, Muraszko KM, Keep RF, and Xi G (2014). "Role of Hemoglobin and Iron in Hydrocephalus after Neonatal Intraventricular Hemorrhage." Neurosurgery **75**(6): 696-705; discussion 706.

Symss NP, and Oi S (2013). "Theories of Cerebrospinal Fluid Dynamics and Hydrocephalus: Historical Trend." J Neurosurg Pediatr **11**(2): 170-177.

Tada T, Kanaji M, and Kobayashi S (1994). "Induction of Communicating Hydrocephalus in Mice by Intrathecal Injection of Human Recombinant Transforming Growth Factor-Beta 1." J Neuroimmunol **50**(2): 153-158.

Tang J, Chen Q, Guo J, Yang L, Tao Y, Li L, Miao H, Feng H, Chen Z, and Zhu G (2015). "Minocycline Attenuates Neonatal Germinal-Matrix-Hemorrhage-Induced Neuroinflammation and Brain Edema by Activating Cannabinoid Receptor 2." Mol Neurobiol.

Tang J, Tao Y, Jiang B, Chen Q, Hua F, Zhang J, Zhu G, and Chen Z (2016). "Pharmacological Preventions of Brain Injury Following Experimental Germinal Matrix Hemorrhage: An up-to-Date Review." Transl Stroke Res **7**(1): 20-32.

Tang J, Tao Y, Tan L, Yang L, Niu Y, Chen Q, Yang Y, Feng H, Chen Z, and Zhu G (2015). "Cannabinoid Receptor 2 Attenuates Microglial Accumulation and Brain

Injury Following Germinal Matrix Hemorrhage Via Erk Dephosphorylation in Vivo and in Vitro." Neuropharmacology **95**: 424-433.

Tsuji M, Saul JP, du Plessis A, Eichenwald E, Sobh J, Crocker R, and Volpe JJ (2000). "Cerebral Intravascular Oxygenation Correlates with Mean Arterial Pressure in Critically Ill Premature Infants." Pediatrics **106**(4): 625-632.

Tully HM, and Dobyns WB (2014). "Infantile Hydrocephalus: A Review of Epidemiology, Classification and Causes." Eur J Med Genet **57**(8): 359-368.

Vassilouthis J, and Richardson AE (1979). "Ventricular Dilatation and Communicating Hydrocephalus Following Spontaneous Subarachnoid Hemorrhage." J Neurosurg **51**(3): 341-351.

Vassilyadi M, Tataryn Z, Shamji MF, and Ventureyra EC (2009). "Functional Outcomes among Premature Infants with Intraventricular Hemorrhage." Pediatr Neurosurg **45**(4): 247-255.

Volpe JJ (2009). "Brain Injury in Premature Infants: A Complex Amalgam of Destructive and Developmental Disturbances." Lancet Neurol **8**(1): 110-124.

Weed LH (1914). "Studies on Cerebro-Spinal Fluid. No. Iii : The Pathways of Escape from the Subarachnoid Spaces with Particular Reference to the Arachnoid Villi." J Med Res **31**(1): 51-91.

Welch K (1975). "The Principles of Physiology of the Cerebrospinal Fluid in Relation to Hydrocephalus Including Normal Pressure Hydrocephalus." Adv Neurol **13**: 247-332.

Welch K, and Friedman V (1960). "The Cerebrospinal Fluid Valves." Brain **83**: 454-469.

Whitelaw A (1993). "Endogenous Fibrinolysis in Neonatal Cerebrospinal Fluid." Eur J Pediatr **152**(11): 928-930.

Whitelaw A, and Aquilina K (2012). "Management of Posthaemorrhagic Ventricular Dilatation." Arch Dis Child Fetal Neonatal Ed **97**(3): F229-223.

Williams B (1976). "Cerebrospinal Fluid Pressure Changes in Response to Coughing." Brain **99**(2): 331-346.

Wong FY, Leung TS, Austin T, Wilkinson M, Meek JH, Wyatt JS, and Walker AM (2008). "Impaired Autoregulation in Preterm Infants Identified by Using Spatially Resolved Spectroscopy." Pediatrics **121**(3): e604-611.

Wright EM (1972). "Mechanisms of Ion Transport across the Choroid Plexus." J Physiol **226**(2): 545-571.

Wyss-Coray T, Feng L, Masliah E, Ruppe MD, Lee HS, Toggas SM, Rockenstein EM, and Mucke L (1995). "Increased Central Nervous System Production of Extracellular Matrix Components and Development of Hydrocephalus in Transgenic Mice Overexpressing Transforming Growth Factor-Beta 1." Am J Pathol **147**(1): 53-67.

Xie L, Kang H, Xu Q, Chen MJ, Liao Y, Thiyagarajan M, O'Donnell J, Christensen DJ, Nicholson C, Iliff JJ, Takano T, Deane R, and Nedergaard M (2013). "Sleep Drives Metabolite Clearance from the Adult Brain." Science **342**(6156): 373-377.

Xue M, Balasubramaniam J, Buist RJ, Peeling J, and Del Bigio MR (2003). "Periventricular/Intraventricular Hemorrhage in Neonatal Mouse Cerebrum." J Neuropathol Exp Neurol **62**(11): 1154-1165.

Xue M, and Del Bigio MR (2005). "Immune Pre-Activation Exacerbates Hemorrhagic Brain Injury in Immature Mouse Brain." J Neuroimmunol **165**(1-2): 75-82.

Yang Y, Salayandia VM, Thompson JF, Yang LY, Estrada EY, and Yang Y (2015). "Attenuation of Acute Stroke Injury in Rat Brain by Minocycline Promotes Blood-Brain Barrier Remodeling and Alternative Microglia/Macrophage Activation During Recovery." J Neuroinflammation **12**: 26.

Zakharov A, Papaiconomou C, Djenic J, Midha R, and Johnston M (2003). "Lymphatic Cerebrospinal Fluid Absorption Pathways in Neonatal Sheep Revealed by Subarachnoid Injection of Microfil." Neuropathol Appl Neurobiol **29**(6): 563-573.

Zervas NT, Liszczak TM, Mayberg MR, and Black PM (1982). "Cerebrospinal Fluid May Nourish Cerebral Vessels through Pathways in the Adventitia That May Be Analogous to Systemic Vasa Vasorum." J Neurosurg **56**(4): 475-481.

Zhang ET, Inman CB, and Weller RO (1990). "Interrelationships of the Pia Mater and the Perivascular (Virchow-Robin) Spaces in the Human Cerebrum." J Anat **170**: 111-123.

Zhao X, Sun G, Zhang J, Strong R, Song W, Gonzales N, Grotta JC, and Aronowski J (2007). "Hematoma Resolution as a Target for Intracerebral Hemorrhage Treatment: Role for Peroxisome Proliferator-Activated Receptor Gamma in Microglia/Macrophages." Ann Neurol **61**(4): 352-362.

Zhao X, Zhang Y, Strong R, Grotta JC, and Aronowski J (2006). "15d-Prostaglandin J2 Activates Peroxisome Proliferator-Activated Receptor-Gamma, Promotes Expression of Catalase, and Reduces Inflammation, Behavioral Dysfunction, and Neuronal Loss after Intracerebral Hemorrhage in Rats." J Cereb Blood Flow Metab **26**(6): 811-820.

Zlokovic BV (2011). "Neurovascular Pathways to Neurodegeneration in Alzheimer's Disease and Other Disorders." Nat Rev Neurosci **12**(12): 723-738.

Zlokovic BV, Segal MB, Davson H, Lipovac MN, Hyman S, and McComb JG (1990). "Circulating Neuroactive Peptides and the Blood-Brain and Blood-Cerebrospinal Fluid Barriers." Endocrinol Exp **24**(1-2): 9-17.

CHAPTER TWO

PPARγ-INDUCED UPREGULATION OF CD36 ENHANCES HEMATOMA RESOLUTION AND ATTENUATES LONG-TERM NEUROLOGICAL DEFICITS AFTER GERMINAL MATRIX HEMORRHAGE IN NEONATAL RATS

Jerry J. Flores[1], Damon Klebe[1], William B. Rolland[1], Tim Lekic[1], Paul R. Krafft[1], John H. Zhang[1, 2]

[1]Department of Physiology & Pharmacology, Loma Linda University School of Medicine, Loma Linda, California USA

[2]Departments of Anesthesiology and Neurosurgery, Loma Linda University School of Medicine, Loma Linda, California, USA

Published: *Neurobiology of Disease*. 2016 Mar; 87: 124-33

Abstract

Germinal matrix hemorrhage remains the leading cause of morbidity and mortality in preterm infants in the United States with little progress made in its clinical management. Survivors are often afflicted with long-term neurological sequelae, including cerebral palsy, mental retardation, hydrocephalus, and psychiatric disorders. Blood clots disrupting normal cerebrospinal fluid circulation and absorption after germinal matrix hemorrhage are thought to be important contributors towards post-hemorrhagic hydrocephalus development. We evaluated if upregulating CD36 scavenger receptor expression in microglia and macrophages through PPARγ stimulation, which was effective in experimental adult cerebral hemorrhage models and is being evaluated clinically, will enhance hematoma resolution and ameliorate long-term brain sequelae using a neonatal rat germinal matrix hemorrhage model. PPARγ stimulation (15d-PGJ_2) increased short-term PPARγ and CD36 expression levels as well as enhanced hematoma resolution, which was reversed by a PPARγ antagonist (GW9662) and CD36 siRNA. PPARγ stimulation (15d-PGJ_2) also reduced long-term white matter loss and post-hemorrhagic ventricular dilation as well as improved neurofunctional outcomes, which were reversed by a PPARγ antagonist (GW9662). PPARγ-induced upregulation of CD36 in macrophages and microglia is, therefore, critical for enhancing hematoma resolution and ameliorating long-term brain sequelae.

Introduction

The ganglionic eminence consists of neuronal and glial precursor cells located at the head of the caudate nucleus below the lateral ventricles of the developing fetus, and the highly vascularized region within the subependymal tissue is the germinal matrix. Cerebral blood flow fluctuation associated with hemodynamic and respiratory instability in preterm infants in conjunction with the inherent fragility of the germinal matrix often leads to germinal matrix hemorrhage, a very common and major neurological complication of prematurity. Germinal Matrix Hemorrhage (GMH) occurs when immature blood vessels rupture within the subependymal (or periventricular) germinal region of the ganglionic eminence in the immature brain (Ballabh 2010). In the United States alone, GMH occurs in approximately 12,000 lives births per year, and the number of moderate-to-severe GMH cases has remained steady over the past two decades (Fanaroff, Stoll et al. 2007; Jain, Kruse et al. 2009; Osterman, Kochanek et al. 2015). Clinical studies indicate GMH afflicted infants often suffer from long-term neurological deficits, cerebral palsy, mental retardation, hydrocephalus, and psychiatric disorders (Kadri, Mawla et al. 2006; Ballabh 2014). Prenatal glucocorticoid treatment remains the best treatment for preventing GMH, yet minimal advancements have been made in GMH clinical management post-ictus (Shankaran, Bauer et al. 1995; Roberts and Dalziel 2006).

Hemodynamic and respiratory instability in preterm infants results in fluctuations of cerebral blood flow in the inherently frail germinal matrix vasculature, often resulting in spontaneous bleeding (Ballabh 2014). The consequent hematoma applies mechanical pressure to glia and neurons, resulting in cytotoxicity and necrosis, as well as evokes an inflammatory response, leading to secretion of destructive proteases and oxidative

species (Lekic, Klebe et al. 2015). In adult cerebral hemorrhage, clinical studies indicate hematoma volume is the best prognostic indicator; larger hematoma volumes have worsened outcomes (Keep, Xi et al. 2005; Xi, Keep et al. 2006). Experimental adult cerebral hemorrhage studies proved more rapid hematoma resolution is necessary for quickly ameliorating inflammation and improving neurological recovery (Zhao, Sun et al. 2007; Zhao, Grotta et al. 2009). Additionally, blood clots directly impair cerebrospinal fluid circulation and absorption after GMH, significantly contributing towards post-hemorrhagic hydrocephalus development (Cherian, Whitelaw et al. 2004; Aquilina, Chakkarapani et al. 2011). Therefore, we hypothesize enhancing hematoma resolution will improve GMH outcomes.

Microglia are resident macrophages of the central nervous system and are critical drivers of the neuro-inflammatory response after GMH and other hemorrhagic brain injuries (Aronowski and Zhao 2011; Tang, Chen et al. 2015). Activated microglia recruit hematogenous phagocytes to the injured site, which engulf the hematoma as well as damaged or dead tissue (Cox, Crossley et al. 1995; Aronowski and Hall 2005). The role microglia play in hemorrhagic brain injury pathogenesis is different in neonates than adults (Woo, Wang et al. 2012). Unlike the adult brain where microglia cells and macrophages contribute to brain injury after stroke through the production of inflammatory cytokines (Vexler and Yenari 2009), neonatal brains demonstrate the opposite as the depletion of these cells enhances injury by removing endogenous protective mechanisms (Faustino, Wang et al. 2011).

Scavenger receptor CD36, a trans-membrane glycoprotein, is involved in several biological functions, such as foam cell formation, immune cell chemotaxis, and

phagocytosis of apoptotic cells (Woo, Wang et al. 2012). CD36 receptor is reportedly located on the cell surface of several cell types, including monocytes, endothelial cells, and microglia. CD36 plays an important role in phagocytosis, and upregulating its expression beneficially enhances hematoma resolution (Zhao, Sun et al. 2007). Transfection of non-phagocytic cells with a CD36-expressing gene converted those cells into phagocytes (Ren, Silverstein et al. 1995). CD36 genetic deletion worsened injury after acute focal stroke in neonatal mice, partially by decreasing removal of apoptotic cells (Woo, Wang et al. 2012).

Peroxisome proliferator-activated receptor gamma (PPARγ), a member of the nuclear hormone receptor superfamily, plays a major role in the upregulating CD36 expression (Zhao, Sun et al. 2007; Zhao, Grotta et al. 2009). PPARγ stimulation exerts anti-inflammatory effects in several central nervous system injuries and disorders (Pereira, Hurtado et al. 2005; Landreth, Jiang et al. 2008). Many studies demonstrated PPARγ is neuroprotective in various experimental stroke models (Pereira, Hurtado et al. 2005; Zhao, Sun et al. 2007; Woo, Wang et al. 2012; Shao and Liu 2015). In adult intracerebral hemorrhage (ICH) experimental models, PPARγ activation was directly associated with upregulation of CD36 expression, leading to enhanced phagocytosis-mediated clearance of the hematoma as well as dead or damaged cells by microglia and macrophages. PPARγ stimulation reduced expression of pro-inflammatory mediators, ameliorated secondary brain injury, and improved functional recovery after ICH (Zhao, Sun et al. 2007). Currently, PPARγ stimulation for enhancing hematoma resolution and ameliorating secondary brain injury is being clinically tested in ICH patients (Gonzales,

Shah et al. 2013). Yet, no clinical trials are evaluating PPARγ stimulation in GMH patients.

In this study, we assess if PPARγ stimulation enhances CD36-mediated hematoma resolution in a neonatal rat germinal matrix hemorrhage model. We hypothesize PPARγ stimulation, using 15d-PGJ_2, will augment microglia/macrophage phagocytosis of blood clots, reducing post-hemorrhagic hydrocephalus, inflammation, behavioral dysfunction, and neuronal loss, which will be reversed by CD36 knockdown or PPARγ antagonist administration.

Materials and methods

Animals and Surgeries

All experimental procedures were conducted in accordance with the National Institutes of Health guidelines for the treatment of animals, and were approved by the Institutional Animal Care and Use Committee of Loma Linda University. Two hundred and sixty P7 Sprague-Dawley neonatal pups (Harlan, Indianapolis, IN) weighing 12-15 g (brain development is comparable to 30-32 week gestation humans) were used in this study. Germinal matrix hemorrhage was achieved by stereotactic-guided injection of bacterial collagenase, as previously described (Lekic, Manaenko et al. 2012). Pups were anesthetized with 3% isoflurane (delivered through medical grade oxygen and mixed air) while being stabilized onto a stereotaxic frame. Isopropyl alcohol followed by betadine was applied to the incision site. Incision was made on the longitudinal plane to expose the skull and reveal bregma. The stereotactic coordinates from bregma were as follows: 1.6 mm (rostral), 1.6 mm (right lateral), and 2.8 mm (depth) from the dura. A burr hole (1

mm) was drilled, into which a 27 gauge needle was inserted at a rate of 1 mm/min. 0.3 units of clostridial collagenase VII-S (Sigma Aldrich, MO) in 1 µL was infused over a period of 3 minutes with a Hamilton syringe guided by a microinfusion pump (Harvard Apparatus, Holliston, MA). After completing infusion, the needle is left into position for an additional 10 minutes after injection to prevent "back-leakage" and then removed at a rate of 1 mm/min. Once the Hamilton is removed, the burr hole is sealed with bone wax and the incision site sutured. Animals are then given buprenorphine and allowed to recover on a 37°C heated blanket. When fully recovered, pups are then placed back with the mother. Surgery time per animal is approximately 30 minutes. Sham animals were subject to needle insertion without collagenase infusion. The same procedures were performed for intraventricular injection of siRNA, except the stereotactic coordinates from bregma were as follows: 1.0 mm (rostral), 1.0 mm (left lateral), and 1.8 mm (depth) of the dura.

Animal Treatments and Experimental Groups

P7 rat pups were randomly divided into the following groups: sham-operated (n=38), Vehicle (n=38), GMH + 15d-PGJ_2 (n=38), GMH + 15d-PGJ_2 + GW9662 (n=38), GMH + CD36 siRNA (n=12), GMH + 15d-PGJ_2 + CD36 (n=12), GMH + scrambled siRNA (n=12). The PPARγ agonist (15d-PGJ_2, 0.1mg/kg; Sigma Aldrich), antagonist (GW9662, 4mg/kg; Sigma Aldrich) + agonist, and saline (for sham and vehicle groups) were administered intraperitoneally to experimental animals at 1 hour post-GMH and then once daily for 7 days. CD36 siRNA (1.2 ng, Cell Signaling & Santa Cruz), and scrambled siRNA (1.2 ng, Santa Cruz) were administered via intraventricular injection to

experimental animals 24 hours prior to GMH induction. Buprenorphine (0.01 mg/kg) was administered subcutaneously to all groups after completing surgery.

Animal Perfusion and Tissue Extraction

Animals were euthanized using isoflurane (≥5%) followed by trans-cardiac perfusion with ice-cold phosphate buffered saline (PBS) for hemoglobin assay and Western blot samples or with ice-cold PBS followed by 10% formalin for histology samples. Forebrains for hemoglobin assay and Western blot were snap-frozen with liquid-nitrogen, then stored in -80°C freezer before protein extractions or spectrophotometric quantification. Histological brain samples were post-fixed in 10% Fomaldehyde for at least 3 days and then 30% sucrose for at least 3 days, all stored in 4°C fridge. Forebrains were next embedded in Optimal Cutting Temperature compound and stored in -20°C freezer.

Hemoglobin Assay

Spectrophotometric measurements were used to assess hemorrhagic volume using well-established protocols (Choudhri, Hoh et al. 1997; Tang, Liu et al. 2004; Lekic, Manaenko et al. 2011). Frozen extracted forebrains were placed into individual glass tubes containing 3 mL of PBS. The tissue was homogenized for 60 seconds (Tissue Miser Homogenizer; Fisher Scientific, Pittsburgh, PA) followed by ultrasonication for 1 minute to lyse erythrocyte membranes. The products were then centrifuged for 30 minutes and the supernatant was separated from the pellets. A 4:1 ratio of Drabkin's reagent (Sigma-Aldrich) and supernatant were combined, which were left to react for 15 minutes.

Absorbance, using a spectrophotometer (540 nm; Genesis 10uv; Thermo Fisher Scientific, Waltham, MA), was calculated into a hemorrhagic volume (μL) on the basis of a standard curve as routinely performed (Lekic, Manaenko et al. 2011).

Intracranial Pressure (ICP) Measurements

At 28 days post-ictus, animals were anesthetized and mounted onto a stereotaxic frame, where the head was inclined downward at a 30 degree angle. A midline skin incision was made to expose the atlanto-occipital membrane. The cisterna magna was punctured with a 26G Hamilton needle, which was connected to a pressure transducer of a Digi-Med LPA 400-low pressure Anayzer (Micro-Med-Louisville, Kentucky, USA) as described (Lackner, Vahmjanin et al. 2013)

Western Blotting

Protein concentrations for immunoblot (Lekic, Manaenko et al. 2011) were determined by DC protein assay (Bio-Rad, Hercules, CA). 30 μg protein per sample were loaded into wells of 4-20% gels, ran for 30 minutes at 50V then 90 minutes at 125V, then transferred onto nitrocellulose membranes at 0.3A for 120 minutes (Bio-Rad). Membranes were incubated for 2 hours in 5% non-fat milk in Tris-buffered saline containing 0.1% Tween20. Then the following primary antibodies were incubated overnight: anti-PPARy (1:1000; Santa Cruz, Dallas, Texas), CD36 (1:500, Santa Cruz, Dallas, Texas), and mannose receptor (CD206) (1:500, ABcam, Cambridge, Massachusetts). Secondary antibodies (1:2000; Santa Cruz Biotechnology, Santa Cruz, CA) were then applied to the membranes and incubated for 2 hours and then processed

with the ECL plus Kit (GE Healthcare and Life Science, Piscataway, NJ). β-actin was used as an internal control against the anti-body (1:1000; Santa Cruz Biotechnology, Santa Cruz, CA). ImageJ software (4.0, Media Cybernetics, Silver Spring, MD) was used to analyze the relative density of the resultant protein immunoblot images as described (Tang, Liu et al. 2004).

Histological Volumetric Analysis

10 μm thick coronal brain sections were cut every 600 μm using a cryostat (Leica Microsystems LM3050S) and were placed onto poly-L-lysine-coated slides. Brain slices were Nissl stained morphometrically analyzed using computer-assisted (ImageJ 4.0, Media Cybernetics, Silver Spring, MD) hand delineation of the ventricle system (lateral, third, cerebral aqueduct, and fourth), hemisphere (cortex, subcortex), caudate, thalamus, hippocampus, and corpus callosum (white matter) (Lekic, Manaenko et al. 2011). These structures were delineated using optical dissector principles from prior stereological studies (Reisert, Wildemann et al. 1984; Oorschot 1996; Tang, Lopez et al. 2001; Bermejo, Jimenez et al. 2003; Avendano, Machin et al. 2005; Ekinci, Acer et al. 2008; Klebe, Krafft et al. 2014). Volumes were calculated using the following equation: [(Average [(Area of coronal section) × Interval × Number of sections) (MacLellan, Silasi et al. 2008).

Immunohistochemistry

10 μm thick slices were first stained with OX-42 (1:1000, ABcam) and mannose receptor (1:1000, ABcam) overnight at 4 °C, followed by incubation with appropriate

fluorescence conjugated secondary antibodies (Jackson Immunoresearch, West Grove, PA). The peri-hemorrhagic area was imaged by a Fluorescent Olympus-BX51 microscope and analyzed using MagnaFire SP 2.1B software (Olympus, Melville, NY). At least six sections per animal group over a microscopic field of 20 × (for microglia) were averaged and expressed as cells/field, as described (Wang and Dore 2007).

Neurobehavioral Analysis

Neurobehavioral function was evaluated in a blinded manner using a battery of tests, described below, to detect sensorimotor and cognitive deficits 28 days after GMH as previously described (Hartman, Lekic et al. 2009; Klebe, Krafft et al. 2014): Foot Fault Test: Rats were placed on a wire grid (20x40 cm) kept above the floor level and allowed to walk on the grid for 2 minutes. Number of foot faults will be recorded when a complete paw falls through the openings in the grid. Rotarod Test: Rats were placed on a rotarod (Columbus Instruments, Columbus, OH), which consists of a rotating horizontal cylinder (7 cm diameter) divided into 9.5-cm-wide lanes. Rats walked forward when the cylinder is rotating to avoid falling down. Rats were tested at a starting 5 RPM or 10 RPM with acceleration at 2 RPM per 5 seconds. A photobeam circuit detected the latency to fall off the cylinder. Water Maze Test: Rats were released in a metal pool (110 cm diameter) filled with water and containing spatial cues on the walls, and they were allowed to swim to find a submerged platform (11 cm diameter). Each animal performed 10 trials per day for 4 days, 5 blocks of 2 consecutive trials, with a 10-min interval between successive blocks. Over the next 3 days, the platform was submerged 1 cm below the water and surface and the rats had to find and remember the platform location.

Additionally, at the end of each day, the platform was removed and animals were allowed to swim to find the platform quadrant. An overhead camera with a computerized tracking system (Noldus Ethovision; Noldus, Tacoma, WA) recorded the swim path and measured the swim distance, swim speed, and time spent in probe quadrant.

Statistical Analysis

A power analysis using a type I error rate of 0.05 and a power of 0.8 on a 2-sided test was used to estimate sample size. Data are expressed in Mean ± Standard Deviation. One-way ANOVA on ranks using the Student-Newman-Keuls post-hoc test was used to analyze behavioral, histological, western blots, and immunohistochemistry. A P-value <0.05 was considered statistically significant.

Results

PPARγ Stimulation Ameliorated Long-term Neurological Deficits

The vehicle group performed significantly worse compared to sham in the Morris Water Maze evaluation, yet PPARγ stimulation improved spatial learning and memory compared to vehicle and was not significantly different from sham. Treatment effect was reversed by the PPARγ antagonist (*P<0.05 versus Sham; #P<0.05 versus Vehicle; †P<0.05 versus GW9662 + 15d-PGJ_2; Figure 2.1.A-B). Treatment also significantly improved sensorimotor function in the foot fault test compared to other GMH groups (*P<0.05 versus Sham; #P<0.05 versus Vehicle; †P<0.05 versus GW9662 + 15d-PGJ_2; Figure 2.1.C). Yet no significant difference was achieved in the treated group compared to vehicle and antagonist groups in the rotarod sensorimotor evaluation (*P<0.05 versus Sham; #P<0.05 versus Vehicle; †P<0.05 versus GW9662 + 15d-PGJ_2; Figure 2.1.D).

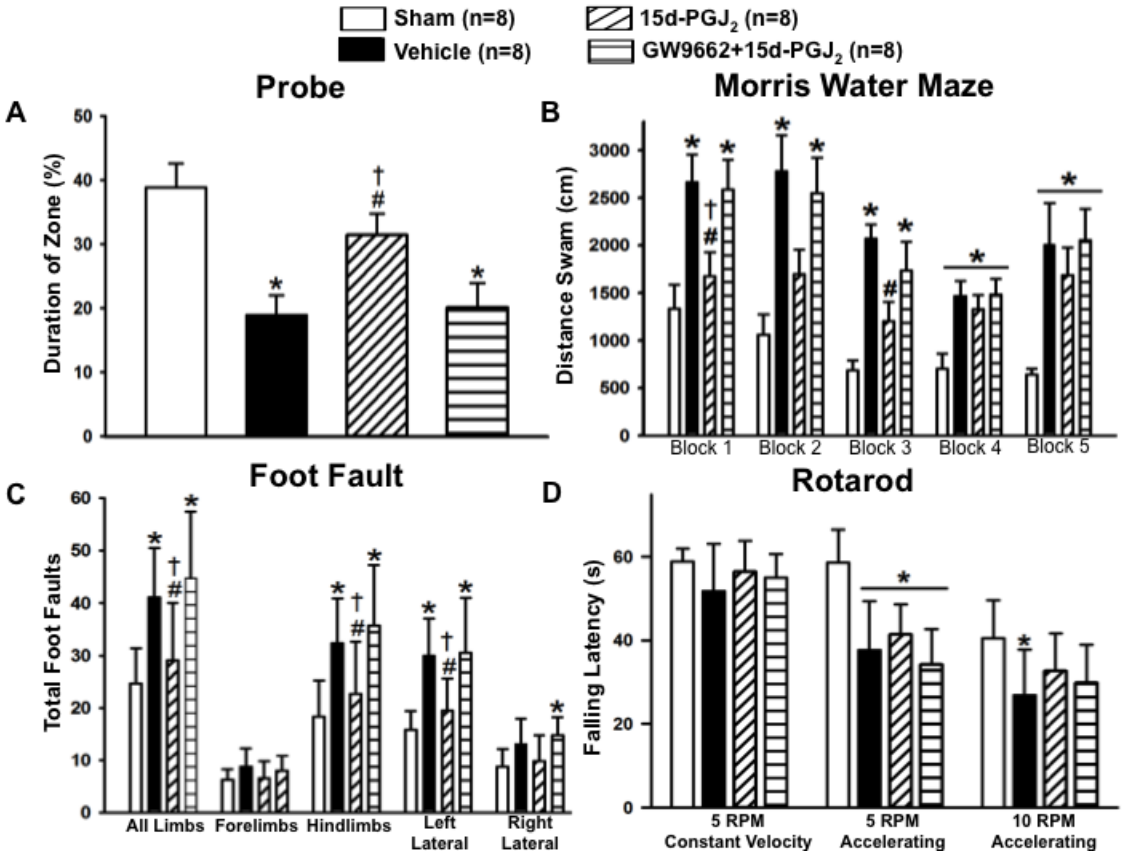

Figure 2.1: Long-term neurocognitive and sensorimotor outcomes after 15d-PGJ$_2$ treatment and PPARγ inhibition with 15d-PGJ$_2$ treatment at 3-4 weeks after GMH. Neurofunctional assessment of (A and B) Morris water maze, (C) foot fault, and (D) rotarod at 21 to 28 days after germinal matrix hemorrhage. Values are expressed as mean±SD. *P<0.05 compared with sham, #P<0.05 compared with vehicle, and †P<0.05 compared with inhibitor and agonist. N=8 per group; and RPM, rounds per minute.

PPARγ Stimulation Improved Long-term Brain Morphology

Since increased intracranial pressure is associated with hydrocephalus, ICP was measured in rats at 4 weeks post-ictus. ICP was significantly decreased in treated groups when compared to vehicle and PPARγ antagonist groups (*P<0.05 versus Sham; #P<0.05 versus Vehicle; †P<0.05 versus GW9662 + 15d-PGJ_2; Figure 2.2.B). Calculated cortical thickness is presented as a ratio to the mean of sham and was significantly deceased in the vehicle and PPARγ antagonist group, but the PPARγ stimulated group had significantly less cortical loss (*P<0.05 versus Sham; #P<0.05 versus Vehicle; †P<0.05 versus GW9662 + 15d-PGJ_2; Figure 2.3.A). Ventricular volume was significantly increased in vehicle and PPARγ antagonist groups, but 15d-PGJ_2 treatment reduced post-hemorrhagic ventricular dilation (*P<0.05 versus Sham; #P<0.05 versus Vehicle; †P<0.05 versus GW9662 + 15d-PGJ_2; Figure 2.3.B). White matter loss is presented as a percentage of white matter present to mean of sham. White matter loss was reduced by PPARγ stimulation, but vehicle and PPARγ antagonist groups had significant white matter loss (*P<0.05 versus Sham; #P<0.05 versus Vehicle; †P<0.05 versus GW9662 + 15d-PGJ_2; Figure 2.3.C). Basal ganglia loss is presented as a percentage of basal ganglia present to mean of sham. The 15d-PGJ_2 treated group had significantly decreased basal ganglia loss compared to the vehicle group. Surprisingly, basal ganglia loss in the GW9662 group was not significantly different from PPARγ agonist or vehicle groups (*P<0.05 versus Sham; #P<0.05 versus Vehicle; †P<0.05 versus GW9662 + 15d-PGJ_2; Figure 2.3.D).

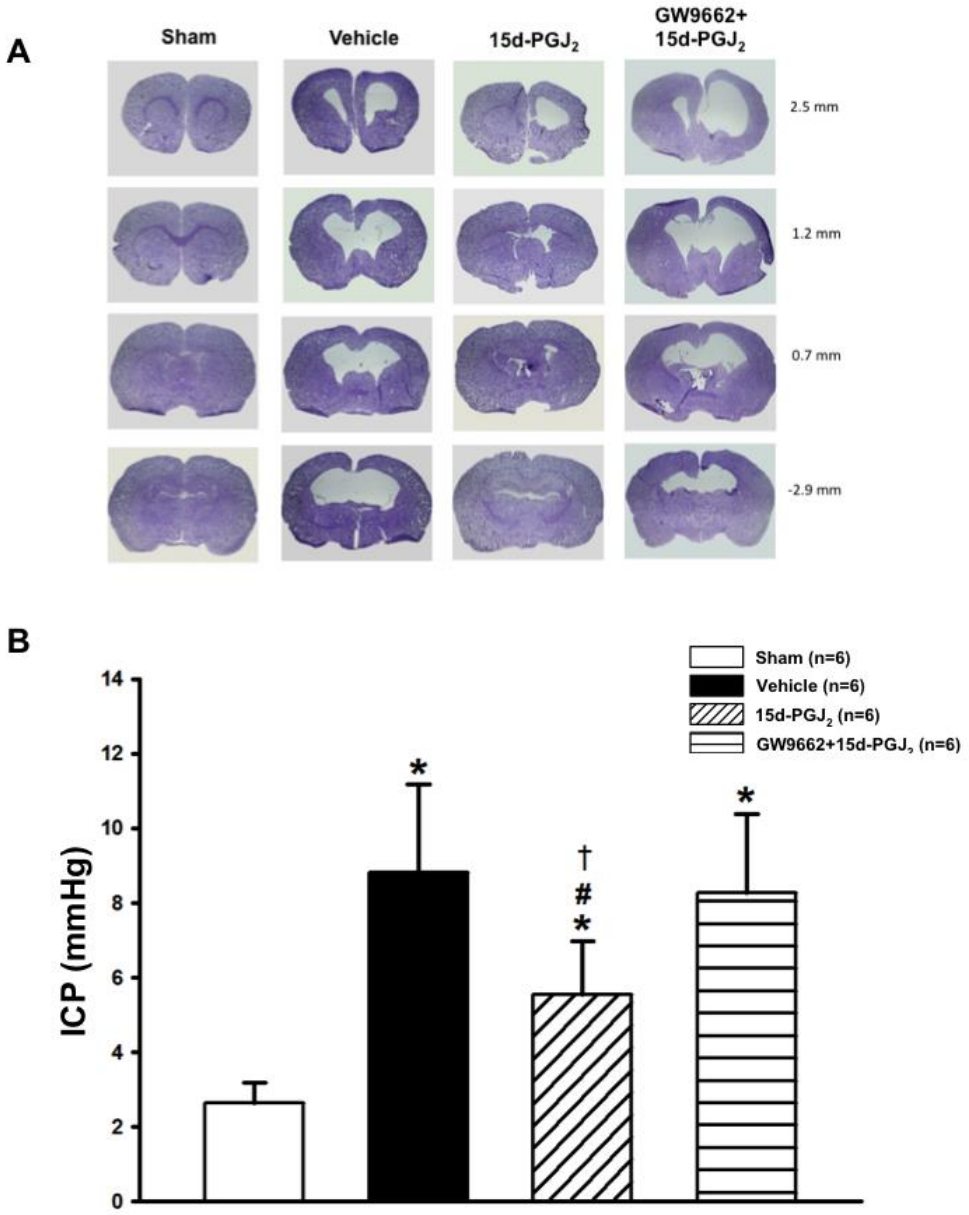

Figure 2.2: Effects of 15d-PGJ$_2$ treatment and PPARγ inhibition with 15d-PGJ$_2$ treatment on brain morphology and intracranial pressure 4 weeks after GMH. 28 days after germinal matrix hemorrhage. Representative microphotographs of (A) Nissl-stained brain sections were taken and (B) Intracranial pressure (ICP) in mm Hg**.** Note: measurement on the right side of the representative pictures indicates the location of the brain section from bregma. Values are expressed as mean±SD. *P<0.05 compared with sham, #P<0.05 compared with vehicle, and †P<0.05 compared with inhibitor and agonist. N=6 per group; and mmHG, millimeters of Mercury.

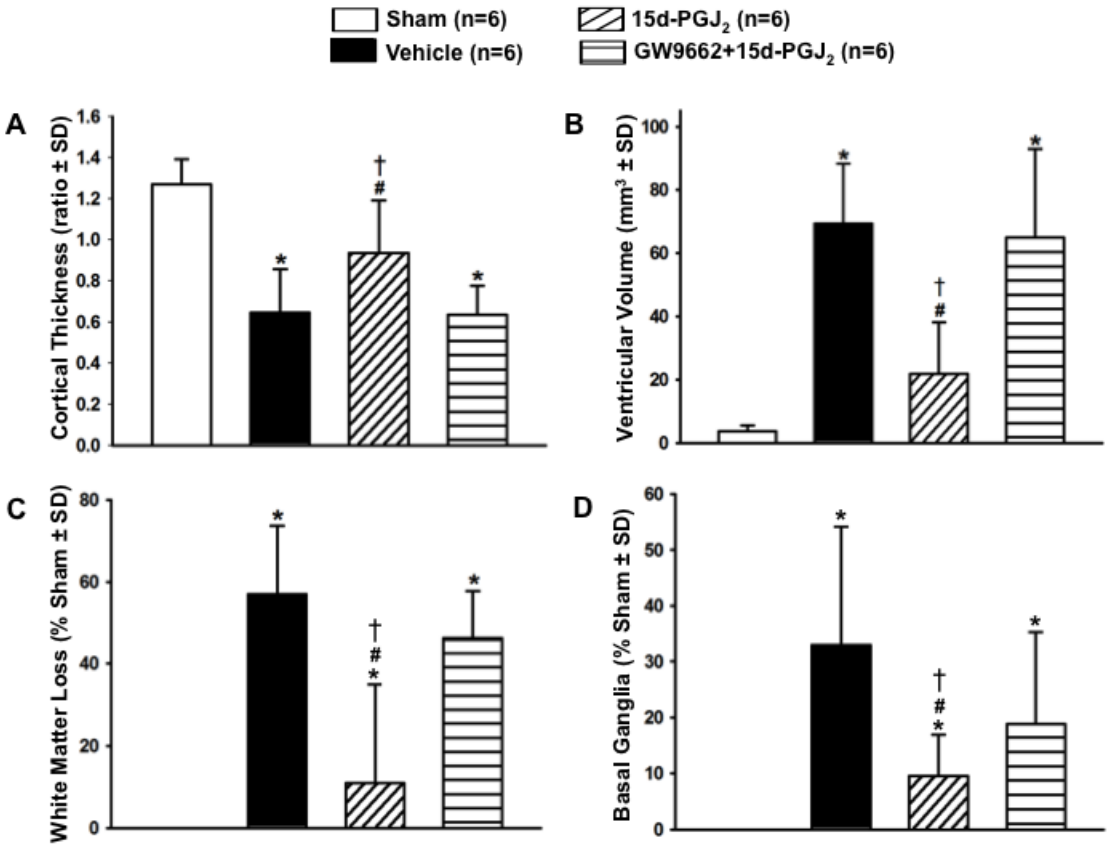

Figure 2.3: Quantification of brain morphological outcomes from 15d-PGJ$_2$ treatment and PPARγ inhibition with 15d-PGJ$_2$ treatment at 4 weeks post-GMH. Quantification of (A) cortical thickness, (B) ventricular volume, (C) white matter loss, and (D) basal ganglia loss at 28 days after germinal matrix hemorrhage. Values are expressed as mean±SD. *P<0.05 compared with sham, #P<0.05 compared with vehicle, and †P<0.05 compared with inhibitor and agonist. N=6 per group.

PPARγ Stimulation Enhanced Hematoma Resolution, Increased Activated Microglia, and Induced M2 Polarization

A hemoglobin assay time-course was conducted at 24 hours, 72 hours, and 7 days to determine PPARγ's role in hematoma resolution. At 24 hours, all groups had significantly greater hemoglobin content in the brain compared to sham (*P<0.05 versus Sham; Figure 2.4.A). At 72 hours, all groups had significantly greater hemoglobin content in the brain compared to sham, but 15d-PGJ_2 treatment had significantly less hemoglobin content compared to vehicle, which was reversed by GW9662 treatment (*P<0.05 versus Sham; #P<0.05 versus Vehicle; †P<0.05 versus GW9662 + 15d-PGJ_2; Figure 2.4.B). At 7 days, only the vehicle and PPARγ antagonist groups had significantly greater hemoglobin content compared to sham, but the PPARγ agonist group had significantly less hemoglobin content compared to vehicle and PPARγ antagonist groups (*P<0.05 versus Sham; #P<0.05 versus Vehicle; †P<0.05 versus GW9662 + 15d-PGJ_2; Figure 2.4.C). Since significantly greater hematoma resolution was observed in the PPARγ stimulated group at 72 hours, representative photographs of immuno-stained activated microglia/macrophages (OX-42) in the peri-hematoma region are presented at this time point (Figure 2.5.A). The 15d-PGJ_2 treated group had relatively increased number of microglia/macrophage compared to sham, vehicle, and PPARγ antagonist group ((*P<0.05 versus Sham; #P<0.05 versus Vehicle; †P<0.05 versus GW9662 + 15d-PGJ_2; Figure 2.5.B). Additionally representative photographs of the co-localization of activated microglia/macrophages (OX-42) and mannose receptor (CD206) in the peri-hematoma region are presented at 72 hours, showing an increase in OX-42/mannose receptor expression in 15d-PGJ_2 treated group in comparison to all other groups (Figure 2.5.A).

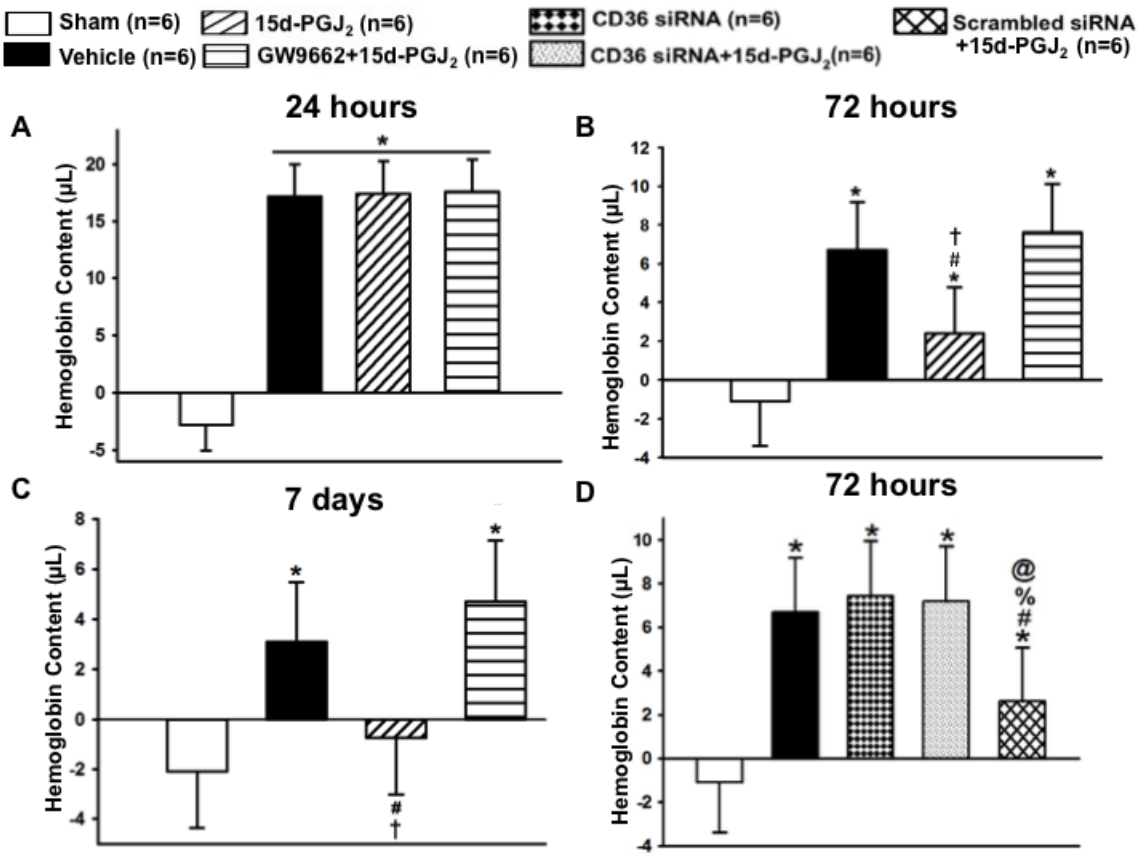

Figure 2.4: Short-term hematoma resolution after GMH from 15d-PGJ2 treatment, PPARγ inhibition with 15d-PGJ2 treatment, CD36 knockdown, and CD36 knockdown with 15d-PGJ2 treatment. Hemoglobin assay at (A) 24 hours, (B) 72 hours, and (C) 7 days. At 72 hours (D) Hemoglobin assay was conducted on siRNA groups. Values are expressed as mean±SD. *P<0.05 compared with sham, #P<0.05 compared with vehicle, and †P<0.05 compared with inhibitor and agonist, %P<0.05 compared CD 36 siRNA, and @P<0.05 compared to scrambled siRNA. N=6 per group.

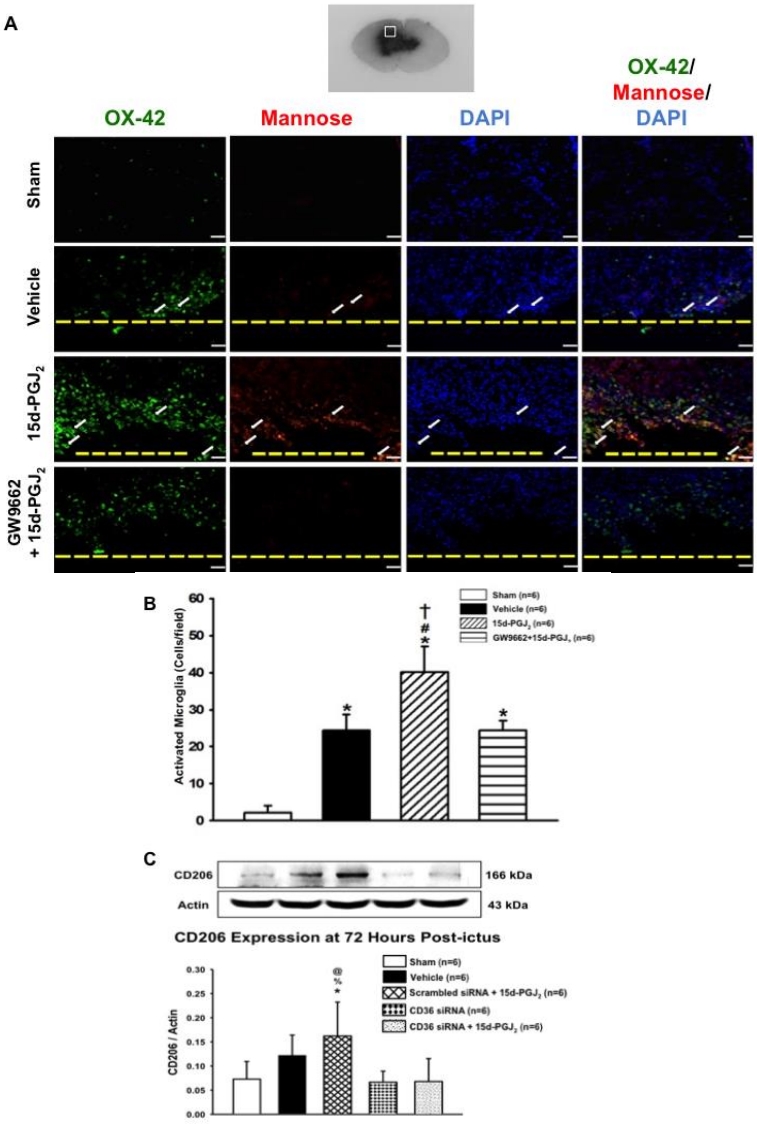

Figure 2.5: Microglia / Macrophage activation and differentiation into M2 subtypes at 3 days post-GMH following 15d-PGJ$_2$ treatment, CD36 knockdown, and CD36 knockdown with 15d-PGJ$_2$ treatment. Immunohistochemistry representative pictures were taken showing the co-localization of (A) activated microglia (OX-42; scale bar: 20 µm) with Mannose Receptor and DAPI staining and (B) quantification of activated microglia was conducted at 72 hours. Western blots were conducted at 72 hours for (C) CD206 Expression. Note: peri-hematoma region is below the yellow broken line (A) and the representative GMH brain indicates where IHC images were taken. Values are expressed as mean±SD. *P<0.05 compared with sham, #P<0.05 compared with vehicle, †P<0.05 compared with inhibitor and agonist, %P<0.05 compared CD36 siRNA, and @P<0.05 compared to scrambled siRNA. N=6 per group; and ICH, Immunohistochemistry. N=6 per group.

PPARγ Stimulation Increased CD36 and PPARγ Expression at 72 Hours

A time-course study was conducted to determine endogenous PPARγ and CD36 expression levels in GMH at 0, 3, 6, 12 hours and 1, 3, 5, and 7 days after GMH. Endogenous PPARγ expression was significantly increased at 3, 6, 12 hours and 1 day compared to 0 hour (*P<0.05 versus 0 hours; Figure 2.6.A). Correspondingly, endogenous CD36 expression was significantly increased at 3, 6, 12 hours, and 1 day compared to 0 hour (*P<0.05 versus 0 hours; Figure 2.6.B), and tended to remain elevated by 7 days. PPARγ and CD36 expression levels were determined at 72 hours for all experimental groups. PPARγ expression was significantly increased in the 15d-PGJ_2 group compared to all other groups (*P<0.05 versus Sham; #P<0.05 versus Vehicle; †P<0.05 versus GW9662 + 15d-PGJ_2; Figure 2.6.C). Much like PPARγ, CD36 expression was significantly increased in the 15d-PGJ_2 group compared to all other groups (*P<0.05 versus Sham; #P<0.05 versus Vehicle; †P<0.05 versus GW9662 + 15d-PGJ_2; Figure 2.6.D).

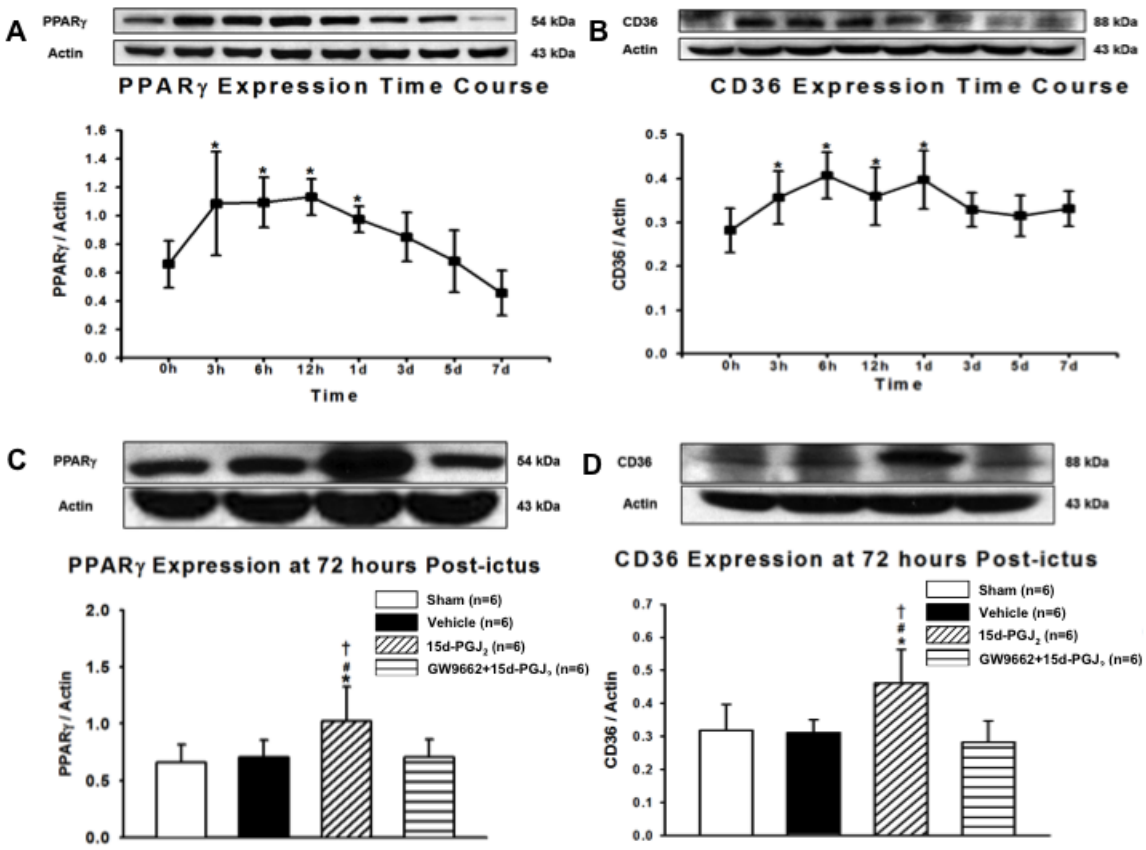

Figure 2.6: Short-term time course of CD36 and PPARγ expression after GMH and the effects of 15d-PGJ$_2$ treatment, PPARγ inhibition with 15d-PGJ$_2$ treatment, CD36 knockdown, and CD36 knockdown with 15d-PGJ$_2$ treatment on CD36 and PPARγ expression levels. Western blot was conducted for time-course studies of (A) PPARγ and (B) CD36 at 0, 3, 6 , 12 hours, 1, 3, 5, 7 days after GMH. Western blot was then conducted at 72 hours for (C) PPAR-Y and (D) CD36. Values are expressed as mean±SD. *P<0.05 compared with sham, #P<0.05 compared with vehicle, and †P<0.05 compared with inhibitor and agonist. N=6 per group; and h and d, hour(s) and day(s).

CD36 Knockdown Reversed PPARγ Agonist-enhanced Hematoma Resolution and M2 Expression at 72 Hours

At 72 hours, CD36 knockdown reversed PPARγ agonist-enhanced hematoma resolution, which was not reversed in the scrambled siRNA group (*P<0.05 versus Sham, #P<0.05 versus Vehicle, %P<0.05 versus CD-36 siRNA + 15d-PGJ_2, @P<0.05 versus scrambled siRNA+15d-PGJ_2, Figure 2.4.D). Additionally, CD36 knockdown reversed PPARγ mannose receptor expression, which was not reversed in the scrambled siRNA group (*P<0.05 versus Sham, #P<0.05 versus Vehicle, %P<0.05 versus CD-36 siRNA + 15d-PGJ_2, @P<0.05 versus scrambled siRNA+15d-PGJ_2, Figure 2.5.C).

Discussion

Neonatal brain hemorrhage is a common affliction of premature infants. The resultant hematoma is thought to play a major role in causing post-hemorrhagic hydrocephalus development because blood clots disrupt cerebrospinal fluid circulation and absorption in the ventricles (Crews, Wyss-Coray et al. 2004). Rapid hematoma resolution was neuroprotective in adult hemorrhagic stroke models (Zhao, Sun et al. 2007; Zhao, Sun et al. 2015). In particular, PPARγ stimulation upregulates CD36 expression in microglia/macrophages, leading to increased phagocytosis of blood products and more rapid hematoma resolution after adult intracerebral hemorrhage (Zhao, Sun et al. 2007). In this study, we examined the effects of stimulating PPARγ with 15d-PGJ_2 on hematoma resolution as well as long-term brain morphological and neurofunctional outcomes after collagenase-induced GMH in neonatal rats. In addition, we determined if PPARγ and CD36 inhibition reversed observed therapeutic effects from

PPARγ stimulation by 15d-PDJ_2. This study is the first to assess this treatment approach in neonates for enhancing hematoma resolution as well as the first to evaluate its therapeutic potential for ameliorating long-term white matter loss, post-hemorrhagic hydrocephalus development, and neurological deficits.

We evaluated the efficacy of 15d-PGJ_2 treatment, a PPARγ agonist, administered 1 hour post-ictus as a potential therapeutic modality for GMH-induced brain injury. Although treatment did not significantly increase hematoma resolution at 24 hours, it did significantly enhance hematoma resolution at 72 hours and 7 days after GMH (Figure 2.4.A-C). PPARγ stimulation demonstrated more rapid hematoma clearance after GMH in neonates, starting at 72 hours, than after ICH in adults, which took 7 days (Zhao, Sun et al. 2007). 15d-PGJ_2 co-admiration with GW9662, a PPARγ antagonist, reversed 15d-PGJ_2 treatment effects on enhanced hematoma resolution at 72 hours and 7 days after GMH. To determine if endogenous expression of PPARγ and CD36 changes after GMH, we performed a Western blot time course using 0, 3, 6, 12 hour, 1, 3, 5, and 7 day endpoints following GMH induction. Endogenous PPARγ expression increased at 3, 6, 12 hour, and 1 day after GMH induction, then returned to baseline by 3 days (Figure 2.6.A). Endogenous CD36 expression significantly increased at 3, 6, 12 hours, and 1 day after GMH induction, and tended to remain elevated through 7 days (Figure 2.6.B). Because endogenous PPARγ and CD36 expression returned near baseline at 72 hours and because 15d-PGJ_2 treatment enhanced hematoma resolution at 72 hours, we determined treatment effects on PPARγ and CD36 expression levels by Western blot at 72 hours. As expected, 15d-PGJ_2 treatment significantly increased PPARγ expression compared to sham and vehicle, and 15d-PGJ_2 co-administration with GW9662 reversed this effect

(Figure 2.6.C). Similarly, 15d-PGJ_2 treatment significantly increased CD36 expression compared to sham and vehicle, and 15d-PGJ_2 co-administration with GW9662 reversed this effect (Figure 2.6.D).

CD36 receptor is an important scavenger receptor located on several cell types, including monocytes, endothelial cells, and microglia/macrophages. CD36 plays an important role in microglia/macrophage phagocytosis, and upregulating its expression beneficially enhances hematoma resolution (Zhao, Sun et al. 2007). More activated microglia were observed in the peri-hematoma region of treated GMH animals than all other groups, providing evidence of PPARγ's treatment effects are dependent upon these critical immune cells (Figure 2.5.A-B). All GMH groups seemed to have increased DAPI stained cells post-ictus compared to sham. The germinal matrix has many growing and dividing neuronal and glial precursor cells. Prior GMH studies have documented increased proliferative cytokines and pathways, such as TGF-β and mTOR, after injury, and we speculate proliferative signaling triggers more profound gliosis after neonatal brain hemorrhage (Lekic, Klebe et al. 2015). While brain cell death is definitely occurring, we speculate proliferative signaling in conjunction with increased leukocyte infiltration contributes towards these observed results in neonatal brains. Although activated microglia/macrophages contribute to brain injury in adults, some evidence suggests microglia/macrophages have important defense mechanisms against injury in neonates, which could be explained by the vital role microglia play in neonatal brain development (Faustino, Wang et al. 2011; Harry and Kraft 2012). Furthermore, activated microglia/macrophages have two differentiated states, a pro-inflammatory classically activated state (M1), and an immune dampening and tissue regenerative alternatively

activated state (M2) (Klebe, McBride et al. 2015). CD36 stimulation can contribute towards microglia/macrophage activation as well as M2 polarization (Kouadir, Yang et al. 2012; Rios, Koga et al. 2013; Chavez-Sanchez, Garza-Reyes et al. 2014). PPARγ stimulation also polarizes microglia/macrophages towards the M2 state (Yoon, Jeon et al. 2008; Pisanu, Lecca et al. 2014; Penas, Mirkin et al. 2015). To corroborate these findings in GMH, immunohistochemical co-localization of activated microglia and mannose receptor (CD206), an M2 marker, demonstrated increased co-expression in 15d-PGJ_2 treated GMH animals compared to other groups, providing more evidence PPARγ induces M2 polarization (Figure 2.5.A). Similarly, CD206 Western blots demonstrated increased CD206 expression levels in treated GMH animals compared to sham, GMH animals with CD36 siRNA alone, and GMH animals with CD36 siRNA and 15d-PGJ_2 treatment. Interestingly, vehicle treated GMH animals showed a small tendency towards having increased CD206 expression levels, which also did not achieve a statistically significant difference compared to 15d-PGJ_2 treated GMH animals. After hemorrhage, M2 microglia/macrophages are expected to increase over time as the peri-hematoma milieu transitions into an immune dampened tissue repair phase in which M2 microglia/macrophages play a pivotal role (Klebe, McBride et al. 2015). CD36 knockdown eliminated the tendency observed in the vehicle group, achieving a significantly reduced expression compared to 15d-PGJ_2 treatment. CD36 knockdown also reversed 15d-PGJ_2 induced upregulation of CD206 expression (Figure 2.5.C). CD36, thus, is important for M2 polarization, particularly after PPARγ stimulation. To further confirm microglial/macrophage CD36 plays a pivotal role in PPARγ-induced blood clot clearance, siRNA was used to knockdown CD36 expression. CD36 knockdown reversed

15d-PGJ_2 treatment effects on enhanced hematoma resolution at 72 hours, which was not reversed by scrambled siRNA (Figure 2.4.D).

In our long-term evaluations, vehicle treated GMH animals had significant cortical, white matter, and basal ganglia loss as well as post-hemorrhagic ventricular dilation, but 15d-PGJ_2 treatment ameliorated these brain morphological maladies, which were reversed by PPARγ antagonist, GW9662, co-administration (Figure 2.3.A-D). Surprisingly, GW9662 co-administration did not completely reverse 15d-PGJ_2's effects on reducing basal ganglia loss, although a tendency was observed. Our ICP measurements agreed with the brain morphological assessment, where ICP levels were significantly lower in treated groups when compared to vehicle and PPARγ antagonist group **(**Figure 2.2.B). Additionally, vehicle treated GMH animals performed poorly in the Morris Water Maze, Foot Fault, and Rotarod tests, but 15d-PGJ_2 treatment significantly improved spatial memory and motor function, which were reversed by GW9662 co-administration (Figure 2.1.A-D). The foot fault test evaluates locomotor function, the rotarod test evaluates sensorimotor coordination and balance, and Morris Water Maze evaluates spatial learning and memory (Schaar, Brenneman et al. 2010). Although 15d-PGJ2 reduced the number of foot faults, it did not significantly improve performance in the rotarod test. GMH and consequent post-hemorrhagic ventricular dilation may cause cerebellar injury that affects motor coordination (Volpe 2009; Brouwer, de Vries et al. 2015; Fumagalli, Bassi et al. 2015). More thorough investigations are needed to elucidate the pathophysiology between GMH and cerebellar injury. Although motor coordination is an important factor in both the rotarod and foot fault tests, the element of balancing on an accelerating cylinder platform leads us to speculate cerebellar injury may more

profoundly affect performances in the rotarod evaluations. 15d-PGJ2 treatment may not be effective enough to ameliorate potential cerebellar injury from GMH and consequent post-hemorrhagic hydrocephalus, and, if this is the case, modulating the immune response after GMH may not be sufficient to promote complete functional recovery. Additionally, the rotarod test may not be sensitive enough for detecting improved sensorimotor outcomes in treatment groups, which is why we performed multiple neurofunctional evaluations. Nonetheless, these results provide sufficient evidence that enhanced hematoma resolution corresponds with improved long-term brain morphological and neurocognitive outcomes after GMH. Most importantly, more rapid blood clot clearance resulted in significantly decreased post-hemorrhagic ventricular dilation, providing evidence that blood products play an important role in post-hemorrhagic hydrocephalus development.

The CD36 scavenger receptor is important in microglia/macrophage-mediated phagocytosis of cellular debris and blood products. Our results suggest PPARγ stimulation by 15d-PGJ_2 increases microglia/macrophage phagocytic function by upregulating CD36 scavenger receptor expression in our experimental GMH model, leading to enhanced hematoma resolution. We are first to report the positive long-term effects on brain morphological and neurofunctional outcomes from more efficient hematoma resolution after GMH. Blood products disrupt cerebrospinal circulation and absorption in the cerebroventricular system, often resulting in post-hemorrhagic hydrocephalus. Herein, we provide evidence that more rapid blood clot clearance reduces long-term post-hemorrhagic ventricular dilation after GMH. Removing the hematoma without damaging surrounding tissues is ideal and clinically relevant. PPARγ

stimulation could be a promising therapeutic approach for GMH patients, especially since PPARγ stimulation by Pioglitazone is already being evaluated in clinical trials for adult cerebral hemorrhage.

References

Aquilina K, Chakkarapani E, Love S, and Thoresen M (2011). "Neonatal Rat Model of Intraventricular Haemorrhage and Post-Haemorrhagic Ventricular Dilatation with Long-Term Survival into Adulthood." Neuropathol Appl Neurobiol **37**(2): 156-165.

Aronowski J, and Hall CE (2005). "New Horizons for Primary Intracerebral Hemorrhage Treatment: Experience from Preclinical Studies." Neurol Res **27**(3): 268-279.

Aronowski J, and Zhao X (2011). "Molecular Pathophysiology of Cerebral Hemorrhage: Secondary Brain Injury." Stroke **42**(6): 1781-1786.

Avendano C, Machin R, Bermejo PE, and Lagares A (2005). "Neuron Numbers in the Sensory Trigeminal Nuclei of the Rat: A Gaba- and Glycine-Immunocytochemical and Stereological Analysis." J Comp Neurol **493**(4): 538-553.

Ballabh P (2010). "Intraventricular Hemorrhage in Premature Infants: Mechanism of Disease." Pediatr Res **67**(1): 1-8.

Ballabh P (2014). "Pathogenesis and Prevention of Intraventricular Hemorrhage." Clin Perinatol **41**(1): 47-67.

Bermejo PE, Jimenez CE, Torres CV, and Avendano C (2003). "Quantitative Stereological Evaluation of the Gracile and Cuneate Nuclei and Their Projection Neurons in the Rat." J Comp Neurol **463**(4): 419-433.

Brouwer MJ, de Vries LS, Kersbergen KJ, van der Aa NE, Brouwer AJ, Viergever MA, Isgum I, Han KS, Groenendaal F, and Benders MJ (2015). "Effects of Posthemorrhagic Ventricular Dilatation in the Preterm Infant on Brain Volumes and White Matter Diffusion Variables at Term-Equivalent Age." J Pediatr.

Chavez-Sanchez L, Garza-Reyes MG, Espinosa-Luna JE, Chavez-Rueda K, Legorreta-Haquet MV, and Blanco-Favela F (2014). "The Role of Tlr2, Tlr4 and Cd36 in Macrophage Activation and Foam Cell Formation in Response to Oxldl in Humans." Hum Immunol **75**(4): 322-329.

Cherian S, Whitelaw A, Thoresen M, and Love S (2004). "The Pathogenesis of Neonatal Post-Hemorrhagic Hydrocephalus." Brain Pathol **14**(3): 305-311.

Choudhri TF, Hoh BL, Solomon RA, Connolly ES, Jr., and Pinsky DJ (1997). "Use of a Spectrophotometric Hemoglobin Assay to Objectively Quantify Intracerebral Hemorrhage in Mice." Stroke **28**(11): 2296-2302.

Cox G, Crossley J, and Xing Z (1995). "Macrophage Engulfment of Apoptotic Neutrophils Contributes to the Resolution of Acute Pulmonary Inflammation in Vivo." Am J Respir Cell Mol Biol **12**(2): 232-237.

Crews L, Wyss-Coray T, and Masliah E (2004). "Insights into the Pathogenesis of Hydrocephalus from Transgenic and Experimental Animal Models." Brain Pathol **14**(3): 312-316.

Ekinci N, Acer N, Akkaya A, Sankur S, Kabadayi T, and Sahin B (2008). "Volumetric Evaluation of the Relations among the Cerebrum, Cerebellum and Brain Stem in Young Subjects: A Combination of Stereology and Magnetic Resonance Imaging." Surg Radiol Anat **30**(6): 489-494.

Fanaroff AA, Stoll BJ, Wright LL, Carlo WA, Ehrenkranz RA, Stark AR, Bauer CR, Donovan EF, Korones SB, Laptook AR, Lemons JA, Oh W, Papile LA, Shankaran S, Stevenson DK, Tyson JE, Poole WK, and Network NNR (2007). "Trends in Neonatal Morbidity and Mortality for Very Low Birthweight Infants." Am J Obstet Gynecol **196**(2): 147 e141-148.

Faustino JV, Wang X, Johnson CE, Klibanov A, Derugin N, Wendland MF, and Vexler ZS (2011). "Microglial Cells Contribute to Endogenous Brain Defenses after Acute Neonatal Focal Stroke." J Neurosci **31**(36): 12992-13001.

Fumagalli M, Bassi L, Sirgiovanni I, Mosca F, Sannia A, and Ramenghi LA (2015). "From Germinal Matrix to Cerebellar Haemorrhage." J Matern Fetal Neonatal Med **28 Suppl 1**: 2280-2285.

Gonzales NR, Shah J, Sangha N, Sosa L, Martinez R, Shen L, Kasam M, Morales MM, Hossain MM, Barreto AD, Savitz SI, Lopez G, Misra V, Wu TC, El Khoury R, Sarraj A, Sahota P, Hicks W, Acosta I, Sline MR, Rahbar MH, Zhao X, Aronowski J, and Grotta JC (2013). "Design of a Prospective, Dose-Escalation Study Evaluating the Safety of Pioglitazone for Hematoma Resolution in Intracerebral Hemorrhage (Shrinc)." Int J Stroke **8**(5): 388-396.

Harry GJ, and Kraft AD (2012). "Microglia in the Developing Brain: A Potential Target with Lifetime Effects." Neurotoxicology **33**(2): 191-206.

Hartman R, Lekic T, Rojas H, Tang J, and Zhang JH (2009). "Assessing Functional Outcomes Following Intracerebral Hemorrhage in Rats." Brain Res **1280**: 148-157.

Jain NJ, Kruse LK, Demissie K, and Khandelwal M (2009). "Impact of Mode of Delivery on Neonatal Complications: Trends between 1997 and 2005." J Matern Fetal Neonatal Med **22**(6): 491-500.

Kadri H, Mawla AA, and Kazah J (2006). "The Incidence, Timing, and Predisposing Factors of Germinal Matrix and Intraventricular Hemorrhage (Gmh/Ivh) in Preterm Neonates." Childs Nerv Syst **22**(9): 1086-1090.

Keep RF, Xi G, Hua Y, and Hoff JT (2005). "The Deleterious or Beneficial Effects of Different Agents in Intracerebral Hemorrhage: Think Big, Think Small, or Is Hematoma Size Important?" Stroke **36**(7): 1594-1596.

Klebe D, Krafft PR, Hoffmann C, Lekic T, Flores JJ, Rolland W, and Zhang JH (2014). "Acute and Delayed Deferoxamine Treatment Attenuates Long-Term Sequelae after Germinal Matrix Hemorrhage in Neonatal Rats." Stroke **45**(8): 2475-2479.

Klebe D, McBride D, Flores JJ, Zhang JH, and Tang J (2015). "Modulating the Immune Response Towards a Neuroregenerative Peri-Injury Milieu after Cerebral Hemorrhage." J Neuroimmune Pharmacol.

Kouadir M, Yang L, Tan R, Shi F, Lu Y, Zhang S, Yin X, Zhou X, and Zhao D (2012). "Cd36 Participates in Prp(106-126)-Induced Activation of Microglia." PLoS One **7**(1): e30756.

Lackner P, Vahmjanin A, Hu Q, Krafft PR, Rolland W, and Zhang JH (2013). "Chronic Hydrocephalus after Experimental Subarachnoid Hemorrhage." PLoS One **8**(7): e69571.

Landreth G, Jiang Q, Mandrekar S, and Heneka M (2008). "Ppargamma Agonists as Therapeutics for the Treatment of Alzheimer's Disease." Neurotherapeutics **5**(3): 481-489.

Lekic T, Klebe D, Poblete R, Krafft PR, Rolland WB, Tang J, and Zhang JH (2015). "Neonatal Brain Hemorrhage (Nbh) of Prematurity: Translational Mechanisms of the Vascular-Neural Network." Curr Med Chem **22**(10): 1214-1238.

Lekic T, Manaenko A, Rolland W, Krafft PR, Peters R, Hartman RE, Altay O, Tang J, and Zhang JH (2012). "Rodent Neonatal Germinal Matrix Hemorrhage Mimics the Human Brain Injury, Neurological Consequences, and Post-Hemorrhagic Hydrocephalus." Exp Neurol **236**(1): 69-78.

Lekic T, Manaenko A, Rolland W, Tang J, and Zhang JH (2011). "A Novel Preclinical Model of Germinal Matrix Hemorrhage Using Neonatal Rats." Acta Neurochir Suppl **111**: 55-60.

MacLellan CL, Silasi G, Poon CC, Edmundson CL, Buist R, Peeling J, and Colbourne F (2008). "Intracerebral Hemorrhage Models in Rat: Comparing Collagenase to Blood Infusion." J Cereb Blood Flow Metab **28**(3): 516-525.

Oorschot DE (1996). "Total Number of Neurons in the Neostriatal, Pallidal, Subthalamic, and Substantia Nigral Nuclei of the Rat Basal Ganglia: A Stereological Study Using the Cavalieri and Optical Disector Methods." J Comp Neurol **366**(4): 580-599.

Osterman MJ, Kochanek KD, MacDorman MF, Strobino DM, and Guyer B (2015). "Annual Summary of Vital Statistics: 2012-2013." Pediatrics.

Penas F, Mirkin GA, Vera M, Cevey A, Gonzalez CD, Gomez MI, Sales ME, and Goren NB (2015). "Treatment in Vitro with Pparalpha and Ppargamma Ligands Drives M1-to-M2 Polarization of Macrophages from T. Cruzi-Infected Mice." Biochim Biophys Acta **1852**(5): 893-904.

Pereira MP, Hurtado O, Cardenas A, Alonso-Escolano D, Bosca L, Vivancos J, Nombela F, Leza JC, Lorenzo P, Lizasoain I, and Moro MA (2005). "The Nonthiazolidinedione Ppargamma Agonist L-796,449 Is Neuroprotective in Experimental Stroke." J Neuropathol Exp Neurol **64**(9): 797-805.

Pisanu A, Lecca D, Mulas G, Wardas J, Simbula G, Spiga S, and Carta AR (2014). "Dynamic Changes in Pro- and Anti-Inflammatory Cytokines in Microglia after Ppar-Gamma Agonist Neuroprotective Treatment in the Mptpp Mouse Model of Progressive Parkinson's Disease." Neurobiol Dis **71**: 280-291.

Reisert I, Wildemann G, Grab D, and Pilgrim C (1984). "The Glial Reaction in the Course of Axon Regeneration: A Stereological Study of the Rat Hypoglossal Nucleus." J Comp Neurol **229**(1): 121-128.

Ren Y, Silverstein RL, Allen J, and Savill J (1995). "Cd36 Gene Transfer Confers Capacity for Phagocytosis of Cells Undergoing Apoptosis." J Exp Med **181**(5): 1857-1862.

Rios FJ, Koga MM, Pecenin M, Ferracini M, Gidlund M, and Jancar S (2013). "Oxidized Ldl Induces Alternative Macrophage Phenotype through Activation of Cd36 and Pafr." Mediators Inflamm **2013**: 198193.

Roberts D, and Dalziel S (2006). "Antenatal Corticosteroids for Accelerating Fetal Lung Maturation for Women at Risk of Preterm Birth." Cochrane Database Syst Rev(3): CD004454.

Schaar KL, Brenneman MM, and Savitz SI (2010). "Functional Assessments in the Rodent Stroke Model." Exp Transl Stroke Med **2**(1): 13.

Shankaran S, Bauer CR, Bain R, Wright LL, and Zachary J (1995). "Relationship between Antenatal Steroid Administration and Grades Iii and Iv Intracranial Hemorrhage in Low Birth Weight Infants. The Nichd Neonatal Research Network." Am J Obstet Gynecol **173**(1): 305-312.

Shao ZQ, and Liu ZJ (2015). "Neuroinflammation and Neuronal Autophagic Death Were Suppressed Via Rosiglitazone Treatment: New Evidence on Neuroprotection in a Rat Model of Global Cerebral Ischemia." J Neurol Sci **349**(1-2): 65-71.

Tang J, Chen Q, Guo J, Yang L, Tao Y, Li L, Miao H, Feng H, Chen Z, and Zhu G (2015). "Minocycline Attenuates Neonatal Germinal-Matrix-Hemorrhage-Induced Neuroinflammation and Brain Edema by Activating Cannabinoid Receptor 2." Mol Neurobiol.

Tang J, Liu J, Zhou C, Alexander JS, Nanda A, Granger DN, and Zhang JH (2004). "Mmp-9 Deficiency Enhances Collagenase-Induced Intracerebral Hemorrhage and Brain Injury in Mutant Mice." J Cereb Blood Flow Metab **24**(10): 1133-1145.

Tang Y, Lopez I, and Baloh RW (2001). "Age-Related Change of the Neuronal Number in the Human Medial Vestibular Nucleus: A Stereological Investigation." J Vestib Res **11**(6): 357-363.

Vexler ZS, and Yenari MA (2009). "Does Inflammation after Stroke Affect the Developing Brain Differently Than Adult Brain?" Dev Neurosci **31**(5): 378-393.

Volpe JJ (2009). "Cerebellum of the Premature Infant: Rapidly Developing, Vulnerable, Clinically Important." J Child Neurol **24**(9): 1085-1104.

Wang J, and Dore S (2007). "Heme Oxygenase-1 Exacerbates Early Brain Injury after Intracerebral Haemorrhage." Brain **130**(Pt 6): 1643-1652.

Woo MS, Wang X, Faustino JV, Derugin N, Wendland MF, Zhou P, Iadecola C, and Vexler ZS (2012). "Genetic Deletion of Cd36 Enhances Injury after Acute Neonatal Stroke." Ann Neurol **72**(6): 961-970.

Xi G, Keep RF, and Hoff JT (2006). "Mechanisms of Brain Injury after Intracerebral Haemorrhage." Lancet Neurol **5**(1): 53-63.

Yoon HJ, Jeon SB, Kim IH, and Park EJ (2008). "Regulation of Tlr2 Expression by Prostaglandins in Brain Glia." J Immunol **180**(12): 8400-8409.

Zhao X, Grotta J, Gonzales N, and Aronowski J (2009). "Hematoma Resolution as a Therapeutic Target: The Role of Microglia/Macrophages." Stroke **40**(3 Suppl): S92-94.

Zhao X, Sun G, Ting SM, Song S, Zhang J, Edwards NJ, and Aronowski J (2015). "Cleaning up after Ich: The Role of Nrf2 in Modulating Microglia Function and Hematoma Clearance." J Neurochem **133**(1): 144-152.

Zhao X, Sun G, Zhang J, Strong R, Song W, Gonzales N, Grotta JC, and Aronowski J (2007). "Hematoma Resolution as a Target for Intracerebral Hemorrhage

Treatment: Role for Peroxisome Proliferator-Activated Receptor Gamma in Microglia/Macrophages." Ann Neurol **61**(4): 352-362.

CHAPTER THREE

ACUTE AND DELAYED DEFEROXAMINE TREATMENT ATTENUATES LONG-TERM SEQUELAE AFTER GERMINAL MATRIX HEMORRHAGE IN NEONATAL RATS

Damon Klebe, BA; Paul R. Krafft, MD; Clotilde Hoffmann, BS; Tim Lekic, MD, PhD; Jerry J. Flores, BS; William Rolland, BS; John H. Zhang, MD, PhD

Department of Physiology & Pharmacology, Loma Linda University School of Medicine, Loma Linda, California, USA

Published: *Stroke*. 2015 Aug; 45(8): 2475-9

Abstract

This study investigated if acute and delayed Deferoxamine treatment attenuates long-term sequelae after germinal matrix hemorrhage (GMH). Bacterial collagenase (0.3 U) was infused intraparenchymally into the right hemispheric ganglionic eminence in P7 rat pups to induce GMH. GMH animals received either Deferoxamine or vehicle twice a day for 7 consecutive days. Deferoxamine administration was initiated at either 1 hour or 72 hours post-GMH. Long-term neurocognitive deficits and motor coordination were assessed using Morris water maze, rotarod, and foot fault tests between day 21-28 post-GMH. At 28 days post-GMH, brain morphology was assessed and extracellular matrix protein (fibronectin and vitronectin) expression was determined. Acute and delayed Deferoxamine treatment improved long-term motor and cognitive function at 21-28 days post-GMH. Attenuated neurofunction was paralleled with improved overall brain morphology at 28 days post-GMH, reducing white matter loss, basal ganglia loss, post-hemorrhagic ventricular dilation, and cortical loss. GMH resulted in significantly increased expression of fibronectin and vitronectin, which was reversed by acute and delayed Deferoxamine treatment. Acute and delayed Deferoxamine administration ameliorated long-term sequelae after GMH.

Introduction

Germinal matrix hemorrhage (GMH) occurs when immature blood vessels rupture within the subventricular tissue in premature infants (Ballabh 2010). GMH occurs in approximately 12000 live births per every year in the US and often results in developmental delays, mental retardation, cerebral palsy, and post-hemorrhagic hydrocephalus, posing significant socioeconomic burdens (Ballabh 2010; Kochanek, Kirmeyer et al. 2012). Because current clinical management is limited, research is needed to investigate innovative therapeutic modalities.

In adult rodent intracerebral hemorrhage and subarachnoid hemorrhage models, red blood cells present in the intraparenchymal tissue are lysed and hemoglobin metabolized to release iron, resulting in a highly oxidative environment and consequent iron toxicity that damages brain tissue (Lee, Keep et al. 2010; Xiong, Wang et al. 2013). Chelation of iron using Deferoxamine improved neurofunctional outcomes after intracerebral hemorrhage and subarachnoid hemorrhage, yet its efficacy has not been evaluated after neonatal GMH (Lee, Keep et al. 2011; Hatakeyama, Okauchi et al. 2013). Blood products and proliferation of extracellular matrix proteins are theorized to disrupt CSF flow dynamics following hemorrhage, leading to consequent post-hemorrhagic hydrocephalus development (Crews, Wyss-Coray et al. 2004).

We hypothesized acute and delayed Deferoxamine treatment will ameliorate extracellular matrix protein proliferation, post-hemorrhagic ventricular dilation, and long-term neurofunctional outcomes after GMH.

Materials and Methods

Animal Surgery and Experimental Groups

All protocols and procedures were approved by the Institutional Animal Care and Use Committee at Loma Linda University. Timed-pregnant rats were purchased from Harlan Laboratories (Indianapolis, IN). Stereotaxic infusion of 0.3 U bacterial collagenase into the right ganglionic eminence was performed to induce GMH in P7 rat pups, as described (Lekic, Manaenko et al. 2012). While some consider P7 rat pups to be equivalent in brain development of a term human infant, recent evidence suggests P7 is closer in brain development to 30-32 week gestation age human infants, which is approximately the point we want to model GMH (Lekic, Manaenko et al. 2012). Briefly, rat pups were anesthetized with isoflurane (3 % in a 30/70 oxygen/medical air mixture) and placed prone with their head secured onto a rodent stereotaxic frame. After sterilizing the rodent's scalp, a small midline incision was made to expose bregma. Next, a cranial burr hole was made 1.8 mm rostral and 1.5 mm right lateral from bregma, using a standard dental drill (1 mm). A 26-gauge needle was inserted through the cranial burr hole and stereotactically lowered 2.8 mm into the brain parenchyma. Following that, bacterial collagenase VII-S (0.3 U, Sigma; St. Louis, MO) was infused into the right hemispheric ganglionic eminence, at a rate of 0.25 µl/minute. Back-leakage of collagenase was prevented by keeping the needle in place for 10 minutes after completed infusion. Following that, the needle was withdrawn at a rate of 1 mm/minute, the burr hole was sealed with bone wax, and the scalp sutured. Sham animals were subjected to needle insertion only. Rat pups were returned to their dams after full recovery from the anesthesia. Forty animals were divided into four groups: Sham, Vehicle (PBS

intraperitoneally BID starting 1 hour post-GMH for 7 days), acute Deferoxamine (100 mg/kg intraperitoneally BID starting 1 hour post-GMH for 7 days), and delayed Deferoxamine (100 mg/kg intraperitoneally BID starting 72 hours post-GMH for 7 days). Each animal group was alternated when undergoing surgeries. Blinded investigators performed the neurobehavioral, histological, and Western blot analyses.

Behavioral Testing

Neurocognitive deficits and motor coordination were evaluated by Morris water maze, rotarod, and foot fault tests between 21-28 days post-GMH (n=10/group). The mentioned neurofunctional tests have been previously utilized for the evaluation of long-term deficits in rodents subjected to unilateral hemorrhagic brain injury (Lekic, Manaenko et al. 2012; Leitzke, Rolland et al. 2013; Rolland, Lekic et al. 2013). All tests were conducted in a blinded fashion. Learning and memory abilities in rats were assessed via the Morris water maze by measuring (1) the swim distance for each animal before detecting a slightly submerged platform in a pool of water (diameter: 110 cm) and (2) the time each animal spent searching the target quadrant, after the platform has been removed from the pool (probe trial). An overhead infrared camera linked to a computerized tracking system (Noldus Ethovision, Tacoma, WA) recorded the swim path and time of each animal. The water maze experiments were conducted on day 21 to 25 post-GMH induction, one block per day followed by the probe trial. Animals that failed to swim or only swam in stationary circles were excluded from further analysis in our study. Motor and coordination function were evaluated on post-operative days 26 to 28. The rotarod apparatus (Columbus Instruments, Columbus, OH), consisting of horizontally rotating

cylinders (7 cm in diameter, 9.5 cm in width) rotate either at constant velocity or accelerate 2 RPM every 5 seconds starting at a speed of 5 or 10 RPM. Continuous walking was required to avoid falling; the latency to fall was recorded for each animal by a photobeam circuit. Foot-fault testing was conducted by placing each animal on a horizontally elevated wire-grid (20 cm x 100 cm) and missteps through the grid were recorded over 2 minutes.

Histopathological Analysis

Ventricular volume, cortical thickness, white matter loss, and basal ganglia loss were calculated in Nissl stained histological brain sections 28 days post-GMH using NIH Image J software (n=5/group). Brain tissue preparation, staining, and volumetric evaluations were conducted as previously described (Lekic, Manaenko et al. 2012; Leitzke, Rolland et al. 2013). Briefly, animals under deep isoflurane anesthesia were euthanized by transcardiac perfusion with PBS and 4% paraformaldehyde. Following that, brains were collected, formalin fixed (in 4% paraformaldehyde for 3 days), dehydrated (in 30 % sucrose for 3 days), and frozen coronal brain slices (10 µl) were obtained, using a cryostat (CM3050S; Leica Microsystems). Nissl stained histological brain sections were evaluated via computer assisted (Image J) hand delineation of cerebral and cerebroventricular structures, based on criteria from stereologic studies using optical dissector principles (Oorschot 1996; Ekinci, Acer et al. 2008). Volumes were calculated as the average delineated area from 10 µm sections taken at approximately 2.5 mm, 1.2 mm, 0.7 mm rostral and 2.9 mm caudal of bregma multiplied by the depth of the cerebroventricular system. The ventricular volume (mm^3) was

calculated as average ventricular area multiplied by the depth of the cerebroventricular system. The cortical thickness was calculated and expressed as ratio of the contralateral brain cortex. Basal ganglia volumes and white matter loss were expressed as % of the sham group. Basal ganglia and white matter volumes were calculated and expressed as % of the sham group by dividing their volumes to the overall average sham volume.

Western Blotting

Fibronectin and vitronectin expressions were quantified by Western blot at 28 days post-GMH (n=5/group). Briefly, whole brain samples were processed according to previously published protocols (Ma, Huang et al. 2011), and equal amounts of protein (50 μg) were separated by SDS-PAGE before being transferred onto nitrocellulose membranes. The latter were then blocked and incubated with the following primary antibodies: anti-fibronectin, anti-vitronectin (1:1000; Abcam) and anti-β-actin (1:4000; Santa Cruz Biotechnology, Santa Cruz, CA). After incubation with the primary and the appropriate secondary antibodies (1:4000; Santa Cruz Biotechnology, Santa Cruz, CA), immunoblots were visualized with the ECL Plus chemiluminescence reagent kit (Amersham Bioscience, Arlington Heights, IL) and bands were quantified using Image J (NIH). Results, expressed as mean±SEM, were normalized to the average values of the sham group.

Statistical Analysis

Sample size estimations were made by power analysis using a type I error rate of 0.05 and a power of 0.8 on a two-sided test. Data are expressed as mean±SEM. Western

blot and histological data were analyzed by one-way ANOVA followed by the Tukey post-hoc test, and behavior data were analyzed by one-way ANOVA on ranks and the Student-Newman-Keuls method. A P value <0.05 was considered statistically significant.

Results

Deferoxamine Improved Brain Morphology after GMH

At 28 days post-GMH, brain morphology was assessed in Nissl stained brain sections (n=5 group). Ventricular volume was found significantly increased in the vehicle group compared to sham, but acute and delayed Deferoxamine treatment significantly reduced GMH-induced ventricular dilation (P<0.05; Figure 3.1.A). Cortical thickness was evaluated as a right hemisphere/left hemisphere ratio to the mean of sham and was significantly decreased in the vehicle group compared to sham-operated animals, but acute and delayed Deferoxamine treatment ameliorated cortical loss (P<0.05, Figure 3.1.B). Basal ganglia volume was evaluated as a percentage to mean sham basal ganglia volume (Figure 3.1.C). Acute and delayed Deferoxamine treated groups had significantly less basal ganglia loss compared to the vehicle group (P<0.05; Figure 3.1.C). White matter loss was evaluated as a percent loss using sham-operated animals as a baseline (Figure 3.1.D). Acute and delayed Deferoxamine treated groups had significantly less white matter loss compared to the vehicle group (P<0.05; Figure 3.1.D).

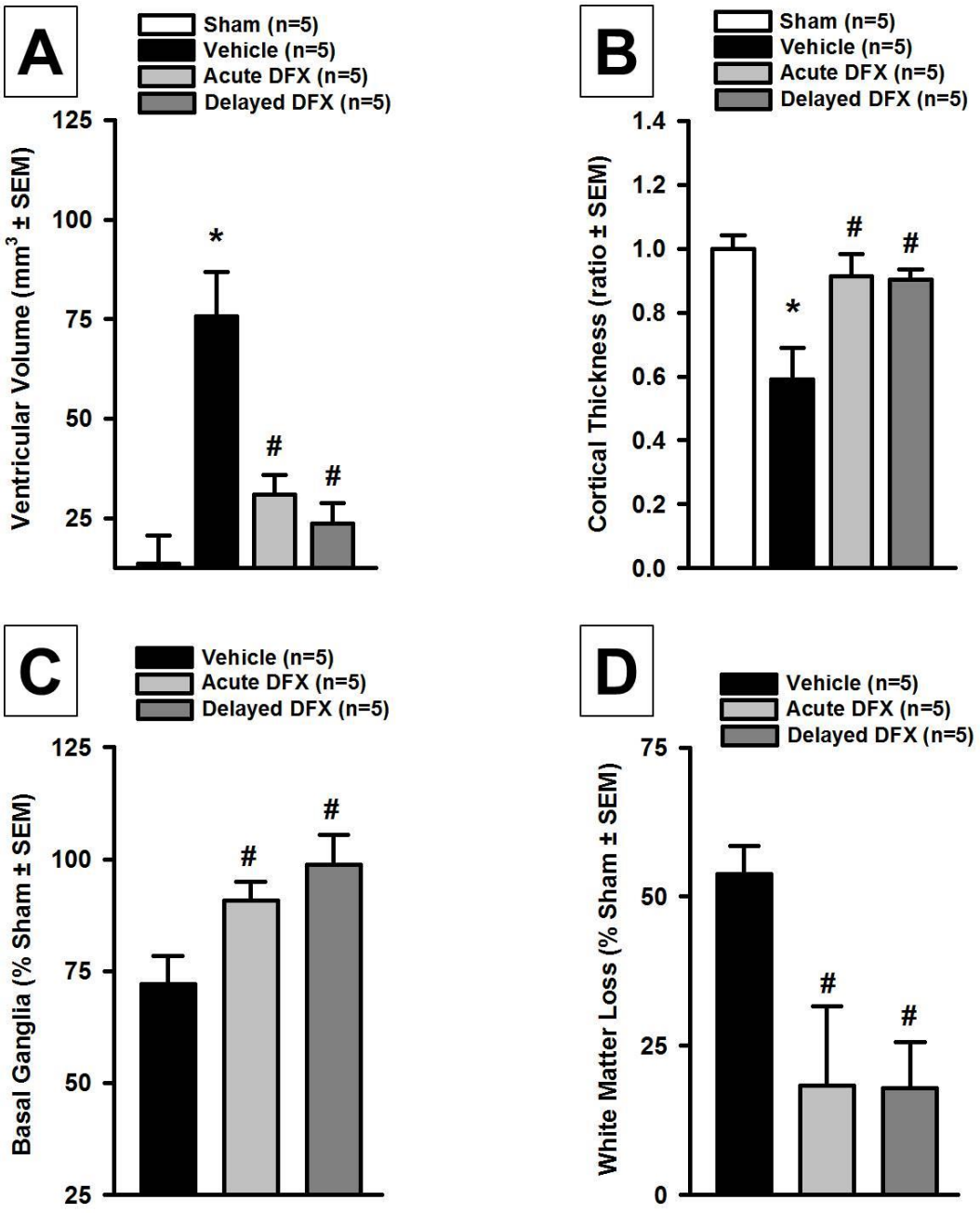

Figure 3.1: Long-term brain morphological outcomes after acute and delayed Deferoxamine treatment at 4 weeks post-GMH. Quantification of (A) ventricular volume, (B) cortical thickness, (C) basal ganglia loss, and (D) white matter loss at 28 days after germinal matrix hemorrhage. Values are expressed as mean±SEM. *P<0.05 compared to sham, and #P<0.05 compared to vehicle. N=5 per group.

Deferoxamine Reduced Extracellular Matrix Protein Expression after GMH

Western blot analyses were conducted at 28 days post-GMH induction (n=5 per group). Fibronectin expression was found increased in the vehicle group compared to sham-operated animals, and acute and delayed Deferoxamine treatment significantly reduced fibronectin expression after GMH ($P<0.05$; Figure 3.2.A). Vitronectin expression was also significantly increased in the vehicle group compared to sham-operated animals, and acute and delayed Deferoxamine treatment tended to reduce vitronectin expression after GMH ($P>0.05$ vs sham; Figure 3.2.B).

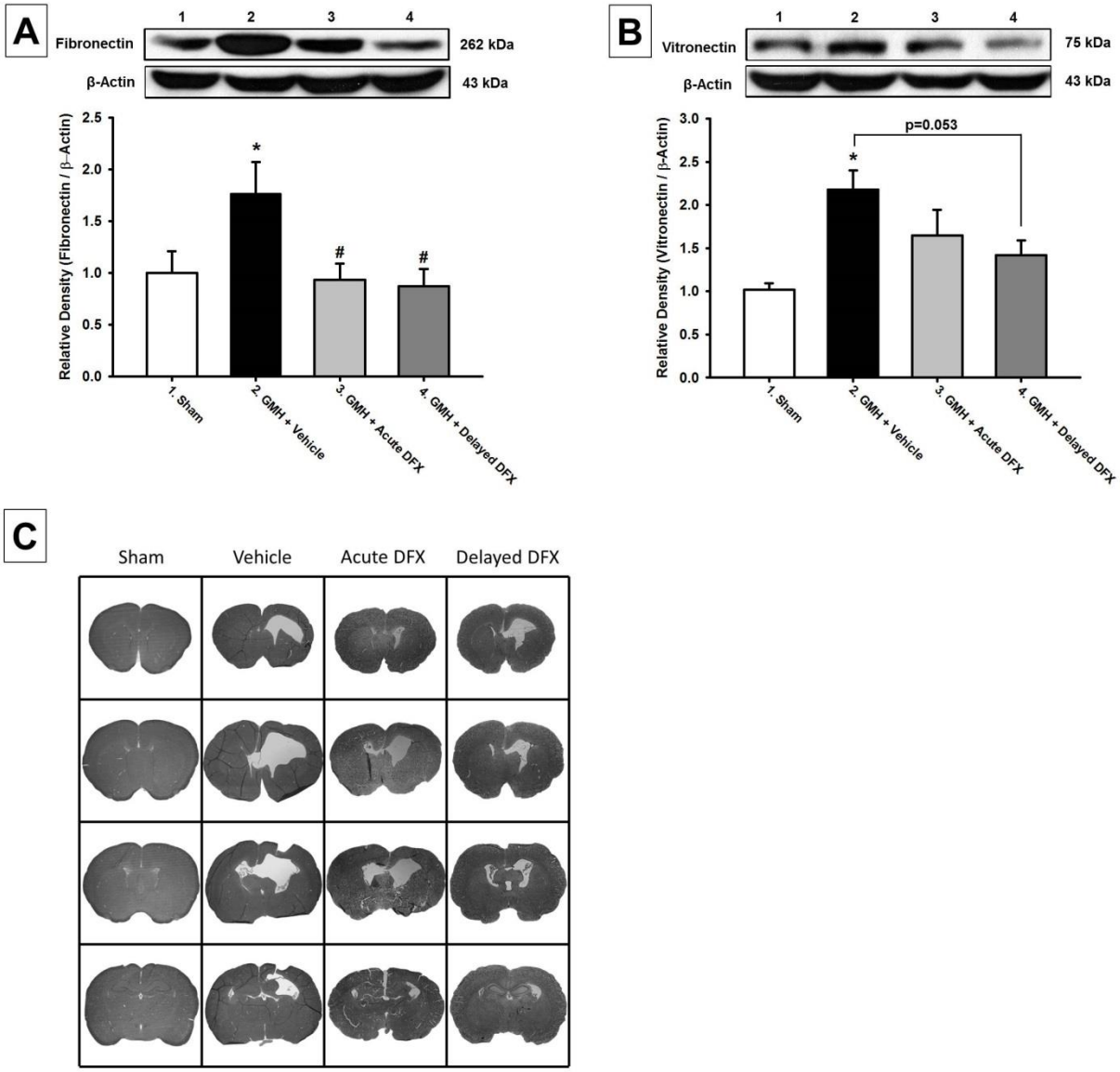

Figure 3.2: Extracellular matrix protein expression levels after acute and delayed Deferoxamine treatment at 4 weeks post-GMH. Western blot analysis of (A) Fibronectin and (B) Vitronectin at 28 days after germinal matrix hemorrhage. Representative microphotographs of Nissl stained brain sections (C) at 28 days after germinal matrix hemorrhage. Values are expressed as mean±SEM. *P<0.05 compared to sham, and #P<0.05 compared to vehicle. N=5 per group.

Deferoxamine Improved Long-term Neurofunctional Outcomes after GMH

Vehicle treated GMH animals demonstrated significant spatial memory loss compared to sham-operated animals in the Morris water maze by swimming greater distances finding the platform ($P<0.05$; Figure 3.3.A) and spending less time in the target quadrant during the probe trials ($P<0.05$; Figure 3.3.B). Acute and delayed treatment animals showed significant cognitive functional recovery by having reduced swimming distances ($P<0.05$; Figure 3.3.A) and tended to spend more time in the target quadrant during the probe trials ($P>0.05$ vs sham; Figure 3.3.B). Furthermore, vehicle animals had significantly more foot faults than sham, but acute and delayed Deferoxamine treated GMH animals had significantly reduced foot faults compared to vehicle ($P<0.05$; Figure 3.3.C). Vehicle animals had significantly worse rotarod performances compared to sham, but acute and delayed Deferoxamine treated animals had significantly better rotarod performances than vehicle rats ($P<0.05$; Figure 3.3.D).

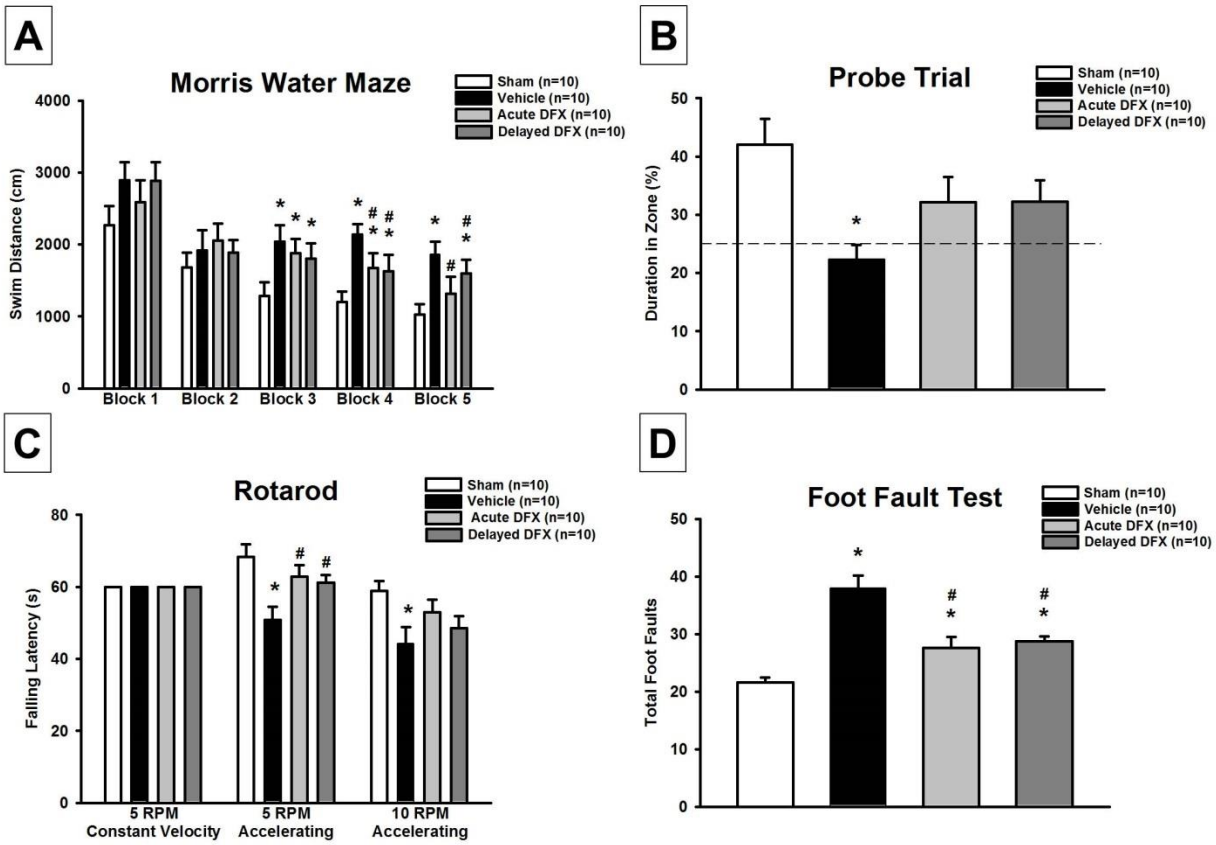

Figure 3.3: Long-term neurocognitive and sensorimotore recovery after acute and delayed Deferoxamine treatment at 3-4 weeks post-GMH. Neurofunctional assessment of (**A**) & (**B**) Morris water maze, (**C**) rotarod, and (**D**) foot fault test at 21-28 days after germinal matrix hemorrhage. Values are expressed as mean±SEM. *P<0.05 compared to sham, and #P<0.05 compared to vehicle. N=10 per group.

Discussion

Iron toxicity is known to play a crucial pathophysiological role in brain injury following hemorrhage, with some evidence indicating iron overload may contribute to hydrocephalus development (Lee, Keep et al. 2010; Chen, Gao et al. 2011; Xiong, Wang et al. 2013). Blood products and extracellular matrix protein proliferation are thought to significantly contribute to post-hemorrhagic hydrocephalus development by disrupting normal cerebrospinal fluid flow in the ventricles (Crews, Wyss-Coray et al. 2004). Deferoxamine treatment attenuated brain injury in adult brain hemorrhage models (Lee, Keep et al. 2011; Hatakeyama, Okauchi et al. 2013), yet it has not been evaluated in neonates nor has it been shown to significantly attenuate neonatal post-hemorrhagic hydrocephalus development and long-term neurofunctional deficits. This study evaluated the efficacy of 1 hour (acute) and 72 hour (delayed) Deferoxamine treatment as a potential therapeutic modality for GMH-induced brain injury, the delayed time point serving as a more clinically relevant treatment regimen. Extracellular matrix protein proliferation is indicative of gliosis and is hypothesized to deposit within the ventricles, disrupting cerebrospinal fluid flow and contributing to post-hemorrhagic hydrocephalus development. Fibronectin and vitronectin were significantly increased in GMH animals compared to sham-operated animals, yet acute and delayed Deferoxamine treated animals had significantly reduced fibronectin and vitronectin expressions compared to vehicle, indicating GMH leads to increased extracellular matrix protein proliferation, which was attenuated by iron chelation.

Additionally, vehicle treated GMH animals demonstrated significantly enlarged ventricular volume, decreased cortical thickness, increased basal ganglia loss, and

increased white matter loss, while acute and delayed Deferoxamine treated animals showed significantly improved brain morphological outcomes across all measures. Consequently, acute and delayed Deferoxamine treated GMH animals had significantly improved spatial memory and motor coordination compared to vehicle animals. Our results corroborate with similar brain hemorrhage animal models depicting Deferoxamine treatment ameliorates post-hemorrhage brain injury. Furthermore, acute and delayed post-GMH iron chelation significantly reduced neonatal post-hemorrhagic ventricular dilation.

Our results suggest that iron toxicity at acute and delayed time points following GMH is associated with post-hemorrhagic ventricular dilation, but the pathophysiological mechanisms remain to be elucidated. The choroid plexus is an epithelial layer in the ventricles specialized for cerebrospinal fluid production and is susceptible to injury following hemorrhage (Simard, Tosun et al. 2011). It also contains high expression levels of iron metabolic proteins relative to other brain tissues (Rouault, Zhang et al. 2009). Iron-overload in the cerebroventricular system following GMH may adversely affect normal functioning of the choroid plexus, leading to pathologically increased cerebrospinal fluid production. Another possible explanation is GMH-induced cerebroventricular iron overload destroys subarachnoid granulations, as is observed in subarachnoid hemorrhage, reducing overall cerebrospinal fluid reabsorption (Okubo, Strahle et al. 2013). Further investigations are needed to determine mechanisms linking GMH-induced iron toxicity with long-term post-hemorrhagic ventricular dilation.

Our study is the first to show Deferoxamine attenuates long-term neurocognitive and sensorimotor deficits, improves overall brain morphology, and reduces post-

hemorrhagic ventricular dilation following GMH when treatment is initiated as late as 72 hours post-ictus in neonates, providing evidence for a potentially clinically translatable therapeutic modality.

References

Ballabh P (2010). "Intraventricular Hemorrhage in Premature Infants: Mechanism of Disease." Pediatr Res **67**(1): 1-8.

Chen Z, Gao C, Hua Y, Keep RF, Muraszko K, and Xi G (2011). "Role of Iron in Brain Injury after Intraventricular Hemorrhage." Stroke **42**(2): 465-470.

Crews L, Wyss-Coray T, and Masliah E (2004). "Insights into the Pathogenesis of Hydrocephalus from Transgenic and Experimental Animal Models." Brain Pathol **14**(3): 312-316.

Ekinci N, Acer N, Akkaya A, Sankur S, Kabadayi T, and Sahin B (2008). "Volumetric Evaluation of the Relations among the Cerebrum, Cerebellum and Brain Stem in Young Subjects: A Combination of Stereology and Magnetic Resonance Imaging." Surg Radiol Anat **30**(6): 489-494.

Hatakeyama T, Okauchi M, Hua Y, Keep RF, and Xi G (2013). "Deferoxamine Reduces Neuronal Death and Hematoma Lysis after Intracerebral Hemorrhage in Aged Rats." Transl Stroke Res **4**(5): 546-553.

Kochanek KD, Kirmeyer SE, Martin JA, Strobino DM, and Guyer B (2012). "Annual Summary of Vital Statistics: 2009." Pediatrics **129**(2): 338-348.

Lee JY, Keep RF, He Y, Sagher O, Hua Y, and Xi G (2010). "Hemoglobin and Iron Handling in Brain after Subarachnoid Hemorrhage and the Effect of Deferoxamine on Early Brain Injury." J Cereb Blood Flow Metab **30**(11): 1793-1803.

Lee JY, Keep RF, Hua Y, Ernestus RI, and Xi G (2011). "Deferoxamine Reduces Early Brain Injury Following Subarachnoid Hemorrhage." Acta Neurochir Suppl **112**: 101-106.

Leitzke AS, Rolland WB, Krafft PR, Lekic T, Klebe D, Flores JJ, Van Allen NR, Applegate RL, 2nd, and Zhang JH (2013). "Isoflurane Post-Treatment Ameliorates Gmh-Induced Brain Injury in Neonatal Rats." Stroke **44**(12): 3587-3590.

Lekic T, Manaenko A, Rolland W, Krafft PR, Peters R, Hartman RE, Altay O, Tang J, and Zhang JH (2012). "Rodent Neonatal Germinal Matrix Hemorrhage Mimics the Human Brain Injury, Neurological Consequences, and Post-Hemorrhagic Hydrocephalus." Exp Neurol **236**(1): 69-78.

Ma Q, Huang B, Khatibi N, Rolland W, 2nd, Suzuki H, Zhang JH, and Tang J (2011). "Pdgfr-Alpha Inhibition Preserves Blood-Brain Barrier after Intracerebral Hemorrhage." Ann Neurol **70**(6): 920-931.

Okubo S, Strahle J, Keep RF, Hua Y, and Xi G (2013). "Subarachnoid Hemorrhage-Induced Hydrocephalus in Rats." Stroke **44**(2): 547-550.

Oorschot DE (1996). "Total Number of Neurons in the Neostriatal, Pallidal, Subthalamic, and Substantia Nigral Nuclei of the Rat Basal Ganglia: A Stereological Study Using the Cavalieri and Optical Disector Methods." J Comp Neurol **366**(4): 580-599.

Rolland WB, Lekic T, Krafft PR, Hasegawa Y, Altay O, Hartman R, Ostrowski R, Manaenko A, Tang J, and Zhang JH (2013). "Fingolimod Reduces Cerebral Lymphocyte Infiltration in Experimental Models of Rodent Intracerebral Hemorrhage." Exp Neurol **241**: 45-55.

Rouault TA, Zhang DL, and Jeong SY (2009). "Brain Iron Homeostasis, the Choroid Plexus, and Localization of Iron Transport Proteins." Metab Brain Dis **24**(4): 673-684.

Simard PF, Tosun C, Melnichenko L, Ivanova S, Gerzanich V, and Simard JM (2011). "Inflammation of the Choroid Plexus and Ependymal Layer of the Ventricle Following Intraventricular Hemorrhage." Transl Stroke Res **2**(2): 227-231.

Xiong XY, Wang J, Qian ZM, and Yang QW (2013). "Iron and Intracerebral Hemorrhage: From Mechanism to Translation." Transl Stroke Res.

CHAPTER FOUR

PROTEASE-ACTIVATED RECEPTOR 1 AND 4 SIGNAL INHIBITION REDUCES PRETERM NEONATAL HEMORRHAGIC BRAIN INJURY

Tim Lekic, MD, PhD[1, 2]; Damon Klebe, BA[1]; Devin W McBride, PhD[1]; Anatol Manaenko, PhD[1]; William B. Rolland, BS[1]; Jerry J. Flores, BS[1]; Orhan Altay, MD[1]; Jiping Tang, MD[1]; and John H. Zhang, MD, PhD[1, 3]

Departments of Physiology and Pharmacology,[1] Neurology,[2] and Neurosurgery,[3] Loma Linda University School of Medicine, Loma Linda, California, 92354, U.S.A.

Published: *Stroke*. 2015 Jun; 46(6): 1710-3.

Abstract

This study examines the role of thrombin's protease-activated receptors (PAR)-1, PAR-4 in mediating cyclooxygenase-2 and mammalian target of rapamycin following germinal matrix hemorrhage. Germinal matrix hemorrhage was induced by intraparenchymal infusion of bacterial collagenase into the right ganglionic eminence of P7 rat pups. Animals were treated with either PAR-1, PAR-4, cyclooxygenase-2, or mammalian target of rapamycin inhibitors by 1 hour and up to ≤5 days. We found increased thrombin activity 6 to24 hours after germinal matrix hemorrhage,, and PAR-1, PAR-4 inhibition normalized cyclooxygenase-2 and mammalian target of rapamycin by 72 hours. Early treatment with NS398 or rapamycin substantially improved long-term outcomes in juvenile animals. Suppressing early PAR signal transduction, and postnatal NS398 or rapamycin treatment, may help reduce germinal matrix hemorrhage severity in susceptible preterm infants.

Introduction

Germinal matrix hemorrhage (GMH) is the leading cause of mortality and morbidity from prematurity because this brain region is selectively vulnerable to spontaneous bleeding within the first 72 hours of preterm life (Ballabh 2010). Cerebroventricular expansion contributes to long-term injury through mechanical compression of surrounding brain tissues (Aquilina, Chakkarapani et al. 2011). Neurological outcomes include hydrocephalus, mental retardation, and cerebral palsy (Ballabh 2010; Heron, Sutton et al. 2010). Current neonatal intensive care treatments are ineffective at preventing GMH, and neurosurgical shunts are prone to devastating complications (Whitelaw 2001).

Importantly, the blood constituent thrombin has been identified as a causative factor in hydrocephalus formation (Gao, Liu et al. 2014). Thrombin activates a subfamily of G protein-coupled receptors, named proteinase-activated receptors (PAR; specifically PAR-1 and PAR-4) (Kataoka, Hamilton et al. 2003), leading to phosphorylation and activation of mammalian target of rapamycin (mTOR) (Jiang, Zhu et al. 2008) and increased cyclooxygenase (COX)-2 expression (Lo, Chen et al. 2009).

Therefore, we hypothesized that modulation of the thrombin- (PAR)-1,-4 – (COX)-2/ mTOR pathway could be a promising strategy to improve outcomes after GMH.

Materials and Methods

Animal Surgeries

All studies, protocols, and procedures were approved by the Loma Linda

University IACUC. One hundred and fifty-seven P7 rat pups (comparable with human 30-32 gestational weeks (Lekic, Manaenko et al. 2012); 14–19 g; Harlan Laboratories, Indianapolis, IN) were randomly subjected to either GMH or sham operations. The number of pups needed for the experiments and study mechanisms was accounted for in each test group. The sample size estimates for all groups assumed type 1 error rate = 0.05 and power = 0.8 on a two-sided test. Sample size estimates were then made using data from our previous experiments (per previous assumptions, mean values, standard deviation, and up to a 20% change in means). A stereotactically guided, 0.3 U bacterial collagenase infusion model was used to mimic preterm right-sided ganglionic eminence bleeds (Lekic, Manaenko et al. 2012; Leitzke, Rolland et al. 2013; Manaenko, Lekic et al. 2014) (except for the cohort using either heat-deactivated collagenase, 30µl of donor blood, or corresponding amount of thrombin [5U], directly injected into the ventricles to study hydrocephalus). Time pregnant rats were purchased from Harlan Laboratories (Indianapolis, IN) and pups of both genders were subjected to spontaneous germinal matrix hemorrhage (GMH) using collagenase infusion (Lekic, Manaenko et al. 2012). Briefly, general anesthesia was achieved by isoflurane (3% in 30/70% Oxygen/Medical Air). The anesthetized rat pup was positioned prone, with its head secured onto a neonatal stereotactic frame (Kopf Instruments, Tujunga, CA). Next, the scalp was sterilized (using betadine solution), and a small midline incision was made to expose the bregma. Then, a 1 mm cranial burr hole was made using a standard dental drill (coordinates from bregma: 1.8 mm anterior, 1.5 mm lateral, 2.8 mm in depth) through which a 26-gauge needle was stereotaxically lowered into the rodent's brain. At this position, clostridial collagenase VII-S (0.3 U, Sigma; St. Louis, MO) was infused at a rate of 0.25µl/min into the right

striatum. The needle was left in place for 10 minutes following infusion completion to prevent backflow of collagenase. Thereafter, the needle was slowly withdrawn at a rate of 1mm/min; the burr hole was sealed with bone wax; and the scalp was sutured closed. All animals were allowed to recover under observation on a 37°C warm heating blanket before being returned to their dams. Shams received needle insertion only without collagenase infusion.

Tissue Processing and Analysis

Rats were euthanized at 72 hours (for Western blot) at various time points between 6 hrs and 21 days (for thrombin assay), and after 28 days (for neuropathological analysis) post-GMH, and analyzed by blinded experts (Lekic, Manaenko et al. 2012; Leitzke, Rolland et al. 2013; Manaenko, Lekic et al. 2014). Standard protocols (Lekic, Manaenko et al. 2012; Leitzke, Rolland et al. 2013; Manaenko, Lekic et al. 2014) were used for Western blot analysis at 72 hours post-GMH. Briefly, deeply anesthetized pups were transcardially perfused using 50ml PBS, and the whole brain tissue samples were collected. Both hemispheres (i.e. bilateral forebrain) were placed into a single test tube for further analysis. Following tissue preparation and protein extractions of the bilateral hemispheres, western blotting was performed using the following primary antibodies: anti-COX-2 (1:200; Cayman Chemical, Ann Arbor, MI), or anti-phospho-mTOR (1:1000; Cell Signaling Technology, Danvers, MA). The appropriate secondary antibodies were obtained from Santa Cruz Biotechnology (Santa Cruz, CA). Immunoblots were visualized using ECL Plus chemiluminescence kit (Amersham Bioscience, Arlington Heights, IL) and further semi-quantitatively analyzed using Image

J (4.0, Media Cybernetics, Silver Springs, MD). Results are expressed as a relative density ratio, adjusted to sham.

Standard protocols (Lekic, Manaenko et al. 2012; Leitzke, Rolland et al. 2013; Manaenko, Lekic et al. 2014) were used for Thrombin assay. Briefly, animals were transcardially perfused with phosphate-buffered saline at 6 hours, 1 day, 5 days, 7 days, 10 days, and 21 days after GMH. Brain samples were then homogenized and thrombin activity was measured using the thrombin-specific chromogenic substrate, S2238 (Anaspec, Fremont, CA) as previously described (Gong, Xi et al. 2008). The final concentration of the s2238 solution was 20mM in phosphate-buffered saline. Thrombin standards were made using rat thrombin (Sigma Aldrich, St. Louis, MO) at concentrations of 0, 1.5625, 3.125, 6.25, 12.5, 25, and 50 mU/ml. Reaction mixtures consisted of 10 µl of brain sample supernatant and 1.5ul of the s2238 chromogenic substrate mixture, which were then added to 90 µl of phosphate-buffered saline. Reaction mixtures were allowed to incubate for 1hr at room temperature, after which the sample absorbance were spectrophotometrically measured at 405 nm.

Standard protocols (Lekic, Manaenko et al. 2012; Leitzke, Rolland et al. 2013; Manaenko, Lekic et al. 2014) were used for histopathological analysis at 28 days post-GMH. Briefly, deeply anesthetized pups were transcardially perfused using 50 ml ice-cold PBS and 10% paraformaldehyde. Whole brain tissue samples were post-fixed in 10% paraformaldehyde solution (at 4°C for 3 days), then dehydrated in 30% sucrose for the same amount of time. 10 µm frozen coronal brain sections were cut every 600 µm using the cryostat (CM3050S, Leica Microsystems), then mounted, and cresyl violet stained on poly-L-lysine-coated slides. Morphometric analysis was conducted using

computer-assisted (ImageJ 4.0, Media Cybernetics, Silver Spring, MD) hand delineation of the ventricle system (lateral, third, cerebral aqueduct, and fourth), hemisphere (cortex, subcortex), corpus callosum (white matter), caudate, thalamus, and hippocampus. Borderlines of these structures are based on criteria derived from stereologic studies using optical dissector principles (Oorschot 1996; Ekinci, Acer et al. 2008; Lekic, Manaenko et al. 2012; Leitzke, Rolland et al. 2013; Manaenko, Lekic et al. 2014). Volumes were calculated: (Average [(Area of coronal section) × Interval × Number of sections]).

Animal Treatments and Experimental Groups

For the 72-hour (short-term; n=49) western blot study: GMH animals received i.p. co-injections of PAR-1 (SCH79797) and PAR-4 (P4pal-10) antagonists (1, 3, 7, 10, or 15 mg/kg given 1, 24, and 48 hrs post-GMH). For thrombin assay time-course study (n=49, n=7/per time point); GMH animals were euthanized at 0 hour, 6 hours, 1 day, 5 days, 7 days, 10 days, and 21 days after GMH. For the 28-day (long-term; n=26) study, COX-2 (NS398) or mTOR (rapamycin) treatment consisted of six intraperitoneal. injections (1, 6, 24, 36, 48, and 60 hours after GMH). Inhibitors were prepared using distilled water containing five percent Dimethyl Sulfoxide (DMSO) solvent. Controls received the vehicle (5% DMSO). All drugs were purchased from Sigma-Aldrich (St. Louis, MO).[10-11]

Assessment of Neurological Deficits

Cognitive (T-maze, Water-maze) and sensorimotor (Rotarod, Foot Fault) testing from 21 to 28 days post-GMH was performed by experienced blinded investigators as

described (Leitzke, Rolland et al. 2013; Manaenko, Lekic et al. 2014). Briefly, the T-Maze1-2 assessed short-term (working) memory ability. For each trial, the pup was placed into the stem (40cm×10cm) and allowed to explore until either the left or right arm was chosen. From the sequence of 10 trials, the rate of spontaneous alternation (0% = none and 100% = complete; alternations/trial) was calculated. The Morris Water-maze (Lekic, Manaenko et al. 2012; Leitzke, Rolland et al. 2013; Manaenko, Lekic et al. 2014) measured spatial learning and memory on three daily blocks. The apparatus consists of a metal pool (110cm diameter) filled with water to within 15cm of the upper edge and containing a small platform (11cm diameter) for the animal to climb onto. The swim path length was digitally analyzed by Noldus Ethovision tracking software. Cued trials (maximum of 60 sec/trial) measured general associative learning, sensorimotor ability, and motivation to escape the water with the platform visible above the water surface. The platform's location changed every other trial. Spatial trials (maximum of 60 sec/trial) measured spatial learning with the platform submerged, but discoverable. Probe trials measured spatial memory by recording the amount of time in the target quadrant after the escape platform was removed. For the rotarod (Lekic, Manaenko et al. 2012; Leitzke, Rolland et al. 2013), this test assessed motor and coordination ability. The apparatus (Columbus Instruments, Columbus, OH) consists of a horizontally rotating cylinder requiring continuous walking in order to avoid falling (7 cm diameter, 9.5 cm width) and programmed to either maintain a constant velocity, or to accelerate 2 rpm every 5 sec. The time to fall was recorded by photobeam circuit. For Foot Fault testing (Lekic, Manaenko et al. 2012; Manaenko, Lekic et al. 2014), this documented the number of completed limb missteps through the openings while the animal explored an elevated

wire (3mm) grid (20cmx100cm) over 120sec. All neurobehavior assessments were conducted in a blinded fashion by experienced investigators.

Statistical Analysis

P values of <0.05 were considered statistically significant. Neurobehavioral data were analyzed using one-way ANOVA on ranks with Student–Newman–Keuls post-hoc test. All other data were analyzed by one-way ANOVA with Tukey post-hoc test. Data are expressed as mean±SEM.

Results

GMH Activated Thrombin

Thrombin activity increased at 6 and 24 hours following collagenase infusion compared to sham ($P<0.05$), and then normalized over 5 to 21 days (Figure 4.1.B).

Molecular Mediators of Post-hemorrhagic Hydrocephalus

Post-hemorrhagic hydrocephalus at 28 days was greatest in the group receiving direct intraparenchymal infusion of collagenase into the ganglionic eminence ($P<0.05$; Figure 4.1.C-D) compared with intracerebroventricular injections of collagenase, heat-deactivated collagenase, donor blood, or thrombin.

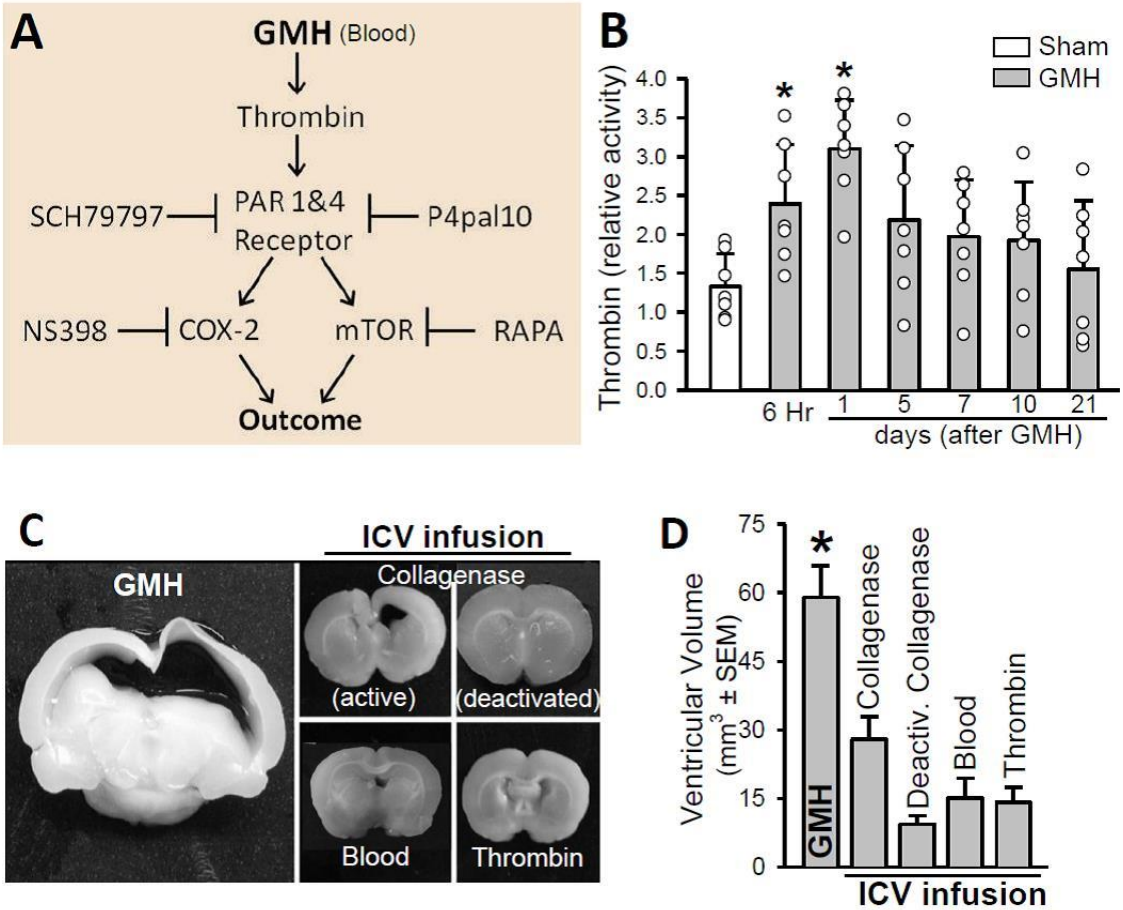

Figure 4.1: Thrombin activity after germinal matrix hemorrhage and association between specific GMH model elements and post-hemorrhagic ventricular dilation development. (A) Proposed mechanism. (B) Time-course of thrombin activity (n=7/group; * $P<0.05$ compared with sham). (C) Representative 2mm coronal brain section pictographs (28 days after infusion). (D) Quantification of ventricular volume (n=6/group; * $P<0.05$ compared with vehicle). ICV indicates intracerebroventricular; RAPA, rapamycin.

Western Blots

Early PAR-1 and PAR-4 signal inhibition reduced mTOR phosphorylation and COX-2 expression ($P<0.05$; Figure 4.2A-B) in a dose responsive fashion at 72 hours post-GMH induction.

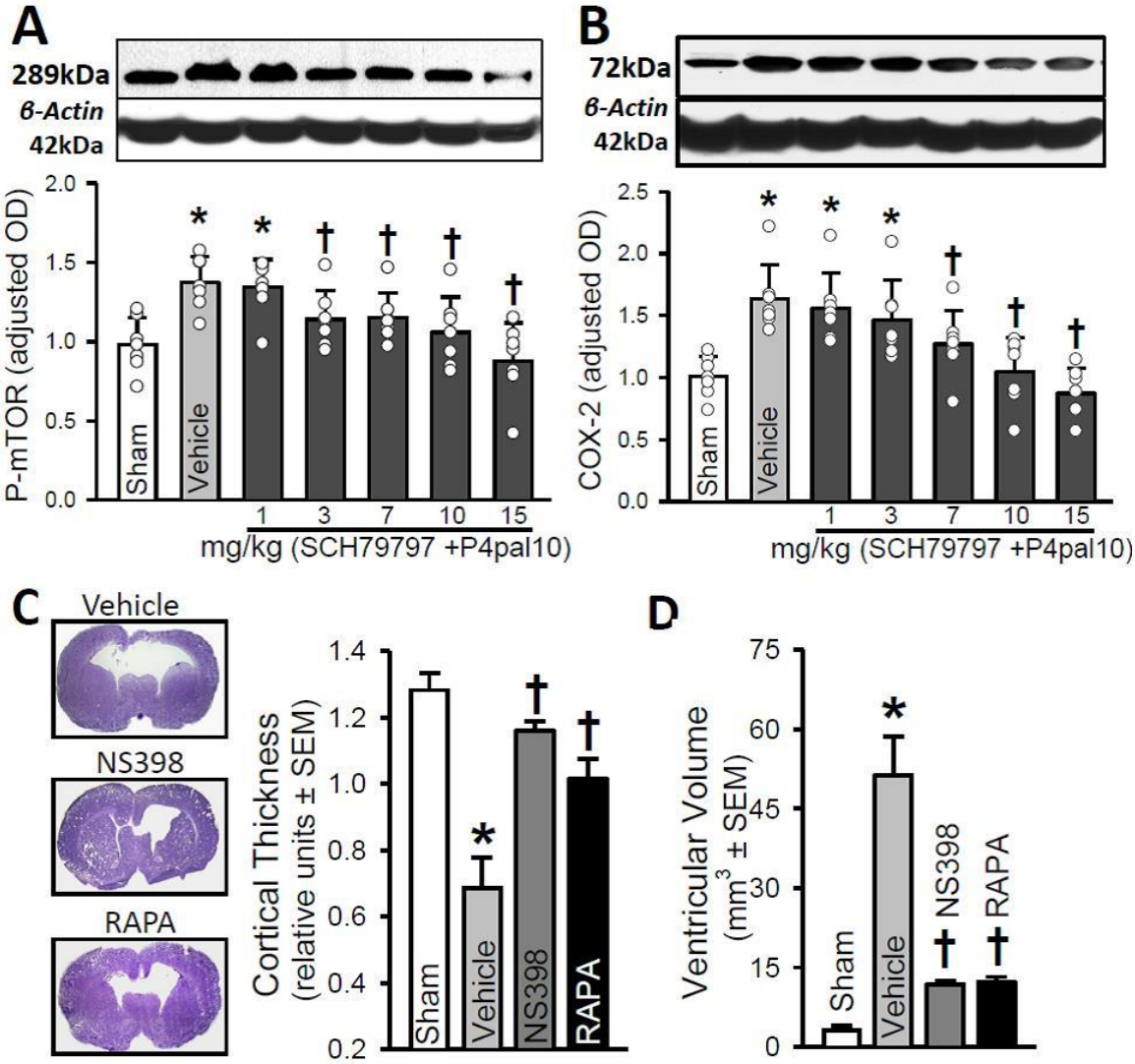

Figure 4.2: Dose-response changes of COX-2 and p-mTOR expression after combinatorial PAR-1 and PAR-4 inhibition at 72 hours post-GMH as well as long-term brain morphological outcomes after COX-2 or mTOR inhibition at 4 weeks post-GMH. (A- B) Western blot analyses of p-mTOR (left) and COX-2 expression (right) at 72 hours after GMH (n=7/group). (C) Representative Nissl stained brain micrograph sections (left), quantification of cortical thickness (right) and (D) ventricular volume at 28 days after GMH. * $P<0.05$ compared with sham; † $P<0.05$ compared with vehicle.

Early Signal Inhibition Improved Long-term Outcomes

Treatments using either COX-2 or mTOR inhibitors significantly ameliorated long-term cortical thickness, ventricular volume ($P<0.05$; Figures 4.2.C-D), and neurodeficits (Figure 4.3.A-D) compared to vehicle treated animals at 28 days post-GMH.

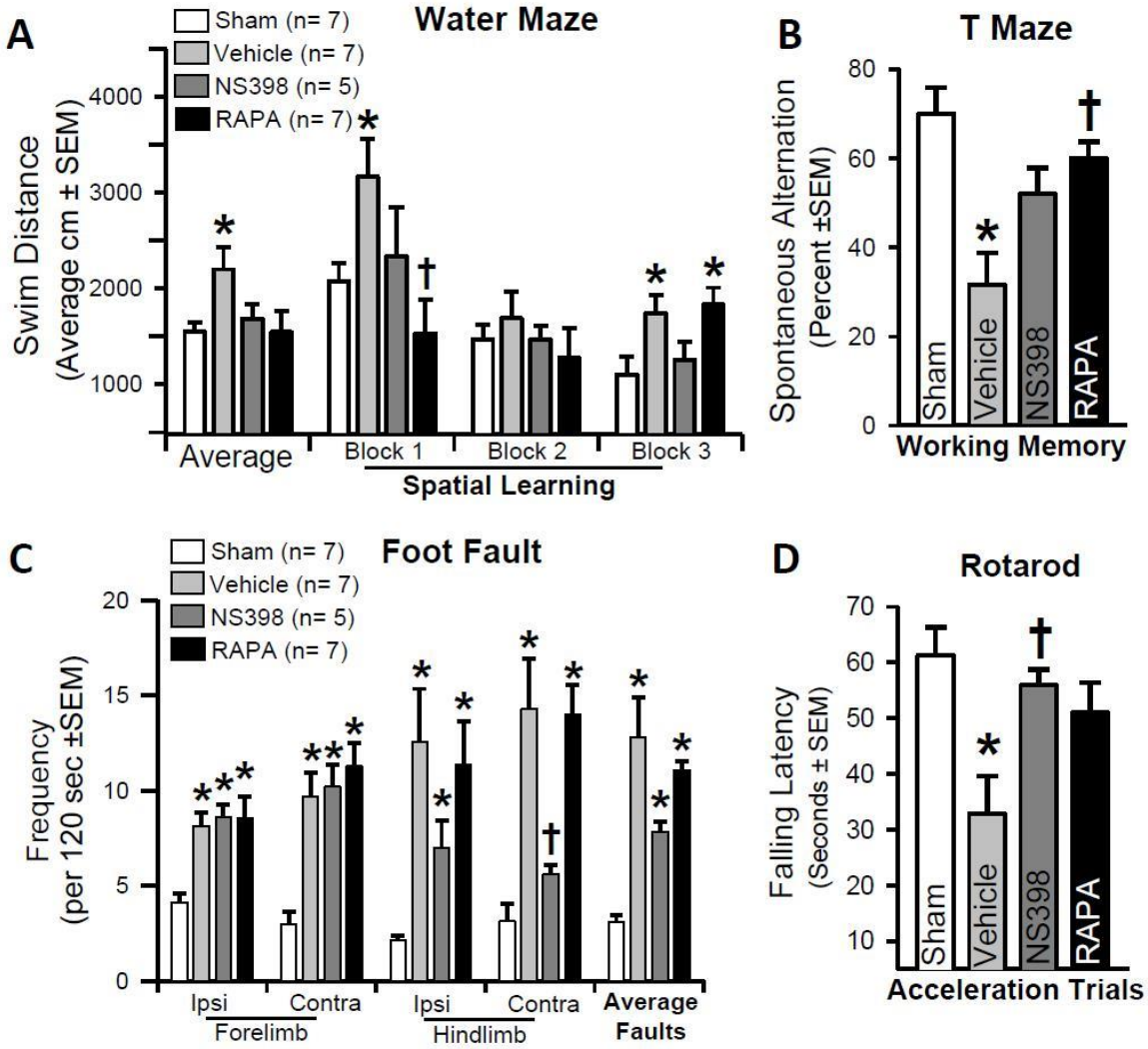

Figure 4.3: Long-term neurocognitive and sensorimotor outcomes after COX-2 or mTOR inhibition at 3-4 weeks post-GMH. Neurological assessments at 21-28 days after GMH using **A.** Morris water maze, **B.** T-maze, **C.** Foot fault, and **D.** Rotarod test (n=5-7/group). * $P<0.05$ compared with sham; † $P<0.05$ compared with vehicle.

Discussion

This study investigated the effectiveness of modulating thrombin- PAR-1 and PAR-4 in reversing COX-2 and p-mTOR upregulation, as well as the effect of direct COX-2 and p-mTOR inhibition upon post-hemorrhagic hydrocephalus and neurological deficits. Previous studies hypothesized the mechanism of hydrocephalus involved increased production of infiltrating extracellular matrix proteins throughout the cerebroventricular system, leading to the disruption of CSF outflow (Crews, Wyss-Coray et al. 2004; Ballabh 2010; Aquilina, Chakkarapani et al. 2011; Strahle, Garton et al. 2012; Manaenko, Lekic et al. 2014). Our results suggest that thrombin-induced PAR-1, PAR-4 stimulation upregulates detrimental signaling: exacerbating inflammatory (COX-2 mediated) and proliferative responses (p-mTOR mediated) that are potentially upstream of extracellular matrix protein dysregulation (Jiang, Zhu et al. 2008; Lo, Chen et al. 2009; Ballabh 2010; Lekic, Manaenko et al. 2012; Gao, Du et al. 2014; Gao, Liu et al. 2014; Manaenko, Lekic et al. 2014).Multiple parallels (especially with thrombin) (Jiang, Zhu et al. 2008; Lo, Chen et al. 2009; Ballabh 2010; Aquilina, Chakkarapani et al. 2011; Lekic, Manaenko et al. 2012; Leitzke, Rolland et al. 2013; Manaenko, Lekic et al. 2014) exist between our study and the pathophysiology of adult intracerebral hemorrhage (Whitelaw 2001; Crews, Wyss-Coray et al. 2004; Strahle, Garton et al. 2012; Gao, Du et al. 2014; Gao, Liu et al. 2014). Thus, in extension, our findings may have a much broader therapeutic implication in terms of further adult stroke mechanistic study (Keep, Zhou et al. 2014).

To address the question of molecular mediators of GMH, our first aim demonstrated that intraparenchymal infusion of collagenase generated the majority of

hydrocephalus. This is likely the sum contribution of blood products (Gao, Du et al. 2014) (red blood cell lysis and inflammation) and thrombin. In fact, thrombin demonstrated greatest activity in the acute phase, between 6 and 24 hours post-ictus, with tendency to remain elevated $\leq$10 days and normalized by 21 days.

We next hypothesized that thrombin binds to PAR-1, PAR-4 receptors, and consequently upregulates COX-2 and p-mTOR. Because thrombin is most active in the acute phase, we examined levels at 72 hours post-ictus and determined COX-2 and p-mTOR were significantly greater in vehicle treated animals than in sham. Furthermore, inhibiting PAR-1, PAR-4 using SCH79797 (PAR-1 antagonist) and p4pal10 (PAR-4 antagonist) significantly normalized COX-2 and p-mTOR levels at 72 hours.

Then, we asked whether directly inhibiting COX-2 or p-mTOR after GMH could circumvent long-term post-hemorrhagic ventricular dilation, cortical cell loss, and improve sensorimotor and neurocognitive outcomes. Our findings demonstrated that vehicle treated animals had significantly worsened outcomes compared to shams, and treating with either NS398 (COX-2 inhibitor) or rapamycin (mTOR inhibitor) significantly improved brain neuropathology and neurological ability. Thus, by attenuating early inflammatory (COX-2), and proliferative (p-mTOR) signaling pathways, we improved long-term outcomes in the juvenile animals.

In summary, this study is the first to show thrombin-PAR-1, thrombin-PAR-4 signal inhibition normalizing early COX-2 and p-mTOR expression levels, and this, in turn, improving long-term neurological outcomes after GMH.

References

Aquilina K, Chakkarapani E, Love S, and Thoresen M (2011). "Neonatal Rat Model of Intraventricular Haemorrhage and Post-Haemorrhagic Ventricular Dilatation with Long-Term Survival into Adulthood." Neuropathol Appl Neurobiol **37**(2): 156-165.

Ballabh P (2010). "Intraventricular Hemorrhage in Premature Infants: Mechanism of Disease." Pediatr Res **67**(1): 1-8.

Crews L, Wyss-Coray T, and Masliah E (2004). "Insights into the Pathogenesis of Hydrocephalus from Transgenic and Experimental Animal Models." Brain Pathol **14**(3): 312-316.

Ekinci N, Acer N, Akkaya A, Sankur S, Kabadayi T, and Sahin B (2008). "Volumetric Evaluation of the Relations among the Cerebrum, Cerebellum and Brain Stem in Young Subjects: A Combination of Stereology and Magnetic Resonance Imaging." Surg Radiol Anat **30**(6): 489-494.

Gao C, Du H, Hua Y, Keep RF, Strahle J, and Xi G (2014). "Role of Red Blood Cell Lysis and Iron in Hydrocephalus after Intraventricular Hemorrhage." J Cereb Blood Flow Metab **34**(6): 1070-1075.

Gao F, Liu F, Chen Z, Hua Y, Keep RF, and Xi G (2014). "Hydrocephalus after Intraventricular Hemorrhage: The Role of Thrombin." J Cereb Blood Flow Metab **34**(3): 489-494.

Gong Y, Xi G, Hu H, Gu Y, Huang F, Keep RF, and Hua Y (2008). "Increase in Brain Thrombin Activity after Experimental Intracerebral Hemorrhage." Acta Neurochir Suppl **105**: 47-50.

Heron M, Sutton PD, Xu J, Ventura SJ, Strobino DM, and Guyer B (2010). "Annual Summary of Vital Statistics: 2007." Pediatrics **125**(1): 4-15.

Jiang X, Zhu S, Panetti TS, and Bromberg ME (2008). "Formation of Tissue Factor-Factor Viia-Factor Xa Complex Induces Activation of the Mtor Pathway Which Regulates Migration of Human Breast Cancer Cells." Thromb Haemost **100**(1): 127-133.

Kataoka H, Hamilton JR, McKemy DD, Camerer E, Zheng YW, Cheng A, Griffin C, and Coughlin SR (2003). "Protease-Activated Receptors 1 and 4 Mediate Thrombin Signaling in Endothelial Cells." Blood **102**(9): 3224-3231.

Keep RF, Zhou N, Xiang J, Andjelkovic AV, Hua Y, and Xi G (2014). "Vascular Disruption and Blood-Brain Barrier Dysfunction in Intracerebral Hemorrhage." Fluids Barriers CNS **11**: 18.

Leitzke AS, Rolland WB, Krafft PR, Lekic T, Klebe D, Flores JJ, Van Allen NR, Applegate RL, 2nd, and Zhang JH (2013). "Isoflurane Post-Treatment Ameliorates Gmh-Induced Brain Injury in Neonatal Rats." Stroke **44**(12): 3587-3590.

Lekic T, Manaenko A, Rolland W, Krafft PR, Peters R, Hartman RE, Altay O, Tang J, and Zhang JH (2012). "Rodent Neonatal Germinal Matrix Hemorrhage Mimics the Human Brain Injury, Neurological Consequences, and Post-Hemorrhagic Hydrocephalus." Exp Neurol **236**(1): 69-78.

Lo HM, Chen CL, Tsai YJ, Wu PH, and Wu WB (2009). "Thrombin Induces Cyclooxygenase-2 Expression and Prostaglandin E2 Release Via Par1 Activation and Erk1/2- and P38 Mapk-Dependent Pathway in Murine Macrophages." J Cell Biochem **108**(5): 1143-1152.

Manaenko A, Lekic T, Barnhart M, Hartman R, and Zhang JH (2014). "Inhibition of Transforming Growth Factor-Beta Attenuates Brain Injury and Neurological Deficits in a Rat Model of Germinal Matrix Hemorrhage." Stroke **45**(3): 828-834.

Oorschot DE (1996). "Total Number of Neurons in the Neostriatal, Pallidal, Subthalamic, and Substantia Nigral Nuclei of the Rat Basal Ganglia: A Stereological Study Using the Cavalieri and Optical Disector Methods." J Comp Neurol **366**(4): 580-599.

Strahle J, Garton HJ, Maher CO, Muraszko KM, Keep RF, and Xi G (2012). "Mechanisms of Hydrocephalus after Neonatal and Adult Intraventricular Hemorrhage." Transl Stroke Res **3**(Suppl 1): 25-38.

Whitelaw A (2001). "Intraventricular Haemorrhage and Posthaemorrhagic Hydrocephalus: Pathogenesis, Prevention and Future Interventions." Semin Neonatol **6**(2): 135-146.

CHAPTER FIVE

DABIGATRAN AMELIORATES POST-HAEMORRHAGIC HYDROCEPHALUS DEVELOPMENT AFTER GERMINAL MATRIX HAEMORRHAGE IN NEONATAL RAT PUPS

Damon Klebe[1], Jerry J Flores[1], Devin W McBride[1], Paul R Krafft[1], William B Rolland[1], Tim Lekic[1], John H Zhang[1, 2]

[1]Department of Physiology and Pharmacology, Loma Linda University School of Medicine, Loma Linda, California, USA

[2]Department of Anesthesiology and Neurosurgery, Loma Linda University School of Medicine, Loma Linda, California, USA

Chapter content currently submitted and under peer-review for publication

Abstract

We aim to determine if direct thrombin inhibition by Dabigatran will improve long-term brain morphological and neurofunctional outcomes and if potential therapeutic effects are dependent upon reduced PAR-1 stimulation and consequent mTOR activation. Germinal matrix hemorrhage was induced by stereotaxically injecting 0.3 U type VII-S collagenase into the germinal matrix of P7 rat pups. Animals were divided into 5 groups: Sham, Vehicle (5% DMSO), Dabigatran intraperitoneal, Dabigatran intraperitoneal + TFLLR-NH_2 (PAR-1 agonist) intranasal, SCH79797 (PAR-1 antagonist) intraperitoneal, and Dabigatran intranasal. Neurofunctional outcomes were determined by Morris water maze, rotarod, and foot fault evaluations at 3 weeks. Brain morphological outcomes were determined by histological Nissl staining at 4 weeks. Expression levels of p-mTOR/p-p70s6k at 3 days and vitronectin/fibronectin at 28 days were quantified. Intranasal and intraperitoneal Dabigatran promoted long-term neurofunctional recovery, improved brain morphological outcomes, and reduced intracranial pressure at 4 weeks after GMH. PAR-1 stimulation tended to reverse Dabigatran's effects on post-hemorrhagic hydrocephalus development. Dabigatran also reduced expression of short-term p-mTOR and long-term extracellular matrix proteins, which tended to be reversed by PAR-1 agonist co-administration. PAR-1 inhibition alone, however, did not achieve the same therapeutic effects as Dabigatran administration. Direct thrombin inhibition ameliorated long-term germinal matrix hemorrhage brain sequelae, which was associated with decreased short-term mTOR activation. PAR-1 stimulation tended to reverse some therapeutic effects, but PAR-1 inhibition alone was not sufficient to improve outcomes.

Introduction

Occurring in approximately 3.5 per 1000 live births, germinal matrix hemorrhage (GMH) remains a leading cause of mortality and lifelong morbidity in premature and/or very low birthweight infants (Heron, Sutton et al. 2010). The rupturing of immature blood vessels in the subependymal brain tissue is thought to result from deficient autoregulatory mechanisms that inadequately function in response to abnormal cerebral blood flow fluctuations spurred by cardiorespiratory and hemodynamic instability (Ballabh 2014). Long-term clinical complications from GMH include developmental delays, learning and psychiatric disorders, cerebral palsy, and post-hemorrhagic hydrocephalus, all of which pose significant economic burdens on both the patients and the US healthcare system (1993; Vohr, Wright et al. 2000; Murphy, Inder et al. 2002). Prenatal glucocorticoid administration remains the best treatment for preventing GMH in premature infants, yet few clinical approaches exist for GMH clinical management post-ictus (Leviton, Kuban et al. 1993; Vinukonda, Dummula et al. 2010). Minimal advancements have also been made in post-hemorrhagic hydrocephalus clinical management, which is mostly limited to surgical insertion of shunts that drain excess cerebrospinal fluid from the ventricles into the peritoneum (Whitelaw 2001; Ballabh 2014). Thus, a non-invasive, safe therapeutic approach that successfully mitigates post-hemorrhagic hydrocephalus development after GMH would significantly improve the quality of life for this patient population.

Immediately after hemorrhage, the coagulation cascade is triggered and thrombin, a serine protease, is activated (Babu, Bagley et al. 2012). In addition to inducing clot formation by converting fibrinogen into fibrin, thrombin also stimulates proteinase-

activated receptors (PARs) (Kataoka, Hamilton et al. 2003; Steinhoff, Buddenkotte et al. 2005; Luo, Wang et al. 2007), leading to phosphorylation and subsequent activation of mammalian target of rapamycin (mTOR) (Lekic, Klebe et al. 2015). Activated mTOR has been associated with extracellular matrix (ECM) protein proliferation in fibroblasts, which possibly disrupts CSF dynamics in the cerebroventricular system (Paul, Leef et al. 2000; Crews, Wyss-Coray et al. 2004; Del Bigio 2004; Xue and Del Bigio 2005; Ballabh, Xu et al. 2007; Dummula, Vinukonda et al. 2010). In our prior studies, long-term post-GMH ventricular dilation was associated with increased expression of vitronectin and fibronectin (Klebe, Krafft et al. 2014), combinatorial PAR-1 and PAR-4 inhibitors reduced p-mTOR expression at 72 hours after GMH, and rapamycin treatment ameliorated long-term neurocognitive deficits and improved brain morphology at 4 weeks post-GMH (Lekic, Klebe et al. 2015). Yet, long-term evaluations for PAR-1 and/or PAR-4 inhibitor administration as well as ECM protein expression levels were not investigated in these studies. Nonetheless, inhibiting the Thrombin/PAR/mTOR pathway seems be a promising strategy for ameliorating post-hemorrhagic hydrocephalus formation after GMH.

Dabigatran, an oral anti-coagulant also known as Pradaxa, is a direct thrombin inhibitor clinically approved for preventing deep vein thrombosis, pulmonary embolism, and stroke from atrial fibrillation (Eisert, Hauel et al. 2010; van Ryn, Stangier et al. 2010). While Dabigatran reduced overall major and minor bleeding events compared to Warfarin, gastrointestinal bleeds were significantly higher (Blommel and Blommel 2011). An antidote, Idarucizumab, was developed to reverse Dabigatran's anti-coagulant effects in the event of major, uncontrolled bleeds (Starke, Komotar et al. 2015). Although

inhibiting thrombin may ameliorate brain injury, Dabigatran's anti-coagulant properties pose a risk of increased bleeding after cerebral hemorrhage. Dabigatran was evaluated in a rodent model of adult intracerebral hemorrhage and was determined to not increase hematoma volume while attenuating brain injury for the doses evaluated (Lauer, Cianchetti et al. 2011), but an additional study suggests high doses of Dabigatran do increase hematoma volume, which can be controlled by intravenous injection of prothrombin complex concentrate (Zhou, Schwarting et al. 2011). We perform a similar dosing study to evaluate Dabigatran's safety for GMH and to determine the best dose for further investigation.

Herein, we evaluate if direct thrombin inhibition by Dabigatran ameliorates long-term neurocognitive deficits, improves brain morphological outcomes, and reduces ECM proliferation. We further investigate if potential therapeutic effects are dependent upon reduced PAR-1 stimulation and subsequent mTOR activation, since PAR-1 inhibition reduced brain injury severity in both adult cerebral ischemic and hemorrhage models. Given Dabigatran's anti-coagulant effects, inhibiting one of thrombin's receptors may be a safer approach if it still achieves the same degree of efficacy, and we aim to determine if PAR-1 inhibition alone will potentially achieve the same therapeutic benefits as direct thrombin inhibition. We further evaluate if PAR-1 stimulation will reverse Dabigatran's therapeutic effects to better confirm this pathway's role in GMH pathophysiology. Additionally, intranasal drug administration has been shown to be an effective, localized delivery route to the brain and we aimed to determine if this route would be efficacious for Dabigatran administration (McMartin, Hutchinson et al. 1987; Djupesland, Messina et al. 2014). We determine the effects of the thrombin/PAR-1 pathway on mTOR

phosphorylation in the short-term as well as ECM protein expression, brain morphology, neurocognitive and sensorimotor function, and intracranial pressure in the long-term.

Materials and Methods

GMH Surgical Procedures

All procedures were approved by the Loma Linda University Institutional Animal Care and Use Committee in accordance with the National Institute of Health's guidelines. For GMH induction, postnatal day 7 rat pups weighing between 12-15 grams (brain development comparable to 30-32 week human gestation) were anesthetized using 2-3% isoflurane delivered in a mixture of medical grade oxygen and air. The scalp was sterilized by topically applying isopropyl alcohol and betadine, and then the heads were fixed onto a stereotaxic frame. An incision was made to expose bregma and a 1 mm burr hole was drilled at 1.6 mm right lateral and 1.5 mm rostral relative to bregma. A 10 µL Hamilton syringe filled with 0.3 U/µL collagenase solution was fixed to an infusion pump (Harvard Apparatus, Holliston, MA) and the needle inserted to a depth of 2.8 mm below the dura with the bevel facing the midline. 0.3 U type VII-S collagenase from *Clostridium hystolyticum* (Sigma Aldrich, St. Louis, MO) was infused at a rate of 0.1 U/min, and the needle was left in place for 5 minutes before being removed at a rate of 1 mm/min to reduce backflow. The burr hole was sealed using bone wax and the incision sutured with 5-0 silk. Animals were allowed to recover on a 37°C heating pad then returned to the dam after awakening from anesthesia. Sham surgery involved needle insertion without collagenase infusion. The average surgery time was approximately 30 minutes per animal.

Experimental Groups and Treatments

For the Dabigatran plasma concentration studies, 72 P7 rat pups were randomly divided into three treatment groups: low dose 3 mg/kg, medium dose 10 mg/kg, or high dose 30 mg/kg administered intraperitoneally. Lyophilized Dabigatran (Boehringer Ingelheim, Ingelheim am Rhein, Germany) was dissolved into a 5% dimethyl sulfoxide (DMSO) solution (Sigma Aldrich, St. Louis, MO). Blood was collected by cardiac puncture prior to euthanization at 2, 4, 8, 12, 18, or 24 hours after Dabigatran administration for all three treatment groups (n=4/group/endpoint). For the hematoma expansion safety study, 48 P7 rat pups were randomly divided into 8 groups (n=6/group): Sham, Vehicle (5% DMSO), 3 mg/kg Dabigatran QD, 3 mg/kg Dabigatran BID, 10 mg/kg Dabigatran QD, 10 mg/kg Dabigatran BID, 30 mg/kg Dabigatran QD, and 30 mg/kg Dabigatran BID. Dabigatran was administered intraperitoneally for this study. For long-term evaluations, 72 P7 rat pups were randomly divided into 6 groups (n=10-12/group, split evenly between histology and Western blot/intracranial pressure): Sham, Vehicle, 3 mg/kg Dabigatran intraperitoneally, 3 mg/kg Dabigatran intraperitoneally + 1 mg/kg TFLLR-NH_2 (PAR-1 agonist) intranasally (Tocris, Minneapolis, MN), 10 mg/kg SCH79797 (PAR-1 antagonist) intraperitoneally (Tocris, Minneapolis, MN), and 3 mg/kg Dabigatran intranasally. All pups were randomized among treatment groups and all treatments commenced 2 hours post-ictus and then twice a day for 3 days. For time course Western blots, 48 P7 rat pups were randomly divided into 8 groups (n=6/group) and euthanized at the indicated time point after GMH: Naïve, 3, 6, 12 hours, 1 3, 5, and 7 days post-ictus. For short-term evaluations, 48 P7 rat pups were randomly divided into 8 groups (n=6/group): Sham, Vehicle BID for 3 days, 3 mg/kg Dabigatran

intraperitoneally; 3 mg/kg Dabigatran intraperitoneally + 1 mg/kg TFLLR-NH_2 intranasally; 10 mg/kg SCH79797 intraperitoneally; 3 mg/kg Dabigatran intranasally; 3 mg/kg Dabigatran intranasally + 1 mg/kg TFLLR-NH_2 intranasally. The TFLLR-NH_2 intranasal dose was derived from a prior *in vivo* rodent study (Aerts, Hamelin et al. 2013), and the SCH79797 intraperitoneal dose was derived from our prior GMH study (Lekic, Klebe et al. 2015).

Intracranial Pressure Measurement

Intracranial pressure was measured as previously described (Lackner, Vahmjanin et al. 2013). At 28 days post-ictus, animals were anesthetized and mounted onto a stereotaxic frame with their heads inclined 30° downward. The atlanto-occipital membrane was exposed by a midline skin excision and the cisterna magna punctured with a 26G needle connected to a pressure transducer (Digi-Med LPA 400, Micro-Med, Louisville, KY).

Neurobehavioral Assessments

A battery of tests was performed, by blinded investigators, to evaluate sensorimotor and cognitive deficits between 21-28 days post-ictus, as previously performed (Klebe, Krafft et al. 2014; Flores, Klebe et al. 2016). Foot Fault Test: Rats were placed on a wire grid (20x40 cm) 2 feet above the ground and allowed to walk for 2 minutes. The left limb faults are reported as a percentage of the total steps taken by the left limbs ((left faults/left steps) x 100). Rotarod: Rats were placed on a rotating cylinder (San Diego Instruments, Columbus, OH), 7 cm diameter, 9.6 cm lanes) accelerating at 2

RPM per 5 seconds (starting speeds of either 5 or 10 RPM), and a photobeam circuit detected the latency to fall off the cylinder. Morris Water Maze: Briefly, rats were trained using a visible platform (10 cm diameter, Cued test) on day 1. Days 2-5, latency to find a submerged platform was measured (Memory Blocks 1-4, 5 trials each block, 1 minute each trial). After completing the memory test, the platform was removed and the rats were tested to determine the amount of time spent within the platform quadrant (Probe Trial, 1 minute trial). An overhead camera with a computerized tracking system (Noldus Ethovision, Tacoma, WA) recorded the swim path and measured swim distance, speed, and time spent in target quadrant.

Perfusions and Tissue Extraction

Deeply anesthetized (5% isoflurane) animals were euthanized by trans-cardiac perfusion with ice-cold phosphate buffered saline (PBS) for hemoglobin assay and Western blot samples or with ice-cold PBS followed by 10% formalin for histology samples. Forebrains were either snap-frozen in liquid nitrogen and stored in -80°C freezer for Western blot and hemoglobin assay or post-fixed in 10% formaldehyde for at least 3 days then dehydrated with 30% sucrose for at least 3 days (4°C) for histology. Histology forebrains were embedded in Optimal Cutting Temperature compound and stored at -20°C.

Hemoclot Assay

Blood was drawn by cardiac puncture and collected in a 0.106 mol/L trisodium citrate solution (1 part anti-coagulant to 9 parts blood). Blood was centrifuged at 2600g

for 10 minutes at 20°C. Platelet poor plasma was collected and snap-frozen in liquid nitrogen then stored at -80°C until analysis. Dabigatran plasma concentration was determined by Hemoclot Assay (Aniara, West Chester, OH) as previously described.(Stangier and Feuring 2012) Briefly, a calibration curve was created using control plasma with 0, 1.25, 2.5, 3.75, and 5 µg/mL Dabigatran. The Hemoclot Assay was performed following the manufacturer guidelines Absorbance was measured on a microplate spectrophotometer (iMark, Bio-Rad, Hercules, CA) at 405 nm against a blank.

Hemoglobin Assay

Frozen forebrains were homogenized in 3 mL PBS for at least 60 seconds then sonicated for at least 60 seconds. The homogenate was centrifuged at 13000 RPM, 20°C for 30 minutes. 200 µL supernatant was combined with 800 µL Drabkin's reagent (Sigma-Aldrich, St. Louis, MO). After 15 minutes, absorbance at 450 nm was measured using a spectrophotometer (Genesis 10 UV; Thermo Fisher Scientific, Waltham, MA). Hemorrhage volume was calculated against a standard curve (created using naïve forebrains and known quantities of blood).

Western Blot

Forebrains were homogenized in RIPA lysis buffer (Santa Cruz Biotechnology, Dallas, TX) for at least 60 seconds. The homogenate was centrifuged at 15000 RPM, 4°C for 20 minutes and supernatant collected, aliquoted, then stored at -80°C. Protein concentrations were determined by DC protein assay (Bio-Rad, Hercules, CA). 50 µg protein per sample were loaded into wells of 10% gels, ran for 30 minutes at 50 V, then

90 minutes at 125 V. Proteins were transferred onto a nitrocellulose membrane at 0.3 A for 120 minutes (Bio-Rad, Hercules, CA). Primary antibodies were applied to the membranes and incubated overnight at 4°C: p-mTOR (1:1000; Cell Signaling Technology, Danvers, MA); p-p70s6k (1:1000; Cell Signaling Technology, Danvers, MA); mTOR (1:1000; Cell Signaling Technology, Danvers, MA); p70s6k (1:1000; Cell Signaling Technology, Danvers, MA); vitronectin (1:1000; Abcam, Cambridge, MA); and actin (1:1000 Santa Cruz Biotechnology, Dallas, TX). Membranes were washed then incubated in secondary antibodies (1:2000; Santa Cruz Biotechnology, Dallas, TX) for 2 hours at 4°C. Proteins were exposed onto radiography film after applying enhanced chemiluminescent solution (GE Healthcare and Life Science, Piscataway, NJ) onto the membranes. ImageJ software (Media Cybernetics, Silver Spring, MD) was used to analyses relative density.

Histology

A cryostat (Leica Microsystems LM3050S, Wetzlar, Germany) was used to cut 10 µm thick coronal sections every 600 µm into the brain. Brain slices were Nissl stained and morphometrically analyzed using ImageJ (Media Cybernetics, Silver Spring, MD) assisted delineation of brain structures, as previously performed in our lab (Lekic, Manaenko et al. 2012). Ventricle volume was calculated as average ventricular area multiplied by the depth of the cerebroventricular system. White matter loss was calculated as the average white matter area multiplied by depth of the cerebroventricular system and expressed as % of the sham group by dividing volumes to the overall average volume of the Sham group.

Statistical Analysis

Data are expressed as mean ± standard deviation. One-way ANOVA using the Newman-Keuls post-hoc test was used to analyses all data. A $p<0.05$ was considered statistically significant in all analyses except neurobehavior; a $p<0.10$ was considered statistically significant for neurobehavioral analyses.

Results

Dabigatran Half-life and Hematoma Volume after GMH

A dosing study was performed to assess the safety and efficacy of Dabigatran. Plasma concentrations reached maximum levels 2 hours after injection and have an approximate half-life of 8-12 hours (Figure 5.1.A). 30 mg/kg Dabigatran administered intraperitoneally QD or BID significantly increased hematoma volume 24 hours after GMH. 10 mg/kg Dabigatran administered intraperitoneally QD or BID had no effect on hematoma volume 24 hours after GMH. 3 mg/kg Dabigatran QD administered intraperitoneally had no effect on hematoma volume while Dabigatran BID tended to decrease hematoma volume (Figure 5.1.B). Excessive bleeding and mortality associated with excessive bleeding, where uncoagulated blood was usually found at the abdomen/intestine, intraperitoneal injection site, and/or surgical suture on the head, was also observed in all groups, particularly the higher dose groups (between 0-33% mortality, data not shown).

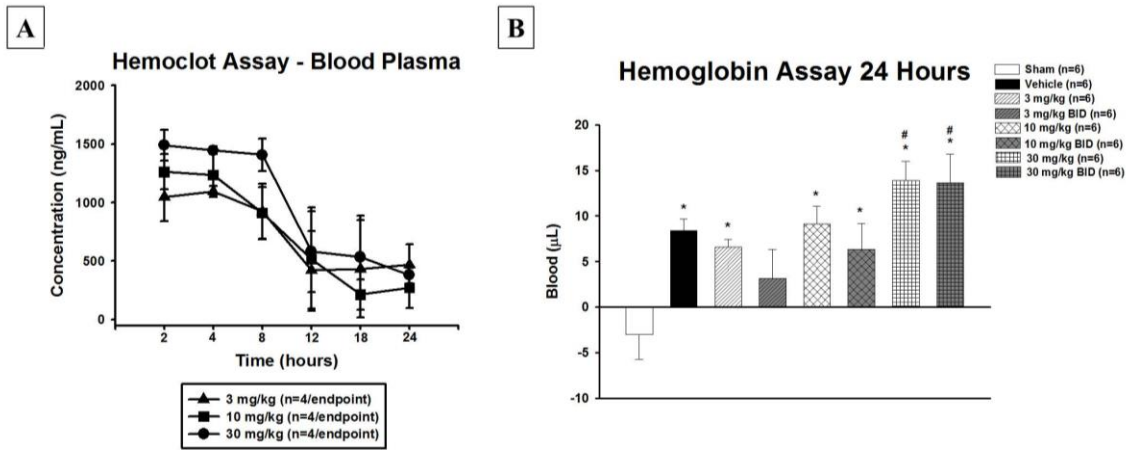

Figure 5.1: Dabigatran dose response for hematoma volume 24 hours post-GMH and plasma concentration time course. Time course of Dabigatran plasma concentrations after intraperitoneal injection of either 3 mg/kg, 10 mg/kg, or 30 mg/kg Dabigatran (**A**). Hematoma volumes 24 hours post-GMH (**B**). *P<0.05 vs Sham; #P<0.05 vs Vehicle.

Thrombin Inhibition Improved Long-term Neurofunctional Recovery, which Was Not Reversed by PAR-1 Stimulation; PAR-1 Inhibition Alone Was Not Sufficient to Promote Recovery

Using the best-tolerated dose, 3 mg/kg Dabigatran administered intraperitoneally BID, we evaluated its efficacy on promoting long-term neurofunctional recovery. After observing the bleeding side effects, particularly bleeding near the injection sites, as well as mortality data from systemic Dabigatran administration, we decided to investigate if a localized intranasal administration would promote long-term recovery. Dabigatran intranasal administration may increase brain concentration compared to intraperitoneal administration and avoids repeated abdominal injections, which may cause the observed bleeding, although the high bioavailability of small drugs after intranasal delivery may make blood plasma concentrations similar to intraperitoneal delivery and have the same bleeding risk (McMartin, Hutchinson et al. 1987). The vehicle group performed significantly worse than sham in the foot fault (Figure 5.2.A), rotarod (Figure 5.2.B), and Morris water maze tests (Figure 5.2.C-D). Dabigatran administered intraperitoneally significantly improved performances on the foot fault and rotarod tests, but did not improve performance in the Morris water maze test compared to vehicle. PAR-1 agonist, TFLLR-NH_2, did not reverse neurobehavioral outcomes from intraperitoneal Dabigatran. PAR-1 antagonist, SCH79797, administration did not improve performances on the foot fault or Morris water maze tests, and only tended to improve performance on the rotarod test compared to vehicle. Intranasal Dabigatran did not improve performance on the foot fault test, tended to improve performance on the rotarod test, and significantly improved performance on the Morris water maze test compared to vehicle.

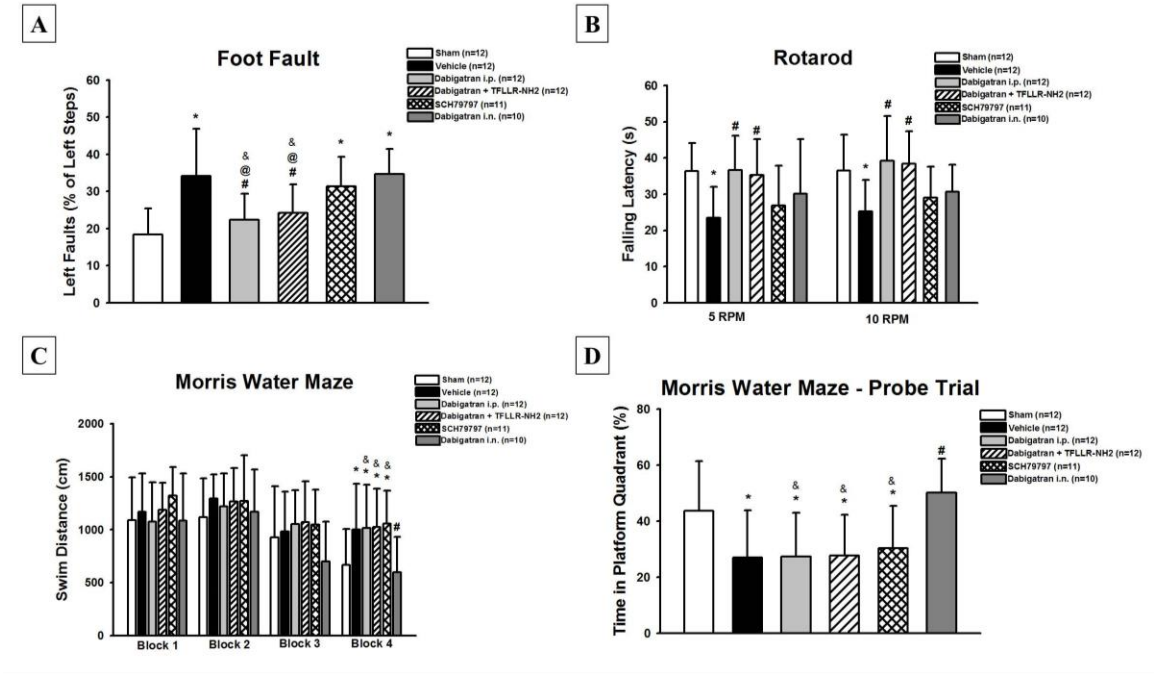

Figure 5.2: Long-term neurobehavioral outcomes after thrombin or PAR-1 inhibition at 3-4 weeks post-GMH. assessment using the foot fault (**A**), rotarod (**B**), and Morris water maze tests for swim distance (**C**) and percentage of time spent in platform quadrant (**D**). *P<0.10 vs Sham; #P<0.10 vs Vehicle; $P<0.10 vs Dabigatran i.p.; &P<0.10 vs Dabigatran i.n.; @P<0.10 vs SCH79797.

Thrombin Inhibition Improved Long-term Brain Morphological Outcomes, which Tended to be Reversed by PAR-1 Stimulation; PAR-1 Inhibition Alone Was Not Sufficient to Promote Recovery

To determine treatment effects on long-term post-hemorrhagic hydrocephalus outcomes, intracranial pressure was measured and brain morphological outcomes determined by histological analysis at 4 weeks post-GMH (Figure 5.3). Dabigatran administered either intraperitoneally or intranasally had significantly diminished post-hemorrhagic ventricular dilation (Figure 5.3.B) and white matter loss (Figure 5.3.C) compared to vehicle. PAR-1 agonist co-administration significantly reversed intraperitoneal Dabigatran's effect on reduced post-hemorrhagic ventricular dilation and tended to reverse intraperitoneal Dabigatran's effect on ameliorating white matter loss. PAR-1 antagonist administration did not significantly diminish post-hemorrhagic ventricular dilation or white matter loss compared to vehicle. Additionally, the vehicle group had significantly increased intracranial pressure compared to sham, which was prevented by Dabigatran (intraperitoneal and intranasal) but not PAR-1 antagonism (Figure 3.D). PAR-1 agonist co-administration significantly reversed intraperitoneal Dabiagatran's effects on diminishing intracranial pressure.

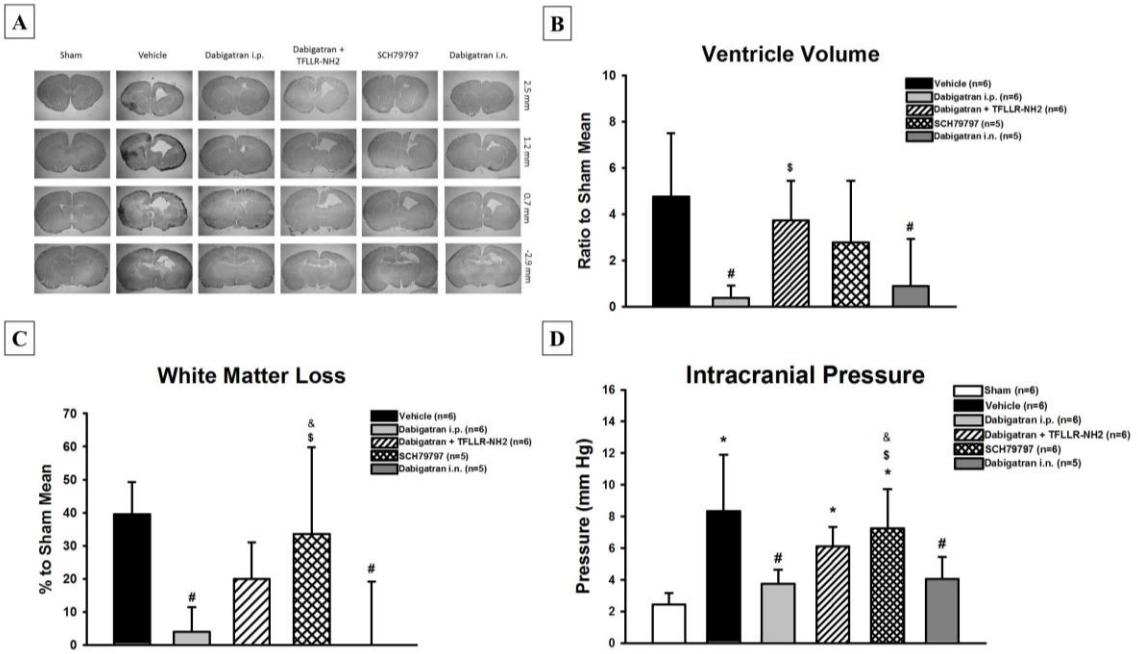

Figure 5.3: **Long-term brain morphological outcomes after thrombin or PAR-1 inhibition at 4 weeks post-GMH.** Long term brain morphological. Representative photomicrographs (**A**), ventricular volumes (ratio to sham mean) (**B**), and white matter loss (percentage to sham mean) (**C**). Intracranial pressure at 4 weeks post-GMH (**D**). *P<.05 vs Sham; #P<.05 vs Vehicle; $P<.05 vs Dabigatran i.p.; &P<.05 vs Dabigatran i.n..

Short-term p-mTOR and Downstream p-p70s6k Expression Levels Are Significantly Increased after GMH

Activated mTOR has been implicated as a potential downstream effector of thrombin-induced PAR stimulation, leading to consequent ECM protein proliferation. We evaluated the expression time course of p-mTOR (Figure 5.4.A) and its downstream effector, p-p70s6k (Figure 5.4.B), after GMH. Activated mTOR (p-mTOR) expression levels were significantly increased 3 hours, and remained elevated up to 7 days post-ictus. Activated p70s6k (p-p70s6k) expression levels were significantly increased 3 hours, and remained increased at 3 days post-ictus, before returning to levels indistinguishable from that of sham at 5 days post-ictus.

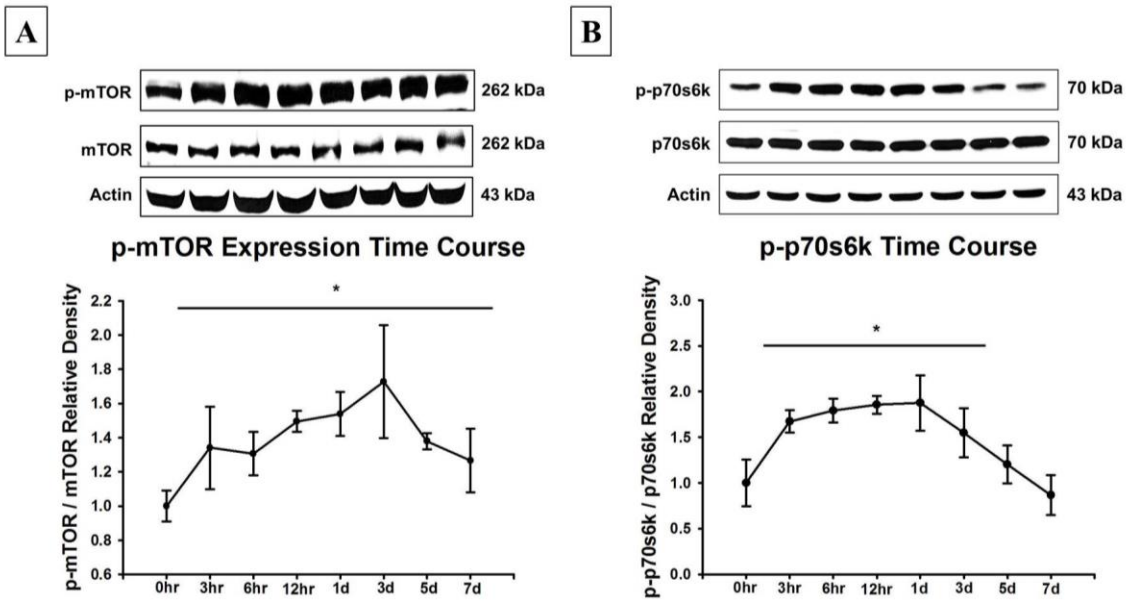

Figure 5.4: Time course of mTOR/p70s6k activation after GMH. Time course of p-mTOR (**A**) and p-p70s6k (**B**) protein expression in the brain after GMH. *P<.05 vs Sham.

Thrombin Inhibition Reduced p-mTOR and p-p70s5k Expression Levels at 3 Days Post-ictus, which Were Reversed by PAR-1 Stimulation; PAR-1 Inhibition Alone Did Not Significantly Reduce p-mTOR and p-p70s6k Expression

Three days post-GMH, the effect of treatment on p-mTOR expression was evaluated (Figure 5.5). Dabigatran (intraperitoneal and intranasal) significantly decreased p-mTOR and p-p70s6k expression levels compared to vehicle, which were reversed by PAR-1 agonist co-administration. Intraperitoneal PAR-1 antagonist administration did not significantly reduce p-mTOR or p-p70s6k expression levels compared to vehicle (Figure 5.5.A-B).

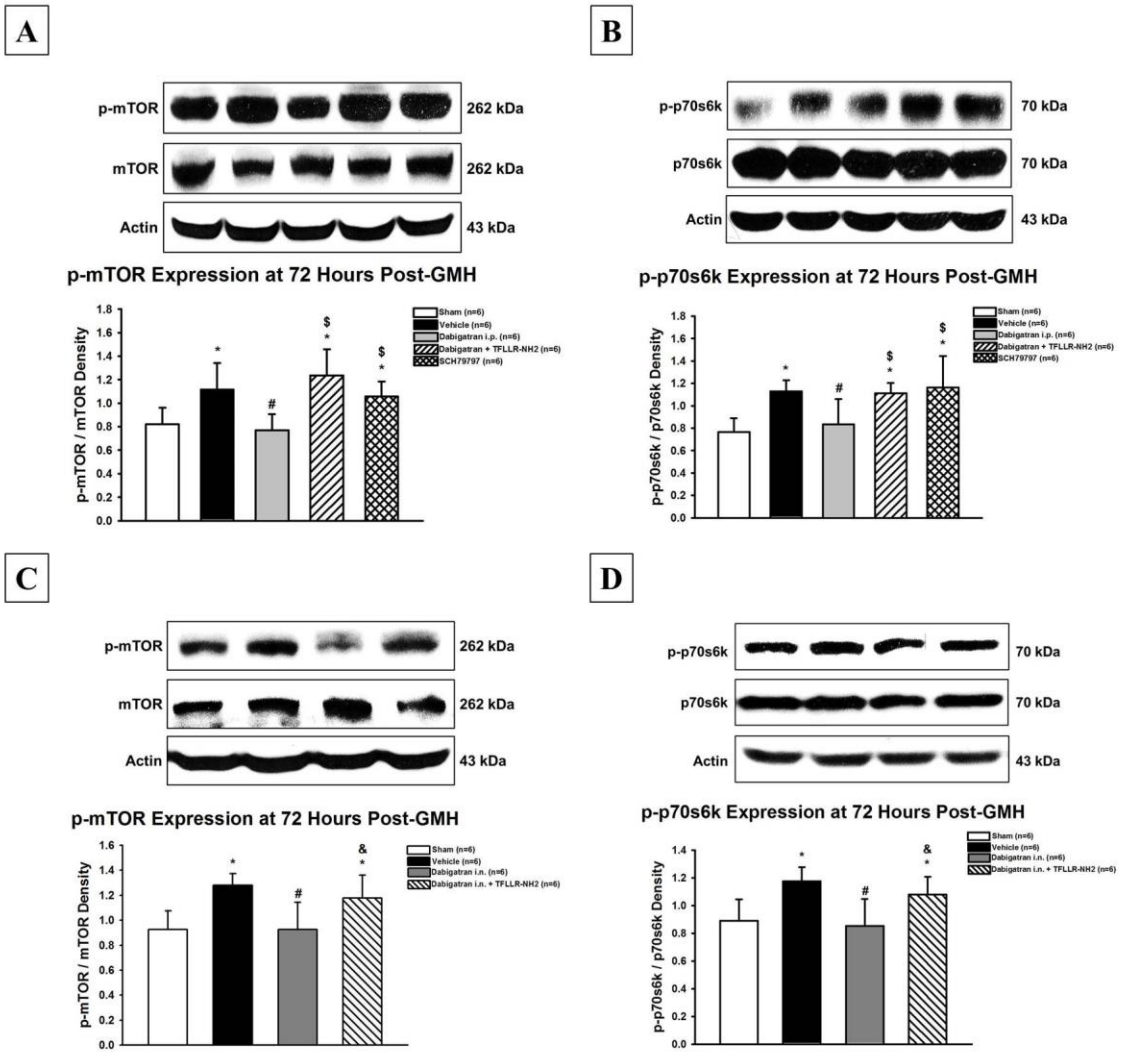

Figure 5.5: Expression of activated mTOR/p70s6k after thrombin inhibition and PAR-1 stimulation at 72 hours after GMH. Expression of p-mTOR and p-p70s6k protein expression in the brain at 3 days post-GMH in rats treated with Dabigatran administered intraperitoneally (**A-B**) or intranasally (**C-D**). *P<.05 vs Sham; #P<.05 vs Vehicle; $P<.05 vs Dabigatran i.p.; &P<.05 vs Dabigatran i.n..

Thrombin Inhibition Significantly Reduced Long-term ECM Protein Proliferation after GMH, which Was Not Reversed by PAR-1 Stimulation; PAR-1 Inhibition Alone Tended to Reduce ECM Protein Proliferation

ECM protein proliferation has been associated with post-hemorrhagic hydrocephalus after GMH, thus we evaluated treatment effects on vitronectin (Figure 5.6.A) and fibronectin (Figure 5.6.B) expression levels 4 weeks post-ictus. The vehicle group had significantly increased expression of both vitronectin and fibronectin compared to sham, which was prevented by Dabigatran (intraperitoneal and intranasal) and tended to decrease by PAR-1 antagonism. PAR-1 agonist co-administration did not significantly reverse intraperitoneal Dabigatran effects on reducing vitronectin expression and only tended to reverse intraperitoneal Dabigatran effects on reducing fibronectin expression.

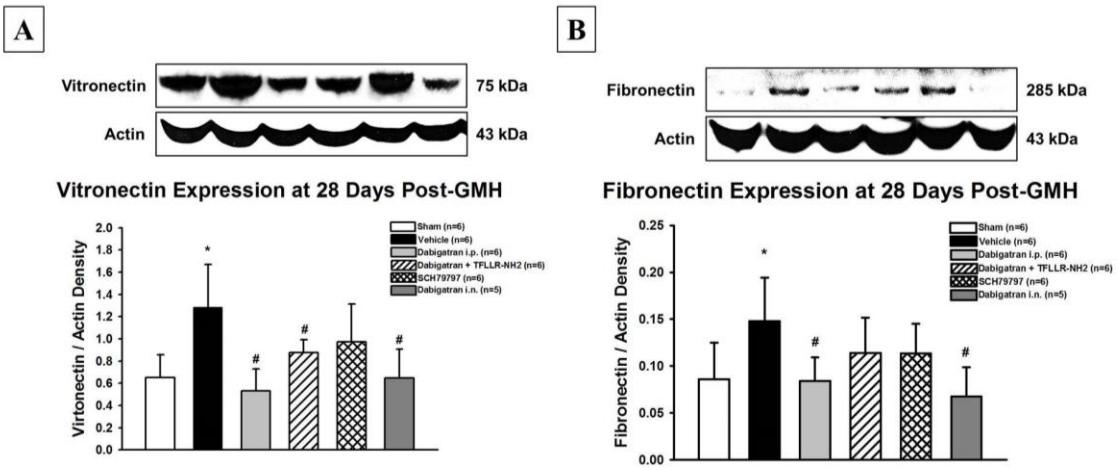

Figure 5.6: Long-term expression of extracellular matrix proteins after thrombin and PAR-1 inhibition at 4 weeks post-GMH. Expression of vitronectin (**A**) and fibronectin (**B**) proteins in the brain at 4 weeks post-GMH. *P<.05 vs Sham; #P<.05 vs Vehicle.

Discussion

Post-hemorrhagic hydrocephalus is a common neurological sequelae afflicting severe grade GMH patients, and a non-invasive therapeutic approach would significantly improve the quality of life for this patient population. Elucidating clinically translatable pathophysiological mechanisms contributing towards post-hemorrhagic hydrocephalus development will hopefully yield novel therapeutic modalities to accomplish this aim. Thrombin has been identified as a potentially critical player since intraventricular thrombin injection results in brain tissue damage and ventricular dilation in adult rats, which was reversed by intraventricular PAR-1 antagonist injection (Gao, Liu et al. 2014). Thrombin activity is significantly upregulated 24 hours after GMH and tends to remain elevated up to 10 days post-ictus (Lekic, Klebe et al. 2015). Additionally, stimulation of thrombin's receptors, protease-activated receptors-1, -3, and -4, upregulates downstream proliferative pathways associated with brain injury, including PI3K/Akt, mTOR, and MAPK (Kataoka, Hamilton et al. 2003; Steinhoff, Buddenkotte et al. 2005; Luo, Wang et al. 2007). Our prior studies determined active p-mTOR is significantly upregulated in GMH rats at 72 hours post-ictus, and co-administration of PAR-1 and PAR-4 inhibitors reduced p-mTOR expression levels. Additionally, mTOR inhibition by rapamycin treatment improved long-term neurofunctional and brain morphological outcomes after GMH (Lekic, Klebe et al. 2015). Thus, this pathway warrants further investigation.

Dabigatran is a novel direct thrombin inhibitor clinically approved for treating deep vein thrombosis and preventing stroke from atrial fibrillation (Eisert, Hauel et al. 2010; van Ryn, Stangier et al. 2010). Similar to Argatroban (Chen 2001), Dabigatran is a competitive inhibitor that reversibly binds to thrombin's active site. We aimed to evaluate

this clinically available drug in our neonatal rat GMH model. We first performed a dosing study to 1) identify the half-life of Dabigatran, and 2) determine the best treatment regimen to prevent hematoma expansion and other adverse effects. Plasma Dabigatran concentrations after intraperitoneal administration was measured at 2, 4, 8, 12, 18, and 24 hours after injection using three doses: 3 mg/kg, 10 mg/kg, and 30 mg/kg. Plasma concentrations for all three doses had peaked by 2 hours and the half-life was 8-12 hours in neonatal rats (Figure 5.1.A).

While thrombin inhibition has yielded positive results in intracerebral hemorrhage models, evidence suggests that high doses of thrombin inhibitors result in increased hematoma volumes due to their anti-coagulant effects (Lauer, Cianchetti et al. 2011; Zhou, Schwarting et al. 2011). Given Dabigatran's 8-12 hour half-life, Dabigatran was given QD and BID. Dabigatran (30 mg/kg) QD and BID resulted in significantly greater hematoma volumes compared to that of the vehicle. Dabigatran (10 mg/kg) QD and BID and Dabigatran (3 mg/kg) QD had hematoma volumes comparable to that of the vehicle, whereas Dabigatran (3 mg/kg) BID tended to decrease hematoma volume (Figure 5.1.B). We speculate Dabigatran's anti-coagulant properties at 3 mg/kg are potent enough to attenuate the accumulation of blood in the brain and cerebroventricular system while preventing excess bleeding and consequent hematoma expansion. These findings are analogous to studies investigating fibrinolytic agents to break down cerebroventricular blood clots after intraventricular hemorrhage (Staykov, Huttner et al. 2009).

During the dosing study, some mortality was observed in the medium and high dose groups, but many of the animals in those groups suffered from adverse bleeding side-effects, particularly in the abdomen. We were concerned systemic administration of

Dabigatran may be risky, so we decided to investigate if intranasal administration, which is more localized to the brain, could be therapeutically beneficial, thus, an intranasal administration group was added to the long-term study, and only 3 mg/kg Dabigatran BID administered either intraperitoneally or intranasally was used, since it was best tolerated. Recognizing that direct thrombin inhibitors have an inherent bleeding risk, we investigated if 1) inhibiting PAR-1, a downstream thrombin receptor, will achieve the same therapeutic results, and 2) stimulating PAR-1 will reverse Dabigatran's therapeutic effects.

Dabigatran treatment ameliorated long-term neurofunctional deficits. Interestingly, intraperitoneal Dabigatran only improved locomotor and sensorimotor outcomes, evidenced by better foot-fault and rotarod performances, while intranasal Dabigatran administration only improved neurocognitive function, evidenced by better Morris water maze performances (Figure 5.2). PAR-1 stimulation did not reverse intraperitoneal Dabigatran's therapeutic effects on foot-fault and rotarod performance, and PAR-1 inhibition did not significantly attenuate any neurofunctional deficits, although it tended to improve performance on the rotarod test. While both administration routes had identical effects in every aspect of this study with neurobehavioral outcomes being the only exception, these results may partially be explained by the inherent error and variability within the tests, but the potential differential effects from the given administration routes cannot be ignored. Regardless, both administration routes showed significant neurofunctional recovery after GMH.

Both Dabigatran administration routes improved long-term brain morphological outcomes by reducing post-hemorrhagic ventricular dilation and white matter loss

compared to vehicle, and both routes reduced long-term intracranial pressure compared to vehicle (Figure 5.3). PAR-1 stimulation showed a strong tendency to reverse intraperitoneal Dabigatran's therapeutic effects on brain morphological and intracranial pressure outcomes since this group did not achieve a statistically significant difference from the vehicle group. PAR-1 inhibition alone failed to ameliorate post-hemorrhagic ventricular dilation, white matter loss, and elevated intracranial pressure. These results suggest thrombin activity is associated with long-term post-hemorrhagic hydrocephalus development, but post-hemorrhagic hydrocephalus development is not exclusively dependent upon thrombin-induced PAR-1 stimulation, although it may play a minor role in conjunction with other pathways. Indeed, activated thrombin also stimulates PAR-3 and PAR-4 as well, and their potential roles in GMH pathophysiology have not been elucidated. PAR-1 inhibition alone also failed to ameliorate short-term subventricular zone damage in a neonatal mouse GMH model (Mao and Del Bigio 2015), which is consistent with our results showing PAR-1 inhibition failed to ameliorate long-term white matter loss. Future investigations should rule out PAR-1 inhibition alone and focus on PAR-3, PAR-4, or a combinatorial treatment approach.

Active thrombin is hypothesized to contribute towards fibrosis and consequent ECM protein proliferation, which disrupt cerebrospinal fluid dynamics in the cerebroventricular system, potentially causing post-hemorrhagic hydrocephalus. PAR stimulation leads to activation of multiple proliferative signaling pathways, including PI3K/Akt, MAPK, and mTOR (Kataoka, Hamilton et al. 2003; Steinhoff, Buddenkotte et al. 2005; Luo, Wang et al. 2007). Previously, mTOR inhibition improved long-term brain morphological and neurofunctional outcomes after GMH, and combinatorial PAR-1,-4

inhibition reduced mTOR activation at 72 hours post-GMH. Yet, neither mTOR inhibition, PAR-1,-4 inhibition, nor ECM protein proliferation have been evaluated for long-term outcomes after GMH (Lekic, Klebe et al. 2015). Herein, p-mTOR expression was increased immediately following GMH and remained elevated to 7 days, and a similar trend was observed for p-p70s6k (Figure 5.4). Dabigatran attenuated the elevated expressions of p-mTOR and p-p70s6k, which was reversed by PAR-1 stimulation. Yet PAR-1 inhibition alone did not significantly decrease p-mTOR or p-p70s6k (Figure 5.5). Our results suggest thrombin inhibition decreases mTOR activation, yet is seems that stimulation of any of thrombin's downstream PARs is sufficient to increase mTOR activation. When thrombin is inhibited, it is not able to stimulate PARs inducing mTOR activation, yet stimulation of one PAR, PAR-1 here, was capable of activating mTOR. This is supported by the current work that inhibition of only PAR-1 was unable to prevent mTOR activation. Additionally, this is supported the work of Lekic et al. that combinational PAR-1,-4 inhibition reduced p-mTOR expression 72 hours after GMH, indicating that combinatorial PAR inhibition may be necessary to completely target this pathway.

Activated mTOR is hypothesized to contribute towards long-term ECM protein proliferation, which was observed in this work. Dabigatran (intraperitoneally and intranasally) significantly decreased vitronectin and fibronectin, and PAR-1 agonist co-administration did not reverse Dabigatran's effects on vitronectin expression but tended to reverse fibronectin expression. PAR-1 inhibition alone tended to reduce vitronectin and fibronectin (Figure 5.6). Long-term ECM protein proliferation weakly correlates with short-term p-mTOR expression levels, suggesting PAR-1/mTOR plays a small role, but

other signaling pathways must be involved as well. Most importantly, ECM protein proliferation does not strongly correlate with brain morphological and intracranial pressure outcomes, but p-mTOR expression levels do correlate, suggesting future investigations into post-GMH hydrocephalus development should focus less on ECM protein proliferation and more on alternative p-mTOR-related pathways, particularly active mTOR's relationship with immunomodulatory and cell survival pathways.

Our study has some limitations that need to be considered. First, neither the time course of Dabigatran plasma concentrations after intranasal injection, nor the time course of Dabigatran brain levels after intraperitoneal or intranasal administration. Second, the effects of intranasal Dabigatran on hematoma volume were also not examined, nor was a dosing study on intranasal Dabigatran performed. Third, thrombin has a plethora of downstream targets in addition to PAR/mTOR-induced ECM proliferation, including immunomodulatory and cell survival pathways (Krenzlin, Lorenz et al. 2016).The scope of this study was on PAR-1/mTOR to isolate a potentially effective pathway downstream of thrombin which may play an important role in post-hemorrhagic hydrocephalus development. PAR-1 agonist and antagonist effects should also be interpreted cautiously, since PAR-1 exhibits biased agonism and responds to various doses of drugs and stimuli differently (Mosnier, Sinha et al. 2012). Fourth, some evidence suggests plasma fibronectin and vitronectin leak into the brain tissue following hemorrhagic transformation after ischemia in adult mice, indicating another source of ECM proteins in addition to those produced from fibrosis (del Zoppo, Frankowski et al. 2012). Increased long-term ECM protein expression after GMH, however, may depend more on chronic fibrosis than acute vascular extravasation. Fifth, the therapeutic window for post-GMH

treatments is poorly defined due to lack of clinically approved or tested therapies, and the initial two hour post-ictus treatment time point examined may be too narrow for clinical translation. Finally, although our model produces consistent hemorrhages with consequent gliosis, neurological deficits, white matter loss, brain atrophy, and post-hemorrhagic hydrocephalus consistent with human neonatal brain hemorrhage, vascular integrity is disrupted by direct protease infusion (Lekic, Manaenko et al. 2012), which does not perfectly model GMH pathophysiology caused by hemodynamic, microvascular, and cardiorespiratory instability emulated in other animal models (Chua, Chahboune et al. 2009; Yang, Baumann et al. 2013). These limitations will be the focus of future studies.

Conclusions

Direct thrombin inhibition by Dabigatran decreased acute mTOR activation, reduced long-term ECM protein proliferation, ameliorated post-hemorrhagic hydrocephalus development, and improved long-term neurofunctional outcomes. Inhibition of PAR-1, a thrombin downstream receptor, was not sufficient to achieve the same observed therapeutic effectiveness as direct thrombin inhibition by Dabigatran. Yet PAR-1 stimulation tended to reverse Dabigatran's therapeutic effects on long-term post-hemorrhagic hydrocephalus development and short-term mTOR activation, suggesting a role for PAR-1 in GMH sequelae. Future investigations should employ combinatorial PAR-1, -3, and/or -4 inhibition treatment modalities and further investigate additional pathways related to thrombin and active mTOR, including inflammatory and cell survival pathways.

References

(1993). "The Vermont-Oxford Trials Network: Very Low Birth Weight Outcomes for 1990. Investigators of the Vermont-Oxford Trials Network Database Project." Pediatrics **91**(3): 540-545.

Aerts L, Hamelin ME, Rheaume C, Lavigne S, Couture C, Kim W, Susan-Resiga D, Prat A, Seidah NG, Vergnolle N, Riteau B, and Boivin G (2013). "Modulation of Protease Activated Receptor 1 Influences Human Metapneumovirus Disease Severity in a Mouse Model." PLoS One **8**(8): e72529.

Babu R, Bagley JH, Di C, Friedman AH, and Adamson C (2012). "Thrombin and Hemin as Central Factors in the Mechanisms of Intracerebral Hemorrhage-Induced Secondary Brain Injury and as Potential Targets for Intervention." Neurosurg Focus **32**(4): E8.

Ballabh P (2014). "Pathogenesis and Prevention of Intraventricular Hemorrhage." Clin Perinatol **41**(1): 47-67.

Ballabh P, Xu H, Hu F, Braun A, Smith K, Rivera A, Lou N, Ungvari Z, Goldman SA, Csiszar A, and Nedergaard M (2007). "Angiogenic Inhibition Reduces Germinal Matrix Hemorrhage." Nat Med **13**(4): 477-485.

Blommel ML, and Blommel AL (2011). "Dabigatran Etexilate: A Novel Oral Direct Thrombin Inhibitor." Am J Health Syst Pharm **68**(16): 1506-1519.

Chen JL (2001). "Argatroban: A Direct Thrombin Inhibitor for Heparin-Induced Thrombocytopenia and Other Clinical Applications." Heart Dis **3**(3): 189-198.

Chua CO, Chahboune H, Braun A, Dummula K, Chua CE, Yu J, Ungvari Z, Sherbany AA, Hyder F, and Ballabh P (2009). "Consequences of Intraventricular Hemorrhage in a Rabbit Pup Model." Stroke **40**(10): 3369-3377.

Crews L, Wyss-Coray T, and Masliah E (2004). "Insights into the Pathogenesis of Hydrocephalus from Transgenic and Experimental Animal Models." Brain Pathol **14**(3): 312-316.

Del Bigio MR (2004). "Cellular Damage and Prevention in Childhood Hydrocephalus." Brain Pathol **14**(3): 317-324.

del Zoppo GJ, Frankowski H, Gu YH, Osada T, Kanazawa M, Milner R, Wang X, Hosomi N, Mabuchi T, and Koziol JA (2012). "Microglial Cell Activation Is a Source of Metalloproteinase Generation During Hemorrhagic Transformation." J Cereb Blood Flow Metab **32**(5): 919-932.

Djupesland PG, Messina JC, and Mahmoud RA (2014). "The Nasal Approach to Delivering Treatment for Brain Diseases: An Anatomic, Physiologic, and Delivery Technology Overview." Ther Deliv **5**(6): 709-733.

Dummula K, Vinukonda G, Xu H, Hu F, Zia MT, Braun A, Shi Q, Wolk J, and Ballabh P (2010). "Development of Integrins in the Vasculature of Germinal Matrix, Cerebral Cortex, and White Matter of Fetuses and Premature Infants." J Neurosci Res **88**(6): 1193-1204.

Eisert WG, Hauel N, Stangier J, Wienen W, Clemens A, and van Ryn J (2010). "Dabigatran: An Oral Novel Potent Reversible Nonpeptide Inhibitor of Thrombin." Arterioscler Thromb Vasc Biol **30**(10): 1885-1889.

Flores JJ, Klebe D, Rolland WB, Lekic T, Krafft PR, and Zhang JH (2016). "Ppargamma-Induced Upregulation of Cd36 Enhances Hematoma Resolution and Attenuates Long-Term Neurological Deficits after Germinal Matrix Hemorrhage in Neonatal Rats." Neurobiol Dis **87**: 124-133.

Gao F, Liu F, Chen Z, Hua Y, Keep RF, and Xi G (2014). "Hydrocephalus after Intraventricular Hemorrhage: The Role of Thrombin." J Cereb Blood Flow Metab **34**(3): 489-494.

Heron M, Sutton PD, Xu J, Ventura SJ, Strobino DM, and Guyer B (2010). "Annual Summary of Vital Statistics: 2007." Pediatrics **125**(1): 4-15.

Kataoka H, Hamilton JR, McKemy DD, Camerer E, Zheng YW, Cheng A, Griffin C, and Coughlin SR (2003). "Protease-Activated Receptors 1 and 4 Mediate Thrombin Signaling in Endothelial Cells." Blood **102**(9): 3224-3231.

Klebe D, Krafft PR, Hoffmann C, Lekic T, Flores JJ, Rolland W, and Zhang JH (2014). "Acute and Delayed Deferoxamine Treatment Attenuates Long-Term Sequelae after Germinal Matrix Hemorrhage in Neonatal Rats." Stroke **45**(8): 2475-2479.

Krenzlin H, Lorenz V, Danckwardt S, Kempski O, and Alessandri B (2016). "The Importance of Thrombin in Cerebral Injury and Disease." Int J Mol Sci **17**(1).

Lackner P, Vahmjanin A, Hu Q, Krafft PR, Rolland W, and Zhang JH (2013). "Chronic Hydrocephalus after Experimental Subarachnoid Hemorrhage." PLoS One **8**(7): e69571.

Lauer A, Cianchetti FA, Van Cott EM, Schlunk F, Schulz E, Pfeilschifter W, Steinmetz H, Schaffer CB, Lo EH, and Foerch C (2011). "Anticoagulation with the Oral Direct Thrombin Inhibitor Dabigatran Does Not Enlarge Hematoma Volume in Experimental Intracerebral Hemorrhage." Circulation **124**(15): 1654-1662.

Lekic T, Klebe D, McBride DW, Manaenko A, Rolland WB, Flores JJ, Altay O, Tang J, and Zhang JH (2015). "Protease-Activated Receptor 1 and 4 Signal Inhibition Reduces Preterm Neonatal Hemorrhagic Brain Injury." Stroke **46**(6): 1710-1713.

Lekic T, Manaenko A, Rolland W, Krafft PR, Peters R, Hartman RE, Altay O, Tang J, and Zhang JH (2012). "Rodent Neonatal Germinal Matrix Hemorrhage Mimics the Human Brain Injury, Neurological Consequences, and Post-Hemorrhagic Hydrocephalus." Exp Neurol **236**(1): 69-78.

Leviton A, Kuban KC, Pagano M, Allred EN, and Van Marter L (1993). "Antenatal Corticosteroids Appear to Reduce the Risk of Postnatal Germinal Matrix Hemorrhage in Intubated Low Birth Weight Newborns." Pediatrics **91**(6): 1083-1088.

Luo W, Wang Y, and Reiser G (2007). "Protease-Activated Receptors in the Brain: Receptor Expression, Activation, and Functions in Neurodegeneration and Neuroprotection." Brain Res Rev **56**(2): 331-345.

Mao X, and Del Bigio MR (2015). "Interference with Protease-Activated Receptor 1 Does Not Reduce Damage to Subventricular Zone Cells of Immature Rodent Brain Following Exposure to Blood or Blood Plasma." J Negat Results Biomed **14**: 3.

McMartin C, Hutchinson LE, Hyde R, and Peters GE (1987). "Analysis of Structural Requirements for the Absorption of Drugs and Macromolecules from the Nasal Cavity." J Pharm Sci **76**(7): 535-540.

Mosnier LO, Sinha RK, Burnier L, Bouwens EA, and Griffin JH (2012). "Biased Agonism of Protease-Activated Receptor 1 by Activated Protein C Caused by Noncanonical Cleavage at Arg46." Blood **120**(26): 5237-5246.

Murphy BP, Inder TE, Rooks V, Taylor GA, Anderson NJ, Mogridge N, Horwood LJ, and Volpe JJ (2002). "Posthaemorrhagic Ventricular Dilatation in the Premature Infant: Natural History and Predictors of Outcome." Arch Dis Child Fetal Neonatal Ed **87**(1): F37-41.

Paul DA, Leef KH, and Stefano JL (2000). "Increased Leukocytes in Infants with Intraventricular Hemorrhage." Pediatr Neurol **22**(3): 194-199.

Stangier J, and Feuring M (2012). "Using the Hemoclot Direct Thrombin Inhibitor Assay to Determine Plasma Concentrations of Dabigatran." Blood Coagul Fibrinolysis **23**(2): 138-143.

Starke RM, Komotar RJ, and Connolly ES (2015). "A Prospective Cohort Study of Idarucizumab for Reversal of Dabigatran-Associated Hemorrhage." Neurosurgery **77**(6): N11-13.

Staykov D, Huttner HB, Struffert T, Ganslandt O, Doerfler A, Schwab S, and Bardutzky J (2009). "Intraventricular Fibrinolysis and Lumbar Drainage for Ventricular Hemorrhage." Stroke **40**(10): 3275-3280.

Steinhoff M, Buddenkotte J, Shpacovitch V, Rattenholl A, Moormann C, Vergnolle N, Luger TA, and Hollenberg MD (2005). "Proteinase-Activated Receptors: Transducers of Proteinase-Mediated Signaling in Inflammation and Immune Response." Endocr Rev **26**(1): 1-43.

van Ryn J, Stangier J, Haertter S, Liesenfeld KH, Wienen W, Feuring M, and Clemens A (2010). "Dabigatran Etexilate--a Novel, Reversible, Oral Direct Thrombin Inhibitor: Interpretation of Coagulation Assays and Reversal of Anticoagulant Activity." Thromb Haemost **103**(6): 1116-1127.

Vinukonda G, Dummula K, Malik S, Hu F, Thompson CI, Csiszar A, Ungvari Z, and Ballabh P (2010). "Effect of Prenatal Glucocorticoids on Cerebral Vasculature of the Developing Brain." Stroke **41**(8): 1766-1773.

Vohr BR, Wright LL, Dusick AM, Mele L, Verter J, Steichen JJ, Simon NP, Wilson DC, Broyles S, Bauer CR, Delaney-Black V, Yolton KA, Fleisher BE, Papile LA, and Kaplan MD (2000). "Neurodevelopmental and Functional Outcomes of Extremely Low Birth Weight Infants in the National Institute of Child Health and Human Development Neonatal Research Network, 1993-1994." Pediatrics **105**(6): 1216-1226.

Whitelaw A (2001). "Intraventricular Haemorrhage and Posthaemorrhagic Hydrocephalus: Pathogenesis, Prevention and Future Interventions." Semin Neonatol **6**(2): 135-146.

Xue M, and Del Bigio MR (2005). "Immune Pre-Activation Exacerbates Hemorrhagic Brain Injury in Immature Mouse Brain." J Neuroimmunol **165**(1-2): 75-82.

Yang D, Baumann JM, Sun YY, Tang M, Dunn RS, Akeson AL, Kernie SG, Kallapur S, Lindquist DM, Huang EJ, Potter SS, Liang HC, and Kuan CY (2013). "Overexpression of Vascular Endothelial Growth Factor in the Germinal Matrix Induces Neurovascular Proteases and Intraventricular Hemorrhage." Sci Transl Med **5**(193): 193ra190.

Zhou W, Schwarting S, Illanes S, Liesz A, Middelhoff M, Zorn M, Bendszus M, Heiland S, van Ryn J, and Veltkamp R (2011). "Hemostatic Therapy in Experimental Intracerebral Hemorrhage Associated with the Direct Thrombin Inhibitor Dabigatran." Stroke **42**(12): 3594-3599.

CHAPTER SIX

DISCUSSION AND CONCLUSION

Summary/Highlights of Findings

Our findings demonstrate blood, iron, and thrombin/PAR-1/mTOR activation contribute to GMH-induced brain injury and long-term PHH development. These findings are supported by the following observations: (1) PPARγ-induced upregulation of CD36 enhances short-term hematoma resolution and attenuates long-term neurological deficits and brain morphological outcomes; (2) acute and delayed iron chelation by Deferoxamine improves long-term brain morphological and neurobehavioral outcomes as well as reduced ECM protein proliferation; (3) combinatorial PAR-1 and PAR-4 inhibition reduced short-term COX-2 and mTOR activation, and COX-2 and mTOR inhibition improved long-term brain morphological and neurocognitive outcomes; (4) direct thrombin inhibition by Dabigatran reduces short-term mTOR activation and ameliorates long-term PHH development and neurocognitive deficits, which was not reversed by PAR-1 stimulation, nor could PAR-1 inhibition alone achieve the same therapeutic benefits as direct thrombin inhibition.

The State of the Field Prior to this Study

The pathophysiological mechanisms leading to PHH development after GMH remain to be clearly elucidated. Thrombin, intracerebroventricular blood clots, and iron have been identified as potentially causative factors of hydrocephalus formation. Thrombin initiates inflammatory responses, gliosis, and ECM protein proliferation that potentially obstruct the cerebroventricular system (Whitelaw 2001; Xue,

Balasubramaniam et al. 2003; Cherian, Whitelaw et al. 2004; Volpe 2009; Aquilina, Chakkarapani et al. 2011). Thrombin activates PARs, which subsequently activate downstream mTOR. Activation of mTOR is associated with ECM protein proliferation and impaired CSF dynamics (Paul, Leef et al. 2000; Kataoka, Hamilton et al. 2003; Crews, Wyss-Coray et al. 2004; Del Bigio 2004; Steinhoff, Buddenkotte et al. 2005; Xue and Del Bigio 2005; Ballabh, Xu et al. 2007; Dummula, Vinukonda et al. 2010). PPARγ stimulation enhances CD36 scavenger receptor-mediated microglial phagocytosis of red blood cells, resulting in increased clot resolution and improved outcomes after adult cerebral hemorrhage (Zhao, Zhang et al. 2006; Zhao, Sun et al. 2007). Iron chelation also improved adult cerebral hemorrhage outcomes (Hatakeyama, Okauchi et al. 2013). Pharmacological modulation of the thrombin/PAR/mTOR pathway, PPARγ, and iron, which all have clinically translatable pharmacological agents that target them available, for neonatal GMH have not been studied. A safe and non-invasive treatment for reducing PHH would significantly improve the quality of life for GMH patients.

How Our Findings Advance the Field

The findings from this investigation further elucidate some of the underlying pathophysiological mechanisms contributing to PHH development after GMH. In particular, we investigate the role of thrombin/PAR-1/mTOR, PPARγ/CD36, and iron. Our study suggests some therapeutic benefit can be achieved by a clinically available direct thrombin inhibitor, Dabigatran. Since thrombin inhibition has the risk of increased bleeding, investigating downstream thrombin pathways may provide more safe therapeutic alternatives. Thrombin inhibition ameliorated long-term PHH, neurological

deficits, and ECM protein proliferation as well as decreased short-term mTOR activity after GMH. Interestingly, PAR-1 inhibition alone did not achieve the same therapeutic benefits as thrombin inhibition, nor did PAR-1 stimulation reverse all therapeutic effects from thrombin inhibition, although brain morphological outcomes and mTOR activity were reversed. PAR-1 inhibition also tended to decrease ECM protein proliferation while PAR-1 stimulation only tended to reverse ECM protein proliferation. Interestingly, combinatorial PAR-1 and PAR-4 inhibition reduced short-term mTOR activity, suggesting inhibiting one PAR is not sufficient to diminish activity of downstream effectors. Future studies should investigate long-term combinatorial inhibition of PARs after GMH. Our findings suggest ECM protein proliferation is weakly associated with long-term PHH development. Furthermore, two Dabigatran administration routes were investigated, intraperitoneal and intranasal, and both achieved the same therapeutic benefits.

Our findings also suggest enhancing hematoma resolution by stimulating PPARγ, which can be targeted by clinically available pharmacological agents, such as thiazolidinediones, enhances short-term hematoma resolution and improves long-term brain morphological and neurocognitive outcomes after GMH. PPARγ antagonization reversed treatment effects, and CD36 knockdown also reversed PPARγ agonist effects on short-term hematoma resolution. Enhanced hematoma resolution was associated with increased presence of alternatively activated M2 microglia/macrophages, suggesting PPARγ stimulation modulates microglia/macrophage differentiation. In addition to enhancing clot resolution, removing iron released from lysed erythrocytes by administering a clinically available iron chelator, Deferoxamine, also ameliorated long-

term PHH, improved neurocognitive function, and reduced ECM proliferation. Therapeutic benefits were achieved when Deferoxamine was administered within hours after GMH as well as three days after GMH, suggesting iron chelation has a large therapeutic window. Our findings provide pertinent information regarding clinically viable therapeutic targets to attenuate long-term PHH development after GMH.

Summary/Conclusion

Direct thrombin inhibition, enhanced hematoma resolution by PPARγ stimulation, and iron chelation all resulted in improved long-term brain morphological (i.e. reduced PHH) and neurocognitive outcomes after experimental GMH in rat pups. Direct thrombin inhibition and combinatorial PAR-1 and PAR-4 inhibition resulted in decreased short-term p-mTOR expression. PAR-1 inhibition alone did not decrease p-mTOR activity, although PAR-1 stimulation with direct thrombin inhibition reversed treatment effects by increasing p-mTOR activity. Rapamycin treatment to inhibit mTOR improved brain morphological and neurocognitive outcomes. Direct thrombin inhibition reduced long-term intracranial pressure, improved brain morphological outcomes, ameliorated neurological deficits, and reduced ECM protein proliferation, but PAR-1 inhibition alone did not achieve the same therapeutic benefits although ECM protein proliferation tended to be reduced. Additionally, PAR-1 stimulation with direct thrombin inhibition only tended to reverse treatment effects on brain morphological outcomes, intracranial pressure, and ECM protein proliferation. Short-term mTOR activity is strongly associated with PHH development after GMH, and ECM protein proliferation is weakly associated with PHH. Additionally, PPARγ stimulation enhanced short-term hematoma resolution,

which was reversed by PPARγ antagonism and CD36 knockdown. PPARγ stimulation improved long-term neurocognitive and brain morphological outcomes, which was reversed by PPARγ antagonism. Iron chelation starting immediately after GMH and 72 hours after GMH improved long-term brain morphology, reduced neurocognitive deficits, and diminished ECM protein proliferation. Thus, the thrombin/PAR/mTOR pathway, the PPARγ/CD36 pathway, and iron play significant roles in long-term PHH development after GMH.

Prospective

Although our findings show blood clots, iron, and the thrombin/PAR/mTOR pathway play important roles in PHH development after GMH, it cannot concluded if PHH developed because of an obstruction in the cerebroventricular system and/or subarachnoid spaces. Indeed, current hydrodynamic theory of CSF dynamics and hydrocephalus development suggests the source for CSF production is choroidal and ependymal capillaries and the source for CSF reabsorption is subarachnoid and parenchymal capillaries as well as perivascular channels following glymphatic-mediated CSF-interstitial fluid exchange. Hydrocephalus results from a disruption in hydrostatic and oncotic pressures in the brain microvasculature as well as possible abnormal distribution of vascular pulsations due to changes in brain compliance (Egnor, Zheng et al. 2002; Greitz 2004; Oreskovic and Klarica 2011; Iliff, Wang et al. 2012). Further investigations into PHH development after GMH should focus less on possible cerebroventricular obstructions and more on alterations in barrier mechanisms of the brain microvasculature as well as the glymphatic system.

References

Aquilina K, Chakkarapani E, Love S, and Thoresen M (2011). "Neonatal Rat Model of Intraventricular Haemorrhage and Post-Haemorrhagic Ventricular Dilatation with Long-Term Survival into Adulthood." Neuropathol Appl Neurobiol **37**(2): 156-165.

Ballabh P, Xu H, Hu F, Braun A, Smith K, Rivera A, Lou N, Ungvari Z, Goldman SA, Csiszar A, and Nedergaard M (2007). "Angiogenic Inhibition Reduces Germinal Matrix Hemorrhage." Nat Med **13**(4): 477-485.

Cherian S, Whitelaw A, Thoresen M, and Love S (2004). "The Pathogenesis of Neonatal Post-Hemorrhagic Hydrocephalus." Brain Pathol **14**(3): 305-311.

Crews L, Wyss-Coray T, and Masliah E (2004). "Insights into the Pathogenesis of Hydrocephalus from Transgenic and Experimental Animal Models." Brain Pathol **14**(3): 312-316.

Del Bigio MR (2004). "Cellular Damage and Prevention in Childhood Hydrocephalus." Brain Pathol **14**(3): 317-324.

Dummula K, Vinukonda G, Xu H, Hu F, Zia MT, Braun A, Shi Q, Wolk J, and Ballabh P (2010). "Development of Integrins in the Vasculature of Germinal Matrix, Cerebral Cortex, and White Matter of Fetuses and Premature Infants." J Neurosci Res **88**(6): 1193-1204.

Egnor M, Zheng L, Rosiello A, Gutman F, and Davis R (2002). "A Model of Pulsations in Communicating Hydrocephalus." Pediatr Neurosurg **36**(6): 281-303.

Greitz D (2004). "Radiological Assessment of Hydrocephalus: New Theories and Implications for Therapy." Neurosurg Rev **27**(3): 145-165; discussion 166-147.

Hatakeyama T, Okauchi M, Hua Y, Keep RF, and Xi G (2013). "Deferoxamine Reduces Neuronal Death and Hematoma Lysis after Intracerebral Hemorrhage in Aged Rats." Transl Stroke Res **4**(5): 546-553.

Iliff JJ, Wang M, Liao Y, Plogg BA, Peng W, Gundersen GA, Benveniste H, Vates GE, Deane R, Goldman SA, Nagelhus EA, and Nedergaard M (2012). "A Paravascular Pathway Facilitates Csf Flow through the Brain Parenchyma and the Clearance of Interstitial Solutes, Including Amyloid Beta." Sci Transl Med **4**(147): 147ra111.

Kataoka H, Hamilton JR, McKemy DD, Camerer E, Zheng YW, Cheng A, Griffin C, and Coughlin SR (2003). "Protease-Activated Receptors 1 and 4 Mediate Thrombin Signaling in Endothelial Cells." Blood **102**(9): 3224-3231.

Oreskovic D, and Klarica M (2011). "Development of Hydrocephalus and Classical Hypothesis of Cerebrospinal Fluid Hydrodynamics: Facts and Illusions." Prog Neurobiol **94**(3): 238-258.

Paul DA, Leef KH, and Stefano JL (2000). "Increased Leukocytes in Infants with Intraventricular Hemorrhage." Pediatr Neurol **22**(3): 194-199.

Steinhoff M, Buddenkotte J, Shpacovitch V, Rattenholl A, Moormann C, Vergnolle N, Luger TA, and Hollenberg MD (2005). "Proteinase-Activated Receptors: Transducers of Proteinase-Mediated Signaling in Inflammation and Immune Response." Endocr Rev **26**(1): 1-43.

Volpe JJ (2009). "Brain Injury in Premature Infants: A Complex Amalgam of Destructive and Developmental Disturbances." Lancet Neurol **8**(1): 110-124.

Whitelaw A (2001). "Intraventricular Haemorrhage and Posthaemorrhagic Hydrocephalus: Pathogenesis, Prevention and Future Interventions." Semin Neonatol **6**(2): 135-146.

Xue M, Balasubramaniam J, Buist RJ, Peeling J, and Del Bigio MR (2003). "Periventricular/Intraventricular Hemorrhage in Neonatal Mouse Cerebrum." J Neuropathol Exp Neurol **62**(11): 1154-1165.

Xue M, and Del Bigio MR (2005). "Immune Pre-Activation Exacerbates Hemorrhagic Brain Injury in Immature Mouse Brain." J Neuroimmunol **165**(1-2): 75-82.

Zhao X, Sun G, Zhang J, Strong R, Song W, Gonzales N, Grotta JC, and Aronowski J (2007). "Hematoma Resolution as a Target for Intracerebral Hemorrhage Treatment: Role for Peroxisome Proliferator-Activated Receptor Gamma in Microglia/Macrophages." Ann Neurol **61**(4): 352-362.

Zhao X, Zhang Y, Strong R, Grotta JC, and Aronowski J (2006). "15d-Prostaglandin J2 Activates Peroxisome Proliferator-Activated Receptor-Gamma, Promotes Expression of Catalase, and Reduces Inflammation, Behavioral Dysfunction, and Neuronal Loss after Intracerebral Hemorrhage in Rats." J Cereb Blood Flow Metab **26**(6): 811-820.

APPENDIX A

MODULATING THE IMMUNE RESPONSE TOWARDS A NEUROREGENERATIVE PERI-INJURY MILIEU AFTER CEREBRAL HEMORRHAGE

Damon Klebe, BA[1]; Devin M[c]Bride, PhD[1]; Jerry J Flores, BS[1]; John H Zhang, MD PhD[1, 2]; Jiping Tang, MD[1]

[1]Department of Physiology & Pharmacology, Loma Linda University School of Medicine, Loma Linda, California, USA

[2]Departments of Anesthesiology and Neurosurgery, Loma Linda University School of Medicine, Loma Linda, California, USA

Published: *Journal of Neuroimmune Pharmacology*. 2015 Dec; 10(4): 576-86

Abstract

Cerebral hemorrhages account for 15-20% of stroke sub-types and have very poor prognoses. The mortality rate for cerebral hemorrhage patients is between 40-50%, of which at least half of the deaths occur within the first two days, and 75% of survivors are incapable of living independently after one year. Current emergency interventions involve lowering blood pressure and reducing intracranial pressure by controlled ventilations or, in the worst case scenarios, surgical intervention. Some hemostatic and coagulatherapeutic interventions are being investigated, although a few that were promising in experimental studies have failed in clinical trials. No significant immunomodulatory intervention, however, exists for clinical management of cerebral hemorrhage. The inflammatory response following cerebral hemorrhage is particularly harmful in the acute stage because blood-brain barrier disruption is amplified and surrounding tissue is destroyed by secreted proteases and reactive oxygen species from infiltrated leukocytes. In this review, we discuss both the destructive and regenerative roles the immune response play following cerebral hemorrhage and focus on microglia, macrophages, and T-lymphocytes as the primary agents directing the response. Microglia, macrophages, and T-lymphocytes each have sub-types that significantly influence the over-arching immune response towards either a pro-inflammatory, destructive, or an anti-inflammatory, regenerative, state. Both pre-clinical and clinical studies of cerebral hemorrhages that selectively target these immune cells are reviewed and we suggest immunomodulatory therapies that reduce inflammation, while augmenting neural repair, will improve overall cerebral hemorrhage outcomes.

Cerebral Hemorrhage Pathophysiology

Incidence, Outcomes, and Clinical Management

Cerebral hemorrhage, the rupturing of blood vessels within the brain tissue, accounts for 10-15% of strokes (Qureshi, Mendelow et al. 2009; Mracsko and Veltkamp 2014). Occurring in approximately 25 per 100,000 people per year, cerebral hemorrhage is the leading cause of morbidity and mortality in stroke patients, having a mortality rate between 30-50% with nearly 75% of survivors incapable of living independently after one year (van Asch, Luitse et al. 2010). Hospital admissions for cerebral hemorrhage cases have increased by 18% over the past decade, and admissions are expected to continue rising due to an increasing elderly population (Qureshi, Mendelow et al. 2009).

Current clinically approved emergency interventions involve lowering blood pressure (Anderson, Huang et al. 2008; Morgenstern, Hemphill et al. 2010; Sakamoto, Koga et al. 2013) or surgical craniotomy (Morgenstern, Hemphill et al. 2010). Hematoma evacuation is also being investigated as a potential surgical intervention, but it has yet to yield positive results (Morgenstern, Frankowski et al. 1998; Mendelow, Gregson et al. 2005; Miller, Vespa et al. 2008; Wang, Jiang et al. 2009; Mendelow, Gregson et al. 2013). Hemostatic therapies have also been investigated in clinical trials, such as recombinant factor VII, but despite showing promise in experimental studies, none have been clinically approved (Mayer, Brun et al. 2006; Mayer, Brun et al. 2008; Diringer, Skolnick et al. 2010). Unfortunately, cerebral hemorrhage is the least treatable stroke subtype, with minimal advancements being made in clinical management, despite its increasing prevalence (Kreitzer and Adeoye 2013).

Primary Brain Injury

Most investigative therapeutic approaches for cerebral hemorrhage focus on ameliorating primary brain injury, which is caused by the mechanical pressure on brain tissue due to the hematoma mass effect, and the potential hematoma expansion (Xi, Keep et al. 2006; Keep, Hua et al. 2012; Mracsko and Veltkamp 2014). Mechanical pressure applied to glia and neurons cause calcium influx and secretion of excitotoxic neurotransmitters, resulting in consequent cytotoxic edema and necrosis (Keep, Xi et al. 2005; Xi, Keep et al. 2006). Indeed, hematoma volume and subsequent hematoma expansion, which occurs in approximately 30% of clinical cerebral hemorrhage cases, are currently the best prognostic indicators (Davis, Broderick et al. 2006; Dowlatshahi, Demchuk et al. 2011; Brouwers and Greenberg 2013). Brain edema, caused by both primary and secondary brain injury mechanisms, is increasingly accepted as a valuable prognostic indicator (Thiex and Tsirka 2007; Staykov, Wagner et al. 2011).

Secondary Brain Injury

Mechanisms for secondary brain injury after cerebral hemorrhage have garnered increased research interests over the past decade. Secondary brain injury results from blood components entering the brain tissue as well as injured brain cells that trigger multiple deleterious mechanisms and subsequently augment oxidative stress, inflammatory pathways, blood-brain barrier disruption, and vasogenic edema (Aronowski and Zhao 2011; Belur, Chang et al. 2013). Coagulation cascade activation increases thrombin formation, which stimulates the complement pathway as well as protease-activated receptors (PARs) (Hua, Keep et al. 2007; Babu, Bagley et al. 2012). PAR

stimulation after hemorrhage, particularly PAR-1 activation in neurons, leads to increased NMDA receptor potentiation and consequent activation of excitotoxicity, apoptosis, and pro-inflammatory pathways (Babu, Bagley et al. 2012). PAR-1 has also been implicated in playing an important role in thrombin-induced cerebral hemorrhaging (Cheng, Xi et al. 2014). Complement activation after cerebral hemorrhage leads to membranous pore formation, called membrane attack complexes, in neurons and red blood cells, causing cytotoxicity and cell lysis (Hua, Xi et al. 2000; Ducruet, Zacharia et al. 2009).

Red blood cell lysis releases hemoglobin, which is metabolized by heme oxygenase 1 to release iron and heme, into the surrounding tissue (Wu, Xi et al. 2006). Heme and iron are critical constituents in redox reactions that produce injurious free radicals and increase oxidative stress, causing significant tissue injury, DNA damage, blood-brain barrier disruption, and inflammation (Wu, Xi et al. 2006; Xi, Keep et al. 2006; Babu, Bagley et al. 2012; Xiong, Wang et al. 2014). Administering Deferoxamine, an iron chelator, resulted in improved neurofunctional outcomes following experimental cerebral hemorrhage and reduced hydrocephalus development in other brain injury models (Nakamura, Keep et al. 2004; Klebe, Krafft et al. 2014; Zhao, Chen et al. 2014). Indeed, post-hemorrhagic hydrocephalus is a common consequence of intracerebral hemorrhage as well, and iron has been implicated as a causative factor (Chen, Zhang et al. 2014; Gao, Du et al. 2014; Meng, Li et al. 2014).

Inflammation is a key component of secondary brain injury following cerebral hemorrhage (Wang 2010; Mracsko and Veltkamp 2014; Zhou, Wang et al. 2014; Chen, Yang et al. 2015). An inflammatory response ensues immediately after blood enters the brain tissue via activation of resident immune cells and subsequent infiltration of

peripheral leukocytes, leading to secretion of pro-inflammatory mediators, extracellular proteases, and reactive oxygen species that further damage brain tissue and disrupt the blood-brain barrier (Aronowski and Hall 2005; Wang and Dore 2007). Immune cells, particularly pro-inflammatory macrophages, also play an important role in cerebral aneurysm formation, a primary cause for cerebral hemorrhage (Hosaka and Hoh 2014; Starke, Raper et al. 2014). Some evidence, however, suggests inflammation may play an important role in repair and recovery following central nervous system injury (Correale and Villa 2004; Hohlfeld, Kerschensteiner et al. 2006; McCombe and Read 2008; Wee Yong 2010). The potential neuroprotective branch in inflammation may be therapeutically exploited following cerebral hemorrhage to promote hematoma resolution as well as tissue repair and regeneration.

Review Scope

In this review, we will discuss microglia, macrophage, and T-helper lymphocyte immunology following cerebral hemorrhagic insult, the roles which the subtypes for each play in neurodegeneration or neuroprotection, as well as possible therapeutic approaches to potentially shift the inflammatory response towards a neuroregenerative phenotype. We will also discuss evidence from current cerebral hemorrhage research and address gaps in the literature that warrant further investigation. Explicating the immune response in its entirety following cerebrovascular insult will discern therapeutic immunomodulatory approaches that dampen the neurodegenerative inflammatory response in favor for a neuroregenerative one, promoting functional recovery and improving overall outcomes. Cerebral hemorrhage pathophysiology is very complex and

multi-modal approaches are being increasingly encouraged, and exploiting immunomodulatory mechanisms may prove beneficial when investigating such approaches since inflammation is an important component of secondary brain injury (Pandey and Xi 2014).

Macrophage, Microglia, and T-helper Lymphocyte Characterization

Macrophage and Microglia Subtypes

Macrophages are a type of white blood cell of myeloid lineage found in almost all tissue types and play a quintessential role in innate (non-specific) immunity by searching for and engulfing potential pathogens (Murray and Wynn 2011). Microglia are the resident macrophages of the central nervous system, and, unfortunately, they are extremely difficult to distinguish from infiltrated macrophages following central nervous system injury (Saijo and Glass 2011). Traditionally, macrophages and microglia phagocytose microbes, cellular debris, apoptotic cells, cancer cells, and foreign substances. Stimulation of microglia/macrophage toll-like receptors, nod-like receptors, scavenger receptors, and/or cytokine receptors from inflammatory cytokines, pathogens, and blood products will potentiate the inflammatory response through further secretion of pro-inflammatory cytokines, such as TNF-α and IL-1β, resulting in leukocyte recruitment. Recent immunology research, however, discerned macrophages can also dampen the immune response, promoting tissue repair and regeneration. Microglia and macrophages have been classified into two predominant subtypes modeled similar to the Th1/Th2 paradigm: classically activated or M1 and alternatively activated or M2 (Murray and Wynn 2011; Saijo and Glass 2011). Further elucidating the role each subtype plays

in cerebral hemorrhage pathophysiology may yield potential therapeutic avenues that coax the immune response to create a neural regenerative milieu in the peri-hematoma region.

Classically activated M1 macrophages and microglia are primarily responsible for the innate immune defense mechanisms, producing a pro-inflammatory response (Murray and Wynn 2011; Saijo and Glass 2011). The M1 phenotype can be induced by lipopolysaccharides, interferon-γ, TNF-α, or stimulation of nod-like receptors (NLR) or toll-like receptors (TLR), primarily TLR-4 (Martinez, Helming et al. 2009; Chen and Nunez 2010). Very few definitive cell surface markers for the M1 subtype have been identified, although CD80 and CD86 are widely used. M1 macrophages and microglia also secrete TNF-α, IL-1β, IL-6, IL-12, and IL-23 pro-inflammatory cytokines (Martinez and Gordon 2014; Wang, Liang et al. 2014). Alternatively, activated M2 macrophages and microglia are primarily responsible for mediating wound healing and produce an anti-inflammatory response (Murray and Wynn 2011; Saijo and Glass 2011). The M2 phenotype can be induced by IL-4, IL-10, TGF-β, and IL-13 stimulation (Martinez, Helming et al. 2009; Martinez and Gordon 2014; Wang, Liang et al. 2014). Common cell surface markers attributed to the M2 subtype include CD163 and CD206, and M2 macrophages and microglia secrete IL-10 and TGF-β anti-inflammatory cytokines (Martinez, Helming et al. 2009; Martinez and Gordon 2014; Wang, Liang et al. 2014). Evidence suggests macrophages and microglia do not exist as terminally differentiated M1 or M2 states, but rather have the ability to switch phenotypes depending upon their microenvironment (Stout and Suttles 2004; Stout, Jiang et al. 2005; Eggen, Raj et al. 2013; Giunti, Parodi et al. 2014). Table A.1 contains the macrophage/microglia

subtypes, cytokines inducing their activation, common markers, secreted cytokines, as well as known mechanisms of action.

The M1/M2 paradigm, however, has limitations. Indeed, M2 microglia are being further classified into 3 subsets based on how differentiation is stimulated: M2a is stimulated by IL-4 and IL-10; M2b is stimulated by toll-like receptor activation; and M2c is stimulated by IL-10, glucocorticoids, and TGF-β (Cherry, Olschowka et al. 2014). M2a and M2c have the typical markers and responses attributed to alternatively activated M2, while M2b lacks certain markers and has a response similar to M1 (Cherry, Olschowka et al. 2014). Additionally, An increasing number of macrophage/microglia subsets in addition to M1/M2 are being classified in other diseases and disorders, such as atherosclerosis, multiple sclerosis, and lupus, including M4, Mox, Mhem, and M(Hb) (Orme and Mohan 2012; Bogie, Stinissen et al. 2014; Chinetti-Gbaguidi, Colin et al. 2015). Furthermore, distinct macrophage/microglia responses have been characterized *in vitro* following stimulation by cytokines and extracellular pathogenic debris as well as *in vivo* following infection, yet the exact roles distinct microglia/macrophage subtypes play in most neurological diseases, disorders, and injuries have yet to be well elucidated. M1 and M2 may represent two extremes on a large spectrum of macrophage/microglia subsets where each subset plays a very critical immunomodulatory role in cerebral hemorrhage pathophysiology, and more research is needed to fill these gaps in our knowledge and help advance immunotherapeutic approaches.

Table A.1: Macrophage/Microglia and T-helper Lymphocyte Subtypes

Cell Types	Activating Cytokines	Markers	Secreted Cytokines	Mechanisms of action	References
M1	IFN-γ, TNF-α, LPS	CD86, CD80, MHC II↑, IL-1R I, TLR2, TLR4, iNOS	TNF-α, IL-12, and IL-23	Inhibits cell proliferation and causes tissue damage	(Martinez, Helming et al. 2009; Chen and Nunez 2010; Cherry, Olschowka et al. 2014; Martinez and Gordon 2014; Wang, Liang et al. 2014)
M2	IL-4, IL-13	CD163, MHC II, SR, CD206↑, (MR↑), TGM2↑, DecoyR, IL-1R II, Ym1, Fizz1, Arg-1	IL-10, TGF-β, and IL-1RA	Promotes cell proliferation and tissue repair	(Martinez, Helming et al. 2009; Murray and Wynn 2011; Saijo and Glass 2011; Cherry, Olschowka et al. 2014; Martinez and Gordon 2014; Wang, Liang et al. 2014)
Th1	IL-12, IL-18	CD4, CXCR3, CCR5	IFN-γ, IL-2, and TNF-α	Activate macrophages and are responsible for cell-mediated immunity and phagocyte-dependent protective responses	(Romagnani 1999; Zhu and Paul 2008; Luckheeram, Zhou et al. 2012)
Th2	IL-4	CRTH2, CCR3, CCR4	IL-4, IL-5, IL-10, and IL-13	Are responsible for strong antibody production, eosinophil activation, and inhibition of several macrophage functions, thus providing phagocyte-independent protective responses	(Romagnani 1999; Zhu and Paul 2008; Luckheeram, Zhou et al. 2012)
Th17	IL-2, IL-6, TGF-β, IL-1β, IL-23	CD4, CCR4, CCR6	IL-17A/F, IL-21, IL-22, CCR6 and RORγ/γt	Creates inflammation and tissue injury in autoimmune diseases	(Stockinger and Veldhoen 2007; Dong 2008; Hirota, Martin et al. 2010; Peck and Mellins 2010; Dong 2011; Zambrano-Zaragoza, Romo-Martinez et al. 2014)
Treg	IL-2, TGF-β	CD4, CD25, and Foxp3	TGF-β, IL-10, and IL-35	Are essential for maintaining peripheral tolerance, preventing autoimmune diseases and limiting chronic inflammatory diseases	(Chen, Jin et al. 2003; Vignali, Collison et al. 2008; Mantel and Schmidt-Weber 2011; Yoshimura and Muto 2011)

T-helper Lymphocyte Subtypes

T-helper cells are $CD4^+$ white blood cells of lymphoid origin that develop within the thymus which are critical in regulating cell-mediated and adaptive immunity (Luckheeram, Zhou et al. 2012). The two predominant paradigms for T-helper cell subtypes, analogous to the M1/M2 macrophage and microglia paradigm in that the two phenotypes oppose each other, are Th1/Th2 and Th17/Treg (Kleinewietfeld and Hafler 2013; Bretscher 2014). Macrophages and microglia are capable of switching phenotypes according to their microenvironment, and some evidence supports T-helper cells switching phenotypes too, particularly between Th17 and Treg, although more conclusive evidence is needed (Stout and Suttles 2004; Stout, Jiang et al. 2005; Xu, Kitani et al. 2007; Kleinewietfeld and Hafler 2013).

Th1 cells direct the immune system towards fighting intracellular pathogens by inducing a cell-mediated response. Th1 cell differentiation is kindled by IL-12 and interferon-γ stimulation, the latter of which Th1 cells secrete to further drive Th1 differentiation. Th2 cells direct the immune system towards fighting extracellular pathogens by inducing a humoral response. Th2 cell differentiation is sparked by IL-4 and IL-2 stimulation, and Th2 cells secrete IL-4, IL-5, IL-6, IL-9, IL-10, and IL-13 (Zhu and Paul 2008; Zhu and Paul 2010; Luckheeram, Zhou et al. 2012). Th1 cells are characterized by CCR5, CXCR3, and T-bet markers, while Th2 cells are identified by CCR3, CCR4, CRTH2, and GATA3 markers. Th1 and Th2 both drive their own differentiation while suppressing differentiation into the other through their cytokine expressions (Zhu and Paul 2008; Zhu and Paul 2010; Luckheeram, Zhou et al. 2012).

The other T-helper phenotype paradigm relies on the promotion or suppression of inflammation. Th17 cells which potentiate inflammation and have been implicated as potential sources for many autoimmune diseases differentiate through IL-6, IL-21, IL-23, and TGF-β stimulation. T17 cells, which express CCR6 and RORγt markers, secrete IL-17, IL-21, and IL-22 (Stockinger and Veldhoen 2007; Dong 2008; Hirota, Martin et al. 2010; Peck and Mellins 2010; Dong 2011). Treg cells which dampen inflammation and mediate immune tolerance to self-antigens, differentiate through IL-2 and TGF-β stimulation (Chen, Jin et al. 2003; Mantel and Schmidt-Weber 2011; Yoshimura and Muto 2011). Treg cells, characterized by CD25 and FOXP3 markers, secrete IL-10 and TGF-β. Evidence suggests plasticity between Th17 and Treg cell differentiation, which is highly dependent upon their surrounding milieu (Zhou, Chong et al. 2009; Kleinewietfeld and Hafler 2013). Interestingly, differentiation of both Th17 and Treg cells can be driven by TGF-β (Li, Wan et al. 2007). TGF-β at low concentrations and in conjunction with IL-6 or IL-21 will drive Th17 differentiation, but TGF-β at high concentrations and in conjunction with IL-10 will drive Treg differentiation (Chen, Jin et al. 2003; Mantel and Schmidt-Weber 2011; Yoshimura and Muto 2011). Table A.1 contains the T-helper lymphocyte subtypes, cytokines inducing their activation, common markers, secreted cytokines, as well as known mechanisms of action.

Macrophage/Microglia and T-helper Lymphocyte Communication

T-helper lymphocytes, macrophages, and microglia are capable of influencing each other's differentiation as well as phenotype switching (Murray and Wynn 2011; Saijo and Glass 2011; Luckheeram, Zhou et al. 2012). M1 macrophages secrete TNF-α,

IL-6, IL-12, and IL23 (Murray and Wynn 2011; Saijo and Glass 2011), which recruits and induces differentiation of both Th1 and Th17 cells. In turn, Th1 cells secrete interferon-γ while Th17 cells secrete IL-17, which further augments M1 macrophage polarization and potentiates the inflammatory response (Fiorentino, Zlotnik et al. 1991; Denning, Wang et al. 2007; Martinez, Sica et al. 2008; Savage, de Boer et al. 2008; Biswas and Mantovani 2010). M1 macrophage and Th1 / Th17 cross-talk acts as a positive feed-back loop that further drives their own differentiation and create a highly inflamed microenvironment. Analogously, M2 macrophages secrete IL-4, IL-10, and TGF-β (Martinez, Sica et al. 2008; Murray and Wynn 2011; Saijo and Glass 2011), which recruits and induces differentiation of both Th2 and Treg cells. In turn, Th2 cells secrete IL-4 and IL-10 while Tregs secrete IL-10 and TGF-β, which further drives M2 polarization, dampening inflammation and promoting tissue repair (Denning, Wang et al. 2007; Martinez, Sica et al. 2008; Savage, de Boer et al. 2008; Biswas and Mantovani 2010). Disproportion between macrophage/microglia and T-helper cells, in which either the M1/Th1/Th17 or M2/Th2/Treg branches are overexpressed, intensify many disorders, including allergies, asthma, cancer, autoimmune diseases, atherosclerosis, and fibrosis. Consequently, many therapeutic approaches have been developed to exploit the cross-talk between macrophages/microglia and T-helper cells, restoring homeostasis between pro-inflammatory and regenerative signaling in those aforementioned disorders (Murray and Wynn 2011; Saijo and Glass 2011; Luckheeram, Zhou et al. 2012).

Inflammation after Cerebral Hemorrhage

Role of Macrophages and Microglia

Explicating the inflammatory component of cerebral hemorrhage pathophysiology and discerning the immune cells involved, particularly the distinct macrophage/microglia and T-helper cell subsets, could lead to novel therapeutic approaches in which the peri-hematoma milieu is switched from a pro-inflammatory microenvironment to a neuroregenerative one. Macrophages, microglia, and T-helper cell subsets are ideal targets because of the cross-talk and capability of potentiating either the damaging branch of inflammation via M1/Th1/Th17 or the repair/regenerative branch via M2/Th2/Treg (Murray and Wynn 2011; Saijo and Glass 2011; Luckheeram, Zhou et al. 2012). The M1/Th1/Th17 branch creates an oxidative, caustic microenvironment to destroy pathogens, but cerebral hemorrhage is a brain injury of endogenous origin, thus attenuating this branch in favor of the M2/Th2/Treg branch may be beneficial (Chen and Nunez 2010). Macrophages and microglia are of particular interest since they are the first to be activated following hemorrhage and are quintessential drivers of the immune response (Mracsko and Veltkamp 2014; Zhou, Wang et al. 2014). Furthermore, microglia and macrophages have great plasticity and aptly switch phenotypes between M1 and M2 in response to the pathophysiology of their microenvironment.

Activated microglia become present within 1-4 hours after cerebral hemorrhage in rodents, peak between 3-7 days, and finally return to basal levels between 3-4 weeks (Wang and Dore 2007; Zhou, Wang et al. 2014). Following microglia activation, peripheral macrophages also infiltrate the injured tissue, although they are extremely difficult to distinguish from microglia. Microglia/macrophages also recruit neutrophils

within hours of activation, which potentiate blood-brain barrier disruption and tissue damage by secreting extracellular proteases (Wang and Dore 2007; Zhao, Sun et al. 2014). While the activated microglia time course has been established in these experimental rodent cerebral hemorrhage models, the time course of M1 and M2 phenotype expression has yet to be well-defined. Determining the ratio of M1/M2 microglia and macrophages could be indicative of the pathophysiological milieu, as a high M1/M2 ratio implies a more oxidative, caustic inflammatory environment while a low M1/M2 ratio implies a more repair, regenerative environment. M2 microglia and macrophages have increased scavenger receptor expression levels as well as augmented phagocytic activity compared to their M1 counterparts, therefore the M2 phenotype may be important for hematoma resolution after cerebral hemorrhage (Cherry, Olschowka et al. 2014). Indeed, hematoma volume peaks 72 hours after experimental cerebral hemorrhage, remains relatively elevated from 3-7 days, and is finally resolved between 2-4 weeks (Zhao, Grotta et al. 2009). Coincidentally, this correlates with the time course of activated microglia number, thus elucidating the time course of the M1/M2 ratio following cerebral hemorrhage may yield more information on the neuroprotective role microglia and macrophage subtypes play, as it is expected the M1/M2 ratio will rise and fall with hematoma volume, implying M2 microglia and macrophages are important for hematoma resolution.

A thoroughly investigated therapy involves enhancing hematoma resolution by peroxisome proliferator receptor gamma (PPARγ) stimulation. PPARγ stimulation enhances hematoma resolution, reduces oxidative stress, ameliorates damaging inflammation, decreases brain edema, and improves functional outcomes starting at 24

hours after cerebral hemorrhage in experimental rodent models (Zhao, Sun et al. 2007; Zhao, Grotta et al. 2009). Furthermore, Pioglitazone, a PPARγ agonist, is being investigated in a clinical trial for enhancing hematoma resolution after cerebral hemorrhage. PPARγ stimulation upregulates the red blood cell scavenger receptor CD36, consequently enhancing red blood cell phagocytosis *in vitro* and *in vivo* (Zhao, Sun et al. 2007). Furthermore, the change in the M1/M2 ratio induced by PPARγ stimulation has not been investigated. However, other studies indicate that PPARγ stimulation polarizes microglia and macrophages towards the M2 phenotype (Pisanu, Lecca et al. 2014). Thus the neuroprotective effect from PPARγ treatment may include polarizing microglia and macrophages towards the M2 phenotype, reducing the M1/M2 ratio, and creating a regenerative peri-hematoma milieu that promotes tissue repair and hematoma resolution.

After cerebral vessel rupture, damage-associated molecular patterns, molecules capable of initiating and perpetuating a non-infectious inflammatory response following injury, stimulate the TLRs and NLRs of microglia, inducing microglia activation (Fang, Wang et al. 2013). TLR-4 stimulation by damage-associated molecular patterns, in addition to hemoglobin degradation products, induces M1 differentiation in macrophages and microglia. In a rodent model of cerebral hemorrhage, TLR-4 knockout mice had decreased microglia activation and macrophage infiltration at 72 hours post ictus (Fang, Wang et al. 2013). Additional studies established that TLR-4 blockade also ameliorates neurological deficits and brain edema after experimental cerebral hemorrhage (Fang, Wang et al. 2013). While TLR-4 stimulation following cerebral hemorrhage activates

microglia and induces an M1-like phenotype, the effect on the M2 phenotype is unknown.

Rather than reduce the M1/M2 phenotype ratio, some studies have aimed at inhibiting microglia activation altogether. Experimental cerebral hemorrhage studies in rodents found that microglia inhibitor factor ameliorates brain injury and improves functional outcomes, which was correlated with overall reduced microglia activation (Wang and Dore 2007; Zhou, Wang et al. 2014). One such microglia activation inhibitor is minocycline. Nervous system injury studies discerned minocycline treatment inhibits M1 microglia and macrophage polarization without affecting M2 polarization. While preclinical studies have reported that minocycline attenuates brain injury and improves functional outcomes, one study challenges minocycline's overall therapeutic potential (Wang and Dore 2007; Zhou, Wang et al. 2014). Indeed, the authors of a study which determined that minocycline is neuroprotective also argued that long-term microglia inhibition may not be beneficial because of the role microglia play in tissue repair, suggesting that M2 microglia and macrophages may play a long-term neuroprotective role. This concept may provide an explanation for the results acquired in the negative minocycline cerebral hemorrhage study. Despite seemingly contradictory studies, minocycline is currently being evaluated in clinical trials for cerebral hemorrhage.

Evidence provided by other brain injury preclinical models suggests manipulating M1/M2 polarization by decreasing the M1 phenotype and/or by increasing the M2 phenotype has beneficial outcomes. Although microglia and macrophages are known to play a very important role in potentiating secondary brain injury after cerebral hemorrhage, since several studies also suggest they are important for functional recovery,

little is known about the roles individual microglia subtypes play. Discerning the exact microglia and macrophage subtypes involved in cerebral hemorrhage pathophysiology, as well as their time course of action following injury, may yield novel, effective therapeutic approaches, since decreasing the M1/M2 ratio by either reducing the M1 pro-inflammatory phenotype and/or increasing the M2 regenerative phenotype may improve overall outcomes.

Role of T-Helper Lymphocytes

Although cerebral hemorrhage is a brain injury of endogenous origin, and mounting an antigen specific adaptive immune response may take nearly one week to occur, increasing evidence suggests that $CD4^+$ T-helper lymphocytes play an important role in secondary brain injury. Clinical evidence shows the presence of T-helper lymphocytes within the peri-hematoma region of patients with cerebral hemorrhage (Guo, Li et al. 2006). Pre-clinical rodent cerebral hemorrhage models indicate T-helper lymphocyte infiltration is delayed, commencing between 2-4 days post-ictus, yet some studies have reported T-helper lymphocyte infiltration occurs within one day post-ictus, peaking at 5 days post-ictus, before subsiding (Mracsko, Javidi et al. 2014). Intuitively, this suggests T-helper cells, which heavily influence the surrounding milieu of injured tissue, direct the delayed immune response of cerebral hemorrhage, at least in part, by encouraging either a highly inflammatory, oxidative microenvironment or a regenerative and repair microenvironment, although preclinical evidence for the exact role of T-helper subtypes is lacking.

Fingolimod, a sphingosine-1 phosphate inhibitor, downregulates sphingosine-1 phosphate receptors in T-helper lymphocytes to reduce their egress from lymphoid tissue and subsequent infiltration into injured tissue. In a rodent model of cerebral hemorrhage, fingolimod reduced brain edema and improved neurofunctional outcomes 24 and 72 hours post-ictus, which was associated with reduced T-helper lymphocyte egress in the blood, decreased T-helper lymphocyte infiltration into the brain, and decreased IL-17 secretion (a pro-inflammatory cytokine typically secreted by Th17 cells (Rolland, Manaenko et al. 2011; Rolland, Lekic et al. 2013). Fingolimod, however, is known to upregulate peripheral regulatory T cells with some evidence suggesting it decreases circulating Th17 cells in clinical and preclinical multiple sclerosis studies. Thus, Fingolimod's neuroprotective effects in cerebral hemorrhage may partially be explained by shifting the predominant T-helper cell response from the inflammatory Th17 subtype to the regenerative Treg phenotype, although this has yet to be confirmed. Fingolimod is currently being investigated in clinical trials for cerebral hemorrhage (Fu, Hao et al. 2014).

Another experimental rodent model of cerebral hemorrhage study investigated adoptive transfer of Treg cells, and observed that Treg cells reduced microglia activation and improved functional outcomes, however the effects on microglia and macrophage polarization were not evaluated (Yang, Yu et al. 2014). Furthermore, neural stem cell transplantation, previously shown to protect the brain from inflammatory damage, resulted in increased peripheral and infiltrated Treg cells, and was associated with increased anti-inflammatory cytokines (IL-4, IL-10, and TGF-β) and decreased pro-inflammatory cytokines (IL-6, interferon-γ) (Gao, Lu et al. 2014). Furthermore,

mammalian target of rapamycin (mTOR) inhibition following cerebral hemorrhage in rats resulted in improved neurofunctional outcomes 24 hours post-ictus which coincided with increased Treg cells, IL-10, and TGF-β, as well as reduced interferon-γ in the blood and brain (Lu, Gao et al. 2014). Unfortunately, investigative studies on the Th1/Th2 paradigm following cerebral hemorrhage are lacking. Yet evidence suggests that inhibiting Th1 proliferation improves outcomes while inhibiting Th2 aggravates brain injury during cerebral ischemia (Theodorou, Marousi et al. 2008; Gu, Xiong et al. 2012).

Table A.2: Current and Past Clinical Trials Evaluating Immunomodulatory Therapies for Cerebral Hemorrhage

Hemorrhage type	Agent	Trial	Phase	Status	References
Supratentorial Intracerebral Hemorrhage	Prophylactic forced normothermia	Systemic Normothermia in Intracerebral Hemorrhage (ICH) (SNICH)	0	Not Yet Recruiting	(Rincon, Friedman et al. 2014)
Intracerebral Hemorrhage	Labetalol/Hydralazine/Enalapril	The Intracerebral Hemorrhage Acutely Decreasing Arterial Pressure Trial II (ICH-ADAPT II)	2	Recruiting	(Butcher, Jeerakathil et al. 2013)
Intracerebral Hemorrhage	Pioglitazone	Safety of Pioglitazone for Hematoma Resolution In Intracerebral Hemorrhage (SHRINC)	2	Ongoing	(Gonzales, Shah et al. 2013)
Intracerebral Hemorrhage	Minocycline	A Pilot Study of Minocycline in Intracerebral Hemorrhage Patients (MACH)	2	Recruiting	(Kohler, Prentice et al. 2013)
Intracerebral Hemorrhage	Rosuvastatin	Effect of Rosuvastatin in Intracerebral Hemorrhage	2	Complete	(Tapia-Perez, Sanchez-Aguilar et al. 2009)
Intracerebral hemorrhage	Nicardipine	IV Double and Triple Concentrated Nicardipine for Stroke and ICH	4	Unknown	(Koga, Arihiro et al. 2014)

Conclusion

In this review, we discussed the distinct macrophage and microglia, and T-helper lymphocyte subtypes, their known roles in cerebral hemorrhage pathophysiology, and current gaps in the literature. Table A.2 contains a brief overview of current and past clinical trials investigating immunomodulatory therapies, which are sparse and often directly target another pathophysiological mechanism with immunomodulation as a secondary effect. Although many pharmacological approaches showed promise experimentally, none have thus far successfully translated to the clinic (Ayer, Hwang et al. 2012). Although the discussion of the M1 and M2 microglia/macrophage subtypes and the Th1/Th2 and Th17/Treg subtypes is not novel, their unknown roles in cerebral hemorrhage pathophysiology warrants further investigation as possible therapeutic targets. Our goal is to advance the discussion of inflammation and secondary brain injury to involve the distinct immune cell subtypes and their probable neurodegenerative or neuroprotective roles and encourage further investigation. Indeed, modulating the immune response by shifting the peri-injury milieu from a highly oxidative, caustic environment, typically mediated by the M1/Th1/Th17 subtypes, to a regenerative and repair environment, mediated by the M2/Th2/Treg subtypes, is being increasingly encouraged in the cerebral ischemia field (Seifert and Pennypacker 2014). Applying the same concept in polarizing towards a regenerative and repair immune response following cerebral hemorrhage may yield positive, novel therapeutic approaches, and may be more desirable than inhibiting inflammation altogether. Applying a multi-modal approach involving immunomodulatory therapies to ameliorate secondary brain injury in

conjunction with conventional therapies targeting primary brain injury may improve both short and long-term outcomes and warrants further investigation.

References

Anderson CS, Huang Y, Wang JG, Arima H, Neal B, Peng B, Heeley E, Skulina C, Parsons MW, Kim JS, Tao QL, Li YC, Jiang JD, Tai LW, Zhang JL, Xu E, Cheng Y, Heritier S, Morgenstern LB, Chalmers J, and Investigators I (2008). "Intensive Blood Pressure Reduction in Acute Cerebral Haemorrhage Trial (Interact): A Randomised Pilot Trial." Lancet Neurol **7**(5): 391-399.

Aronowski J, and Hall CE (2005). "New Horizons for Primary Intracerebral Hemorrhage Treatment: Experience from Preclinical Studies." Neurol Res **27**(3): 268-279.

Aronowski J, and Zhao X (2011). "Molecular Pathophysiology of Cerebral Hemorrhage: Secondary Brain Injury." Stroke **42**(6): 1781-1786.

Ayer A, Hwang BY, Appelboom G, and Connolly ES, Jr. (2012). "Clinical Trials for Neuroprotective Therapies in Intracerebral Hemorrhage: A New Roadmap from Bench to Bedside." Transl Stroke Res **3**(4): 409-417.

Babu R, Bagley JH, Di C, Friedman AH, and Adamson C (2012). "Thrombin and Hemin as Central Factors in the Mechanisms of Intracerebral Hemorrhage-Induced Secondary Brain Injury and as Potential Targets for Intervention." Neurosurg Focus **32**(4): E8.

Belur PK, Chang JJ, He S, Emanuel BA, and Mack WJ (2013). "Emerging Experimental Therapies for Intracerebral Hemorrhage: Targeting Mechanisms of Secondary Brain Injury." Neurosurg Focus **34**(5): E9.

Biswas SK, and Mantovani A (2010). "Macrophage Plasticity and Interaction with Lymphocyte Subsets: Cancer as a Paradigm." Nat Immunol **11**(10): 889-896.

Bogie JF, Stinissen P, and Hendriks JJ (2014). "Macrophage Subsets and Microglia in Multiple Sclerosis." Acta Neuropathol **128**(2): 191-213.

Bretscher PA (2014). "On the Mechanism Determining the Th1/Th2 Phenotype of an Immune Response, and Its Pertinence to Strategies for the Prevention, and Treatment, of Certain Infectious Diseases." Scand J Immunol **79**(6): 361-376.

Brouwers HB, and Greenberg SM (2013). "Hematoma Expansion Following Acute Intracerebral Hemorrhage." Cerebrovasc Dis **35**(3): 195-201.

Butcher KS, Jeerakathil T, Hill M, Demchuk AM, Dowlatshahi D, Coutts SB, Gould B, McCourt R, Asdaghi N, Findlay JM, Emery D, Shuaib A, and Investigators IA (2013). "The Intracerebral Hemorrhage Acutely Decreasing Arterial Pressure Trial." Stroke **44**(3): 620-626.

Chen GY, and Nunez G (2010). "Sterile Inflammation: Sensing and Reacting to Damage." Nat Rev Immunol **10**(12): 826-837.

Chen Q, Zhang J, Guo J, Tang J, Tao Y, Li L, Feng H, and Chen Z (2014). "Chronic Hydrocephalus and Perihematomal Tissue Injury Developed in a Rat Model of Intracerebral Hemorrhage with Ventricular Extension." Transl Stroke Res.

Chen S, Yang Q, Chen G, and Zhang JH (2015). "An Update on Inflammation in the Acute Phase of Intracerebral Hemorrhage." Transl Stroke Res **6**(1): 4-8.

Chen W, Jin W, Hardegen N, Lei KJ, Li L, Marinos N, McGrady G, and Wahl SM (2003). "Conversion of Peripheral Cd4+Cd25- Naive T Cells to Cd4+Cd25+ Regulatory T Cells by Tgf-Beta Induction of Transcription Factor Foxp3." J Exp Med **198**(12): 1875-1886.

Cheng Y, Xi G, Jin H, Keep RF, Feng J, and Hua Y (2014). "Thrombin-Induced Cerebral Hemorrhage: Role of Protease-Activated Receptor-1." Transl Stroke Res **5**(4): 472-475.

Cherry JD, Olschowka JA, and O'Banion MK (2014). "Neuroinflammation and M2 Microglia: The Good, the Bad, and the Inflamed." J Neuroinflammation **11**: 98.

Chinetti-Gbaguidi G, Colin S, and Staels B (2015). "Macrophage Subsets in Atherosclerosis." Nat Rev Cardiol **12**(1): 10-17.

Correale J, and Villa A (2004). "The Neuroprotective Role of Inflammation in Nervous System Injuries." J Neurol **251**(11): 1304-1316.

Davis SM, Broderick J, Hennerici M, Brun NC, Diringer MN, Mayer SA, Begtrup K, Steiner T, and Recombinant Activated Factor VIIIHTI (2006). "Hematoma Growth Is a Determinant of Mortality and Poor Outcome after Intracerebral Hemorrhage." Neurology **66**(8): 1175-1181.

Denning TL, Wang YC, Patel SR, Williams IR, and Pulendran B (2007). "Lamina Propria Macrophages and Dendritic Cells Differentially Induce Regulatory and Interleukin 17-Producing T Cell Responses." Nat Immunol **8**(10): 1086-1094.

Diringer MN, Skolnick BE, Mayer SA, Steiner T, Davis SM, Brun NC, and Broderick JP (2010). "Thromboembolic Events with Recombinant Activated Factor Vii in Spontaneous Intracerebral Hemorrhage: Results from the Factor Seven for Acute Hemorrhagic Stroke (Fast) Trial." Stroke **41**(1): 48-53.

Dong C (2008). "Th17 Cells in Development: An Updated View of Their Molecular Identity and Genetic Programming." Nat Rev Immunol **8**(5): 337-348.

Dong C (2011). "Genetic Controls of Th17 Cell Differentiation and Plasticity." Exp Mol Med **43**(1): 1-6.

Dowlatshahi D, Demchuk AM, Flaherty ML, Ali M, Lyden PL, Smith EE, and Collaboration V (2011). "Defining Hematoma Expansion in Intracerebral Hemorrhage: Relationship with Patient Outcomes." Neurology **76**(14): 1238-1244.

Ducruet AF, Zacharia BE, Hickman ZL, Grobelny BT, Yeh ML, Sosunov SA, and Connolly ES, Jr. (2009). "The Complement Cascade as a Therapeutic Target in Intracerebral Hemorrhage." Exp Neurol **219**(2): 398-403.

Eggen BJ, Raj D, Hanisch UK, and Boddeke HW (2013). "Microglial Phenotype and Adaptation." J Neuroimmune Pharmacol **8**(4): 807-823.

Fang H, Wang PF, Zhou Y, Wang YC, and Yang QW (2013). "Toll-Like Receptor 4 Signaling in Intracerebral Hemorrhage-Induced Inflammation and Injury." J Neuroinflammation **10**: 27.

Fiorentino DF, Zlotnik A, Vieira P, Mosmann TR, Howard M, Moore KW, and O'Garra A (1991). "Il-10 Acts on the Antigen-Presenting Cell to Inhibit Cytokine Production by Th1 Cells." J Immunol **146**(10): 3444-3451.

Fu Y, Hao J, Zhang N, Ren L, Sun N, Li YJ, Yan Y, Huang D, Yu C, and Shi FD (2014). "Fingolimod for the Treatment of Intracerebral Hemorrhage: A 2-Arm Proof-of-Concept Study." JAMA Neurol **71**(9): 1092-1101.

Gao C, Du H, Hua Y, Keep RF, Strahle J, and Xi G (2014). "Role of Red Blood Cell Lysis and Iron in Hydrocephalus after Intraventricular Hemorrhage." J Cereb Blood Flow Metab **34**(6): 1070-1075.

Gao L, Lu Q, Huang LJ, Ruan LH, Yang JJ, Huang WL, ZhuGe WS, Zhang YL, Fu B, Jin KL, and ZhuGe QC (2014). "Transplanted Neural Stem Cells Modulate Regulatory T, Gammadelta T Cells and Corresponding Cytokines after Intracerebral Hemorrhage in Rats." Int J Mol Sci **15**(3): 4431-4441.

Giunti D, Parodi B, Cordano C, Uccelli A, and Kerlero de Rosbo N (2014). "Can We Switch Microglia's Phenotype to Foster Neuroprotection? Focus on Multiple Sclerosis." Immunology **141**(3): 328-339.

Gonzales NR, Shah J, Sangha N, Sosa L, Martinez R, Shen L, Kasam M, Morales MM, Hossain MM, Barreto AD, Savitz SI, Lopez G, Misra V, Wu TC, El Khoury R, Sarraj A, Sahota P, Hicks W, Acosta I, Sline MR, Rahbar MH, Zhao X, Aronowski J, and Grotta JC (2013). "Design of a Prospective, Dose-Escalation Study Evaluating the Safety of Pioglitazone for Hematoma Resolution in Intracerebral Hemorrhage (Shrinc)." Int J Stroke **8**(5): 388-396.

Gu L, Xiong X, Zhang H, Xu B, Steinberg GK, and Zhao H (2012). "Distinctive Effects of T Cell Subsets in Neuronal Injury Induced by Cocultured Splenocytes in Vitro and by in Vivo Stroke in Mice." Stroke **43**(7): 1941-1946.

Guo FQ, Li XJ, Chen LY, Yang H, Dai HY, Wei YS, Huang YL, Yang YS, Sun HB, Xu YC, and Yang ZL (2006). "[Study of Relationship between Inflammatory Response and Apoptosis in Perihematoma Region in Patients with Intracerebral Hemorrhage]." Zhongguo Wei Zhong Bing Ji Jiu Yi Xue **18**(5): 290-293.

Hirota K, Martin B, and Veldhoen M (2010). "Development, Regulation and Functional Capacities of Th17 Cells." Semin Immunopathol **32**(1): 3-16.

Hohlfeld R, Kerschensteiner M, Stadelmann C, Lassmann H, and Wekerle H (2006). "The Neuroprotective Effect of Inflammation: Implications for the Therapy of Multiple Sclerosis." Neurol Sci **27 Suppl 1**: S1-7.

Hosaka K, and Hoh BL (2014). "Inflammation and Cerebral Aneurysms." Transl Stroke Res **5**(2): 190-198.

Hua Y, Keep RF, Hoff JT, and Xi G (2007). "Brain Injury after Intracerebral Hemorrhage: The Role of Thrombin and Iron." Stroke **38**(2 Suppl): 759-762.

Hua Y, Xi G, Keep RF, and Hoff JT (2000). "Complement Activation in the Brain after Experimental Intracerebral Hemorrhage." J Neurosurg **92**(6): 1016-1022.

Keep RF, Hua Y, and Xi G (2012). "Intracerebral Haemorrhage: Mechanisms of Injury and Therapeutic Targets." Lancet Neurol **11**(8): 720-731.

Keep RF, Xi G, Hua Y, and Hoff JT (2005). "The Deleterious or Beneficial Effects of Different Agents in Intracerebral Hemorrhage: Think Big, Think Small, or Is Hematoma Size Important?" Stroke **36**(7): 1594-1596.

Klebe D, Krafft PR, Hoffmann C, Lekic T, Flores JJ, Rolland W, and Zhang JH (2014). "Acute and Delayed Deferoxamine Treatment Attenuates Long-Term Sequelae after Germinal Matrix Hemorrhage in Neonatal Rats." Stroke **45**(8): 2475-2479.

Kleinewietfeld M, and Hafler DA (2013). "The Plasticity of Human Treg and Th17 Cells and Its Role in Autoimmunity." Semin Immunol **25**(4): 305-312.

Koga M, Arihiro S, Hasegawa Y, Shiokawa Y, Okada Y, Kimura K, Furui E, Nakagawara J, Yamagami H, Kario K, Okuda S, Tokunaga K, Takizawa H, Takasugi J, Sato S, Nagatsuka K, Minematsu K, Toyoda K, Stroke Acute Management with Urgent Risk-factor A, and Improvement Study I (2014). "Intravenous Nicardipine Dosing for Blood Pressure Lowering in Acute Intracerebral Hemorrhage: The Stroke Acute Management with Urgent Risk-

Factor Assessment and Improvement-Intracerebral Hemorrhage Study." J Stroke Cerebrovasc Dis **23**(10): 2780-2787.

Kohler E, Prentice DA, Bates TR, Hankey GJ, Claxton A, van Heerden J, and Blacker D (2013). "Intravenous Minocycline in Acute Stroke: A Randomized, Controlled Pilot Study and Meta-Analysis." Stroke **44**(9): 2493-2499.

Kreitzer N, and Adeoye O (2013). "An Update on Surgical and Medical Management Strategies for Intracerebral Hemorrhage." Semin Neurol **33**(5): 462-467.

Li MO, Wan YY, and Flavell RA (2007). "T Cell-Produced Transforming Growth Factor-Beta1 Controls T Cell Tolerance and Regulates Th1- and Th17-Cell Differentiation." Immunity **26**(5): 579-591.

Lu Q, Gao L, Huang L, Ruan L, Yang J, Huang W, Li Z, Zhang Y, Jin K, and Zhuge Q (2014). "Inhibition of Mammalian Target of Rapamycin Improves Neurobehavioral Deficit and Modulates Immune Response after Intracerebral Hemorrhage in Rat." J Neuroinflammation **11**: 44.

Luckheeram RV, Zhou R, Verma AD, and Xia B (2012). "Cd4(+)T Cells: Differentiation and Functions." Clin Dev Immunol **2012**: 925135.

Mantel PY, and Schmidt-Weber CB (2011). "Transforming Growth Factor-Beta: Recent Advances on Its Role in Immune Tolerance." Methods Mol Biol **677**: 303-338.

Martinez FO, and Gordon S (2014). "The M1 and M2 Paradigm of Macrophage Activation: Time for Reassessment." F1000Prime Rep **6**: 13.

Martinez FO, Helming L, and Gordon S (2009). "Alternative Activation of Macrophages: An Immunologic Functional Perspective." Annu Rev Immunol **27**: 451-483.

Martinez FO, Sica A, Mantovani A, and Locati M (2008). "Macrophage Activation and Polarization." Front Biosci **13**: 453-461.

Mayer SA, Brun NC, Begtrup K, Broderick J, Davis S, Diringer MN, Skolnick BE, Steiner T, and Investigators FT (2008). "Efficacy and Safety of Recombinant Activated Factor Vii for Acute Intracerebral Hemorrhage." N Engl J Med **358**(20): 2127-2137.

Mayer SA, Brun NC, Broderick J, Davis SM, Diringer MN, Skolnick BE, Steiner T, and United States NovoSeven ICHTI (2006). "Recombinant Activated Factor Vii for Acute Intracerebral Hemorrhage: Us Phase Iia Trial." Neurocrit Care **4**(3): 206-214.

McCombe PA, and Read SJ (2008). "Immune and Inflammatory Responses to Stroke: Good or Bad?" Int J Stroke **3**(4): 254-265.

Mendelow AD, Gregson BA, Fernandes HM, Murray GD, Teasdale GM, Hope DT, Karimi A, Shaw MD, Barer DH, and investigators S (2005). "Early Surgery Versus Initial Conservative Treatment in Patients with Spontaneous Supratentorial Intracerebral Haematomas in the International Surgical Trial in Intracerebral Haemorrhage (Stich): A Randomised Trial." Lancet **365**(9457): 387-397.

Mendelow AD, Gregson BA, Rowan EN, Murray GD, Gholkar A, Mitchell PM, and Investigators SI (2013). "Early Surgery Versus Initial Conservative Treatment in Patients with Spontaneous Supratentorial Lobar Intracerebral Haematomas (Stich Ii): A Randomised Trial." Lancet **382**(9890): 397-408.

Meng H, Li F, Hu R, Yuan Y, Gong G, Hu S, and Feng H (2014). "Deferoxamine Alleviates Chronic Hydrocephalus after Intraventricular Hemorrhage through Iron Chelation and Wnt1/Wnt3a Inhibition." Brain Res.

Miller CM, Vespa P, Saver JL, Kidwell CS, Carmichael ST, Alger J, Frazee J, Starkman S, Liebeskind D, Nenov V, Elashoff R, and Martin N (2008). "Image-Guided Endoscopic Evacuation of Spontaneous Intracerebral Hemorrhage." Surg Neurol **69**(5): 441-446; discussion 446.

Morgenstern LB, Frankowski RF, Shedden P, Pasteur W, and Grotta JC (1998). "Surgical Treatment for Intracerebral Hemorrhage (Stich): A Single-Center, Randomized Clinical Trial." Neurology **51**(5): 1359-1363.

Morgenstern LB, Hemphill JC, 3rd, Anderson C, Becker K, Broderick JP, Connolly ES, Jr., Greenberg SM, Huang JN, MacDonald RL, Messe SR, Mitchell PH, Selim M, Tamargo RJ, American Heart Association Stroke C, and Council on Cardiovascular N (2010). "Guidelines for the Management of Spontaneous Intracerebral Hemorrhage: A Guideline for Healthcare Professionals from the American Heart Association/American Stroke Association." Stroke **41**(9): 2108-2129.

Mracsko E, Javidi E, Na SY, Kahn A, Liesz A, and Veltkamp R (2014). "Leukocyte Invasion of the Brain after Experimental Intracerebral Hemorrhage in Mice." Stroke **45**(7): 2107-2114.

Mracsko E, and Veltkamp R (2014). "Neuroinflammation after Intracerebral Hemorrhage." Front Cell Neurosci **8**: 388.

Murray PJ, and Wynn TA (2011). "Protective and Pathogenic Functions of Macrophage Subsets." Nat Rev Immunol **11**(11): 723-737.

Nakamura T, Keep RF, Hua Y, Schallert T, Hoff JT, and Xi G (2004). "Deferoxamine-Induced Attenuation of Brain Edema and Neurological Deficits in a Rat Model of Intracerebral Hemorrhage." J Neurosurg **100**(4): 672-678.

Orme J, and Mohan C (2012). "Macrophage Subpopulations in Systemic Lupus Erythematosus." Discov Med **13**(69): 151-158.

Pandey AS, and Xi G (2014). "Intracerebral Hemorrhage: A Multimodality Approach to Improving Outcome." Transl Stroke Res **5**(3): 313-315.

Peck A, and Mellins ED (2010). "Plasticity of T-Cell Phenotype and Function: The T Helper Type 17 Example." Immunology **129**(2): 147-153.

Pisanu A, Lecca D, Mulas G, Wardas J, Simbula G, Spiga S, and Carta AR (2014). "Dynamic Changes in Pro- and Anti-Inflammatory Cytokines in Microglia after Ppar-Gamma Agonist Neuroprotective Treatment in the Mptpp Mouse Model of Progressive Parkinson's Disease." Neurobiol Dis **71**: 280-291.

Qureshi AI, Mendelow AD, and Hanley DF (2009). "Intracerebral Haemorrhage." Lancet **373**(9675): 1632-1644.

Rincon F, Friedman DP, Bell R, Mayer SA, and Bray PF (2014). "Targeted Temperature Management after Intracerebral Hemorrhage (Ttm-Ich): Methodology of a Prospective Randomized Clinical Trial." Int J Stroke **9**(5): 646-651.

Rolland WB, 2nd, Manaenko A, Lekic T, Hasegawa Y, Ostrowski R, Tang J, and Zhang JH (2011). "Fty720 Is Neuroprotective and Improves Functional Outcomes after Intracerebral Hemorrhage in Mice." Acta Neurochir Suppl **111**: 213-217.

Rolland WB, Lekic T, Krafft PR, Hasegawa Y, Altay O, Hartman R, Ostrowski R, Manaenko A, Tang J, and Zhang JH (2013). "Fingolimod Reduces Cerebral Lymphocyte Infiltration in Experimental Models of Rodent Intracerebral Hemorrhage." Exp Neurol **241**: 45-55.

Romagnani S (1999). "Th1/Th2 Cells." Inflamm Bowel Dis **5**(4): 285-294.

Saijo K, and Glass CK (2011). "Microglial Cell Origin and Phenotypes in Health and Disease." Nat Rev Immunol **11**(11): 775-787.

Sakamoto Y, Koga M, Yamagami H, Okuda S, Okada Y, Kimura K, Shiokawa Y, Nakagawara J, Furui E, Hasegawa Y, Kario K, Arihiro S, Sato S, Kobayashi J, Tanaka E, Nagatsuka K, Minematsu K, Toyoda K, and Investigators SS (2013). "Systolic Blood Pressure after Intravenous Antihypertensive Treatment and Clinical Outcomes in Hyperacute Intracerebral Hemorrhage: The Stroke Acute Management with Urgent Risk-Factor Assessment and Improvement-Intracerebral Hemorrhage Study." Stroke **44**(7): 1846-1851.

Savage ND, de Boer T, Walburg KV, Joosten SA, van Meijgaarden K, Geluk A, and Ottenhoff TH (2008). "Human Anti-Inflammatory Macrophages Induce Foxp3+

Gitr+ Cd25+ Regulatory T Cells, Which Suppress Via Membrane-Bound Tgfbeta-1." J Immunol **181**(3): 2220-2226.

Seifert HA, and Pennypacker KR (2014). "Molecular and Cellular Immune Responses to Ischemic Brain Injury." Transl Stroke Res **5**(5): 543-553.

Starke RM, Raper DM, Ding D, Chalouhi N, Owens GK, Hasan DM, Medel R, and Dumont AS (2014). "Tumor Necrosis Factor-Alpha Modulates Cerebral Aneurysm Formation and Rupture." Transl Stroke Res **5**(2): 269-277.

Staykov D, Wagner I, Volbers B, Hauer EM, Doerfler A, Schwab S, and Bardutzky J (2011). "Natural Course of Perihemorrhagic Edema after Intracerebral Hemorrhage." Stroke **42**(9): 2625-2629.

Stockinger B, and Veldhoen M (2007). "Differentiation and Function of Th17 T Cells." Curr Opin Immunol **19**(3): 281-286.

Stout RD, Jiang C, Matta B, Tietzel I, Watkins SK, and Suttles J (2005). "Macrophages Sequentially Change Their Functional Phenotype in Response to Changes in Microenvironmental Influences." J Immunol **175**(1): 342-349.

Stout RD, and Suttles J (2004). "Functional Plasticity of Macrophages: Reversible Adaptation to Changing Microenvironments." J Leukoc Biol **76**(3): 509-513.

Tapia-Perez H, Sanchez-Aguilar M, Torres-Corzo JG, Rodriguez-Leyva I, Gonzalez-Aguirre D, Gordillo-Moscoso A, and Chalita-Williams C (2009). "Use of Statins for the Treatment of Spontaneous Intracerebral Hemorrhage: Results of a Pilot Study." Cent Eur Neurosurg **70**(1): 15-20.

Theodorou GL, Marousi S, Ellul J, Mougiou A, Theodori E, Mouzaki A, and Karakantza M (2008). "T Helper 1 (Th1)/Th2 Cytokine Expression Shift of Peripheral Blood Cd4+ and Cd8+ T Cells in Patients at the Post-Acute Phase of Stroke." Clin Exp Immunol **152**(3): 456-463.

Thiex R, and Tsirka SE (2007). "Brain Edema after Intracerebral Hemorrhage: Mechanisms, Treatment Options, Management Strategies, and Operative Indications." Neurosurg Focus **22**(5): E6.

van Asch CJ, Luitse MJ, Rinkel GJ, van der Tweel I, Algra A, and Klijn CJ (2010). "Incidence, Case Fatality, and Functional Outcome of Intracerebral Haemorrhage over Time, According to Age, Sex, and Ethnic Origin: A Systematic Review and Meta-Analysis." Lancet Neurol **9**(2): 167-176.

Vignali DA, Collison LW, and Workman CJ (2008). "How Regulatory T Cells Work." Nat Rev Immunol **8**(7): 523-532.

Wang J (2010). "Preclinical and Clinical Research on Inflammation after Intracerebral Hemorrhage." Prog Neurobiol **92**(4): 463-477.

Wang J, and Dore S (2007). "Inflammation after Intracerebral Hemorrhage." J Cereb Blood Flow Metab **27**(5): 894-908.

Wang N, Liang H, and Zen K (2014). "Molecular Mechanisms That Influence the Macrophage M1-M2 Polarization Balance." Front Immunol **5**: 614.

Wang WZ, Jiang B, Liu HM, Li D, Lu CZ, Zhao YD, and Sander JW (2009). "Minimally Invasive Craniopuncture Therapy Vs. Conservative Treatment for Spontaneous Intracerebral Hemorrhage: Results from a Randomized Clinical Trial in China." Int J Stroke **4**(1): 11-16.

Wee Yong V (2010). "Inflammation in Neurological Disorders: A Help or a Hindrance?" Neuroscientist **16**(4): 408-420.

Wu G, Xi G, and Huang F (2006). "Spontaneous Intracerebral Hemorrhage in Humans: Hematoma Enlargement, Clot Lysis, and Brain Edema." Acta Neurochir Suppl **96**: 78-80.

Xi G, Keep RF, and Hoff JT (2006). "Mechanisms of Brain Injury after Intracerebral Haemorrhage." Lancet Neurol **5**(1): 53-63.

Xiong XY, Wang J, Qian ZM, and Yang QW (2014). "Iron and Intracerebral Hemorrhage: From Mechanism to Translation." Transl Stroke Res **5**(4): 429-441.

Xu L, Kitani A, Fuss I, and Strober W (2007). "Cutting Edge: Regulatory T Cells Induce Cd4+Cd25-Foxp3- T Cells or Are Self-Induced to Become Th17 Cells in the Absence of Exogenous Tgf-Beta." J Immunol **178**(11): 6725-6729.

Yang Z, Yu A, Liu Y, Shen H, Lin C, Lin L, Wang S, and Yuan B (2014). "Regulatory T Cells Inhibit Microglia Activation and Protect against Inflammatory Injury in Intracerebral Hemorrhage." Int Immunopharmacol **22**(2): 522-525.

Yoshimura A, and Muto G (2011). "Tgf-Beta Function in Immune Suppression." Curr Top Microbiol Immunol **350**: 127-147.

Zambrano-Zaragoza JF, Romo-Martinez EJ, Duran-Avelar Mde J, Garcia-Magallanes N, and Vibanco-Perez N (2014). "Th17 Cells in Autoimmune and Infectious Diseases." Int J Inflam **2014**: 651503.

Zhao J, Chen Z, Xi G, Keep RF, and Hua Y (2014). "Deferoxamine Attenuates Acute Hydrocephalus after Traumatic Brain Injury in Rats." Transl Stroke Res **5**(5): 586-594.

Zhao X, Grotta J, Gonzales N, and Aronowski J (2009). "Hematoma Resolution as a Therapeutic Target: The Role of Microglia/Macrophages." Stroke **40**(3 Suppl): S92-94.

Zhao X, Sun G, Zhang H, Ting SM, Song S, Gonzales N, and Aronowski J (2014). "Polymorphonuclear Neutrophil in Brain Parenchyma after Experimental Intracerebral Hemorrhage." Transl Stroke Res **5**(5): 554-561.

Zhao X, Sun G, Zhang J, Strong R, Song W, Gonzales N, Grotta JC, and Aronowski J (2007). "Hematoma Resolution as a Target for Intracerebral Hemorrhage Treatment: Role for Peroxisome Proliferator-Activated Receptor Gamma in Microglia/Macrophages." Ann Neurol **61**(4): 352-362.

Zhou L, Chong MM, and Littman DR (2009). "Plasticity of Cd4+ T Cell Lineage Differentiation." Immunity **30**(5): 646-655.

Zhou Y, Wang Y, Wang J, Anne Stetler R, and Yang QW (2014). "Inflammation in Intracerebral Hemorrhage: From Mechanisms to Clinical Translation." Prog Neurobiol **115**: 25-44.

Zhu J, and Paul WE (2008). "Cd4 T Cells: Fates, Functions, and Faults." Blood **112**(5): 1557-1569.

Zhu J, and Paul WE (2010). "Peripheral Cd4+ T-Cell Differentiation Regulated by Networks of Cytokines and Transcription Factors." Immunol Rev **238**(1): 247-262.